University of Arizona
Carnegie Institution of Washington
The Johns Hopkins University

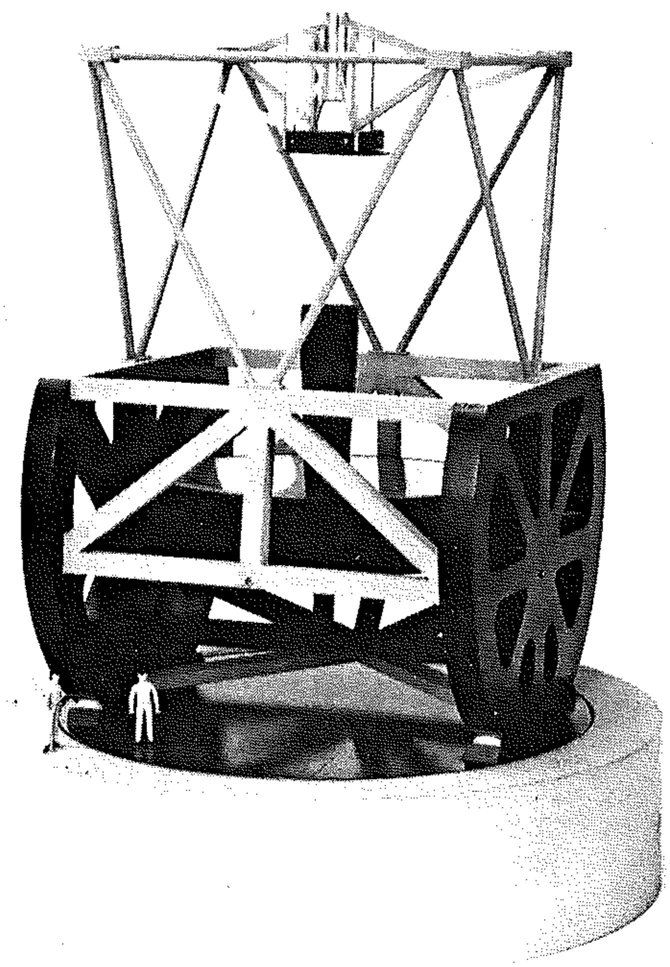

Preliminary Design
Magellan Project 8-Meter Telescope

L & F Industries
Huntington Park, California
July 1988
Revised April 1989
No. 5

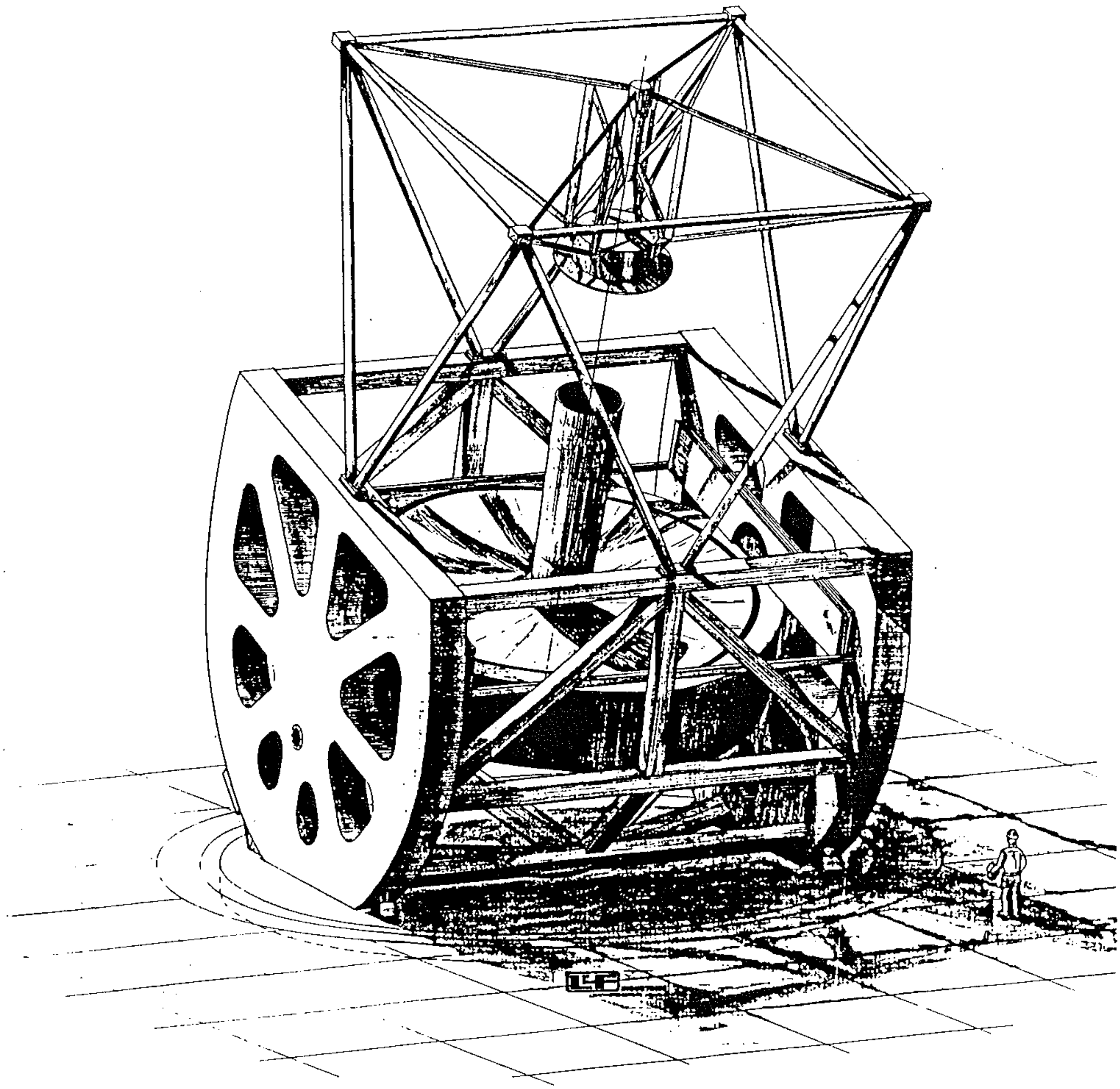

INDEX

ERRATA TO:

"ENGINEERING REPORT

PRELIMINARY DESIGN

MAGELLAN PROJECT 8 METER TELESCOPE

(dated) July 1988"

April 11, 1989

The above-referenced report summarized results of finite element analyses, using Algor Interactive Systems' Supersap software. Recent revisions to the software incorporated a more accurate (and less stiff) plate element, while the beam element stiffnesses remained unchanged. All affected analyses were again run using the more accurate versions of the software. The affected sheets from the report were revised and are included on the following sheets.

Generally, since major portions of the models relied upon beam elements, the changes were small. However, since optical misalignments (static runs) are comparing secondary deflections (predominant stiffness due to beam elements) with the primary mirror target deflections (predominant stiffness due to plate elements), some of these effects were more significant.

In some cases static misalignments worsened, but in more cases they actually improved. This is due to the fact that secondary motions, in general, are greater than primary (mirror target) motions, and the softer primary mirror cell actually reduces misalignments in many cases.

(Note added April 28, 1989). The revised pages referred to above have replaced those in the original report. The pages are 11 REV to 13 REV and 27 REV to 36 REV. The gravity misalignments have recently been calculated for a 1500 lb. secondary assembly. This calculation, which was not in the original report, is given on three pages, all numbered 11 ADD. Except for this one isolated calculation all others in this report were made with a 5000 lb. secondary in place.

INTRODUCTION

The purpose of this report is to:

1.) Define the telescope in its current preliminary design configuration.

2.) Summarize the expected performance of the current telescope design.

3.) Document other design configurations which have been investigated since the previous (October 1987) report, but which are now obsolete. These data are included in the appendix in order to avoid confusion with the current design.

The primary goal of the work performed in this phase (that is, since October 1987) has been to improve the lowest resonant frequencies of the structure. This has been accomplished, and will be summarized herein. Four considerably different structural configurations were analyzed in this effort:

1.) Much larger, stiffer "conventional fork" structures (but using the same general structural configuration as was used in the previous work).

2.) A "conventional Nasmyth Alt-Az Disk" structure (to be defined in the body of this report).

3.) A plate or monocoque structure Alt-Az Disk system.

4.) An "eccentric Nasmyth Alt-Az Disk" telescope, which has proven to be the most efficient from various standpoints, and which is the current design of choice.

In addition, detailed structural variations (particularly in the secondary support vane system) were investigated. The result is a system which is both stiff and very convenient from the operational standpoint.

Results of the finite element analyses are presented herein, with emphasis on the current design. Also, a video presentation of the work, including animated vibrational modeshapes, is being supplied.

Layout drawings, data reductions, and information pertinent to the current design are included at the end of the body of this report. Drawings, discussion and data from obsolete designs, but which were created since the last (October 1987) report, are included in the appendix for historical purposes. Therefore, all information not in the appendix of this report is current.

STRUCTURAL AND MECHANICAL CONFIGURATION

SYSTEM DESCRIPTION:

The Magellan Project 8 Meter Telescope design summarized herein consists of an Alt-Az Disk mount as shown on drawings E271030, E271029, and E271032 (end of report body). The f1.2 primary and f6.5 wide field secondary mirrors focus at the Cassegrain instrument location. Alternatively, the fx.x infrared secondary mirror may be used. In addition, two Nasmyth instrument locations are provided.

The two main rotating structural components of the mount are the Optical Support Structure ("O.S.S.") and the Azimuth Disk.

The O.S.S. Assembly consists of two major subassemblies:

1.) The Primary Support Structure includes the primary mirror, primary mirror cell, altitude disks, lateral braces, and truss main planes.

2.) The Secondary End consists of the main truss, square frame, vane system, and wide field and infrared secondaries.

The Azimuth Disk is a large diameter, relatively thin structure, which contains all of the hydrostatic bearing pads which define the altitude and azimuth axes. The azimuth pads run against two large diameter bearing surfaces which are integral with the large concrete pier support (ref dwg E271029 sht. 2).

STRUCTURAL DESIGN:

The current preliminary design configuration has been selected in order to maximize stiffness and reduce weight. This effects both low deflections due to gravity and wind loading, and high structural resonant frequencies. In addition, the reduced weight may effect cost savings, but will certainly improve thermal response of the structure to ambient temperature changes. This, then, should have a beneficial effect on seeing.

This "Alt-Az Disk" mount has been found to have considerably higher (lateral and fore-aft translation) natural frequencies than the earlier conventional fork design.

Lateral translation is improved due to the fact that lateral bracing can be integral with the O.S.S., and therefore rotate with it while always remaining clear of the Cassegrain instrument. Conversely, a large open area is required between the altitude bearings in a conventional fork design, in order to clear the Cassegrain instrument near zenith, and the O.S.S. near horizon. A large bending moment must therefore be reacted by the fork tines in the conventional fork design, causing a lower natural frequency in lateral translation.

Fore-aft translation is improved due mainly to the large in-plane stiffness of the altitude disks reacting moment more efficiently than the fork tines in the conventional fork design.

Another, perhaps simpler, way of looking at this improved efficiency is to say that, in the conventional fork system, for any attitude of the O.S.S. the (lateral and fore-aft translation) load path is less direct for the lower half of the O.S.S. Its load path actually begins at a low level and travels up to the altitude bearings before then "changing direction" and travelling back down the fork tines to ground. In the Alt-Az Disk system, the load is always travelling "down". The average moment arm upon which the average mass acts, is then lower in the Alt-Az Disk configuration than with the conventional fork.

Although the Alt-Az Disk O.S.S. is a little heavier than in the conventional fork design (288 kips vs. 204 kips), the azimuth disk is much lighter (127 kips vs. 300 kips). This is due to the fact that the azimuth disk is designed in such a way that it reacts no out-of-plane bending. It therefore can be a large diameter but relatively thin structure (ref dwg E271029 shts 1 and 2), and thus light in weight. It is a fabricated structure, with numerous bulkheads and gussets separating the main top and bottom (1/2" thick) plates.

The altitude disks serve three functions. Their individual members complete the main trussed or braced structure of the O.S.S., they carry local bending and torsional stresses due to point loading from the hydrostatic pads, and they support the Nasmyth instruments. The radial "spoke" members are generally 30" square box sections fabricated from 1/4" steel plate. The circumferential "rim" members are nominally 30" x 48" sections fabricated from 1/2" plate except for heavier 2" plates locally where the hydrostatic pads run.

The primary mirror cell is supported by the Primary Support Structure at four points. Its perimeter wall is integral with the cell and capable of supporting the primary mirror with an edge support system. If transverse support of the mirror is finally done with a back support system, some reduction of the thickness of the mirror cell perimeter wall can be effected to reduce the size and weight of the entire structure and improve its performance. The mirror cell is constructed predominantly of 1/2" steel plate.

The truss main plane weldment is fabricated from 16" square structural tubing, with 1/2" wall thickness. Heavy steel pads are welded and machined at all bolted connections.

The lateral braces connect the two altitude disks and one of the main plane weldments. They are specially fabricated box sections due to the need for large cross-sectional area; thus limiting the lateral translation vibration mode to an acceptable value. They have welded, machined pads at their ends so that they can be individually removed for clearance by the mirror cell during its removal.

The 8-member secondary end main truss is a "M.I.L.T." truss, or modified Surrurier rotated 45 degrees about the optical axis. This provides the maximum clearance for vertical removal or installation of the wide field secondary mirror when the telescope is pointed to horizon. The main truss is fabricated from 8" outside diameter by 3/4" wall steel tubing.

The secondary square frame members are 7" outside diameter by 3/4" wall steel tubing. They not only complete the secondary end truss system, but also react the vane system pretensioning with a light compression stress.

The "universal" vane system is shown best on drawing E271032. This unique system provides a mounting point for both the wide field and infrared secondary mirrors, but still presents a rather small radiation in the infrared configuration. In this way, the infrared mirror can be permanently installed, and the wide field secondary simply installed or removed as necessary. This eliminates the need for an "exchangeable" top end, including the undesirable requirement of storing a large secondary support structure. The vanes are pretensioned at the ends (where they interface with the secondary square frame) with a total load of 100,000 lbs. at each of the four corners. This does create a small compression reaction in the four members which parallel the optical axis. However, their compression stability is adequate with the 8" by 2" by 3/8" wall rectangular tube as shown and this end view as seen in the infrared is thought to be acceptable. The static and modal performance of this system is thought to be good and is discussed in detail later in this report.

BEARINGS:

Hydrostatic bearings are used on both major rotation axes in this system (ref drawing E271029).

The altitude axis is defined by four hydrostatic pads mounted on the top side of the Azimuth Disk, two each supporting each altitude disk with contact angles 30 degrees from vertical.

The azimuth axis is defined using four vertical pads (each directly under the altitude axis pads) running on a large diameter flat bearing mounted to the top of the pier, as well as two horizontal pads at the perimeter of the azimuth disk running on the inside of a large diameter cylindrical bearing, also pier mounted.

In addition, one horizontal pad defines the O.S.S. laterally to the azimuth disk.

Of course, one preload hydrostatic pad (that is, a hydrostatic pad preloaded with a hydraulic cylinder) is required opposite the altitude disk lateral positioning pad, as well two opposite the azimuth disk horizontal pads.

It is intended that all 14 (stiffness load path and preload) hydrostatic pads will have internal spherical hydrostatic seats to assure equal pad loading when running against these rather large diameter bearings.

DRIVES:

Both the altitude and azimuth axis drives will be friction roller type. A friction-disk reducer will provide the necessary reduction between the servo-motor and the drive roller, so that no backlash exists in the system. This selection will provide the maximum possible smoothness and will be designed to maximize stiffness and natural frequencies.

The altitude axis consists of two drives; one driving each altitude disk. They are flexure-mounted so that the friction preload can be controlled while maintaining maximum stiffness in the tangential (drive) direction. (Ref dwg E271029 sht. 1).

The azimuth axis also uses two drives, mounted and preloaded in a similar manner to the altitude drives (ref dwg E271029 sht. 2).

FINITE ELEMENT ANALYSIS

INTRODUCTION

An Intermediate-level finite element analysis was performed during this phase of the preliminary design of the Magellan Project 8 Meter Telescope. The purpose of this work has been to improve the lowest resonant frequencies and other performance and operational features of the structure. The following discussion and data are pertinent to the current design of choice; that is, the Eccentric Nasmyth Alt-Az Disk Telescope with Universal Vane System.

Numerous models were created to accomplish this task. Results from 8 FEA models are included herein. A typical model is represented by:

680	nodes
680	thin plate/shell elements
207	beam elements
405	nodal masses
3153	degrees of freedom

The models are briefly defined in "Summary of Results" and as described below:

STATIC ANALYSIS:

In this Alt-Az Disk design some distortion of the altitude disks will occur as the O.S.S. is rotated from zenith to horizon. Therefore, it was felt that gravity loading must be applied to the entire telescope in order to evaluate motions of the secondary mirror(s) relative to the primary. (In the previous Conventional Fork design a local model of the O.S.S. was used for both zenith and horizon gravity loading).

Therefore, four models were created for static analysis:

Optical (wide field) Configuration, zenith attitude. (That is, with wide field secondary installed).

Optical Configuration, horizon attitude.

Infrared Configuration, zenith attitude. (That is, with wide field secondary removed.)

Infrared Configuration, horizon attitude.

Wind load criteria used were as follows:

It was assumed that under a relatively high wind load (that is, when it is not quite windy enough to halt observing), that the wind screen would be up. Therefore, only the upper end of the telescope should be exposed to significant wind forces when operating near zenith. A wind pressure of 0.46 psf was then applied above the midlength point of the main truss members under zenith front wind conditions. This represents a wind velocity of 15 mph acting upon the structure, at 7000 ft. elevation. It is believed that this is representative of an ambient wind velocity remote from the enclosure of 25 to 35 mph.

It was likewise assumed that when operating at low altitude angles (far from zenith) that the entire front view of the telescope would be exposed to the wind under horizon front wind loading.

Since it is less clear how side wind components originate, side wind was conservatively taken as acting upon the entire side profile view of the telescope, at both zenith and horizon.

In all of the above cases, it was reasoned that the wind could act at angles slightly off the nominal ("global") directions, and thus considerably increase the areas of the structure exposed to wind.

MODAL ANALYSIS:

Standard linear finite element programs are not capable of considering secondary effects such as those caused by member preloads acting on a distorted structure. However, a special purpose program (although somewhat limited in scope) is available from Algor Interactive Systems. The program "Modal Analysis with Load Stiffening" is capable of geometric stiffness addition (to the stiffness matrix) due to member preloads. However, it is not capable of working with plate elements.

Therefore, since it is desirable to understand the modal performance of the "universal vane system" with vane pretensions present, the following modal analyses were performed:

Model AADTELM1 is representative of the complete telescope in the worst (modal performance) attitude; 17 degrees off zenith. It includes no preload in any member. However, the secondary support vane members' bending stiffnesses (about the weak axis only) were increased artificially. In this way, numerous low (invalid) local vane vibrational modes were eliminated from the modal analysis results. Therefore all modes from this model are valid except for mode 1, secondary rotation about the optical axis (which will be affected by vane pretension).

However, the results from this model alone are not complete because the vane local modes are not included. Therefore, models

OP2NDRY and IR2NDRY were created (using only beam elements) to be run with the load stiffening program. This model (due to an anomaly in the program) included only the secondary vane system and secondary assemblies; that is, it did not include the square frame, main truss, or any of the rest of the telescope. The effect, then, of a 100,000# preload applied at each of the four corners of the system is included in these results. These results are thought to be valid relative to a structure preloaded in this manner, that is:

> Optical configuration (both wide field and infrared assemblies in place) with a 100,000# preload applied (total each corner) subsequent to the attachment of the wide field secondary mirror assembly.
>
> Infrared configuration (infrared assembly only, in place) with a 100,000# preload applied after the removal of the wide field secondary.

It should be noted, then, that to achieve the 5.2 hz wide field secondary rotation mode the pretension would have to be adjusted after installing the wide field assembly. If the preload is not adjusted, but rather the wide field assembly is simply attached to the (already preloaded) vane system, this mode will probably be about 2 or 3 hz.

It would seem that a reasonable strategy in this regard would be:

1.) Try this design without adjusting the preload when changing to the wide field configuration. If the 2 or 3 hz rotation about the optical axis mode causes some performance problem, then:

2.) Adjust the preload after installing the wide field secondary. If the 5.2 hz mode is still objectionable, then:

3.) Add antirotation wires and bring this natural frequency up to any desired value, and live with some operational inconvenience. (It is still much less work than exchanging the entire secondary end).

In addition to the above, Model AADTELM2 was run (again, of the complete telescope without preloads) with only one altitude drive effective. The results are somewhat poorer than in previous similar models. This is thought to be due to the beneficial effect of the previous dual vane system in keeping the Primary Support Structure from twisting about an axis parallel to the altitude axis. This, then, is still an open (and now somewhat more significant) question: Would the control system cause or allow the two altitude disks to act synchronously, limiting the lowest major vibrational mode to 7.3 hz?

(cont'd)

Two possible strategies are apparent:

Create and execute a math model of the control system to see how it will, in fact, respond with these structural resonances.

Increase the "one-drive" mode natural frequency through structural means (this has not yet been attempted). It is believed that this may be effective; however the possibility exists that some other modes may also suffer since it may require the addition of structural mass to the system.

For a better understanding of the significant modeshapes summarized herein, refer to the video presentation.

MAGELLAN PROJECT 8 METER TELESCOPE

FINITE ELEMENT ANALYSIS

SUMMARY OF RESULTS

NOTE - All models are representative of the Alt-Az Disk Telescope, with eccentric Nasmyth, universal vane system, f1.2 primary and f6.5 secondary f-ratios as follows:

AADTELOZ - Zenith pointing, optical (wide field) configuration.
load case 1 = gravity
load case 2 = front wind
load case 3 = side wind

AADTELOH - Horizon pointing, optical (wide field) configuration.
load case 1 = gravity
load case 2 = front wind
load case 3 = side wind

AADTELIZ - Zenith pointing, infrared configuration.
load case 1 = gravity
load case 2 = front wind
load case 3 = side wind

AADTELIH - Horizon pointing, infrared configuration.
load case 1 = gravity
load case 2 = front wind
load case 3 = side wind

AADTELM1 - Modal analysis, optical configuration, 17° off zenith. Both altitude drives effective with equal ("locked rotor") stiffness. Effect of vane preload is not included in these models of the complete telescope. Therefore, to preclude many invalid local vane modes, artificially high bending stiffness (about the weak axis only) was used for vanes. All modes except no. 1 are valid. Mode 1 (secondary rotation about the optical axis) and local vane modes are valid in local vane models (listed below). See body of text for further explanation.

AADTELM2 - Same as AADTELM1 but with only one altitude drive.

OP2NDRY - Modal analysis of secondary vane system with load stiffening effect due to 100,000# preload at each corner, optical configuration. See body of text.

IR2NDRY - Same as OP2NDRY but in the infrared configuration.

FINITE ELEMENT ANALYSIS

SUMMARY OF RESULTS

REVISED 4-11-89

GRAVITY MISALIGNMENTS

(If optics are perfectly aligned at zenith, the following misalignments will develop between the subject optical element and the primary mirror as the O.S.S. is rotated to horizon).

CONFIGURATION/ELEMENT	NET PISTON	NET SAG	NET TILT
Optical/Secondary Mirror	.040 in. 1.016 mm	.011 in. .28 mm	.0029 deg 50 microrad 10 arcsec
Infrared/Secondary Mirror	.027 in.	.0024 in.	.00013 deg 0.48 arcsec
(Both)/Focal Plane	.0056 in.	-	.0029 deg 10.4 arcsec

MAGELLAN PROJECT 8 METER TELESCOPE

GRAVITY MISALIGNMENTS

1,500# VS. 5,000# SECONDARY ASSEMBLY

REVISED 4-11-89

(If optics are perfectly aligned at zenith, the following misalignments will develop between the subject optical element and the primary mirror as the O.S.S. is rotated to horizon)

CONFIGURATION	NET PISTON	NET SAG	NET TILT
5,000# Optical Assy	.040 in. 1.016 mm	.011 in. .28 mm	.0029 deg 50 microrad 10 arcsec
1,500# Optical Assy	.013 in.	.001 in.	.00003 deg 0.11 arcsec

CAUTION:

Some small nominal misalignments result from subtraction of two much larger motions (e.g. primary mirror target net rotation vs. secondary vertex rotation). No tolerance is directly implied by these numbers.

DISPLACEMENTS WITH 1500# (TOTAL) SECONDARY MIRROR ASSEMBLY

REVISED 4-11-89

**** DISPLACEMENT POST-PROCESSING OF ATOZ1.DO

LOAD CASE 1 SCALE FACTOR -1.000E+00

ZENITH GRAVITY GOING AWAY

NODE	GLOBAL X TRANSLATION	GLOBAL Y TRANSLATION	GLOBAL Z TRANSLATION	GLOBAL X ROTATION (DEGREE)	GLOBAL Y ROTATION (DEGREE)	GLOBAL Z ROTATION (DEGREE)
322	-7.2354E-03	1.0416E-02	3.4992E-02	-2.0255E-03	8.7924E-07	2.3795E-04
684	-7.2355E-03	1.3758E-02	4.7572E-02	-2.5845E-03	8.6289E-07	2.3795E-04

**** DISPLACEMENT POST-PROCESSING OF ATOH1.DO

LOAD CASE 1 SCALE FACTOR 1.000E+00

HORIZON GRAVITY APPLIED

NODE	GLOBAL X TRANSLATION	GLOBAL Y TRANSLATION	GLOBAL Z TRANSLATION	GLOBAL X ROTATION (DEGREE)	GLOBAL Y ROTATION (DEGREE)	GLOBAL Z ROTATION (DEGREE)
322	1.9000E-03	2.0099E-03	-5.9910E-02	6.2127E-03	-9.2577E-07	-2.3802E-04
684	1.8990E-03	1.8743E-03	-6.4224E-02	6.7416E-03	-8.9650E-07	-2.3679E-04

NOTES:

NODE 322 - PRIMARY MIRROR TARGET

NODE 684 - SECONDARY MIRROR VERTEX

ATOZ1 / ATOH1 DATA REDUCTION

REVISED 4-11-89

SMG
4-11-9

ROTATING THRU GRAVITY FIELD:

A. NET PISTON:

(ZTXL) LET Z = DUE TO ZENITH GRAVITY GOING AWAY
(YTXL) " H = " " HORIZON " APPLIED

1.) Z: .047572 - .035 = .0126 SEPARATION
H: .00201 - .001874 = .00014 SEPARATION

NET PISTON OPTICAL = .013 IN. SEPARATION

B.) NET SAG:

(YTXL) - "Z"
(ZTXL) - "H"

1.) Z: .013758 - .010416 = .0033 2NDRY ABOVE PMT
H: .064224 - .05991 = .0043 " BELOW "

NET SAG OPTICAL (DECENTER) = .0010 IN. 2NDRY BELOW PMT

C.) NET TILT:

(X ROTN) - "Z"
(" ") - "H"

1.) Z: (.0025845 - .0020255) = - .000559 DEG 2ND. REL/PRI.
H: (.0067416 - .0062127) = + .000529 " " "

NET TILT = -.00003 DEG 2NDRY REL TO PRIMARY

FINITE ELEMENT ANALYSIS

SUMMARY OF RESULTS

REVISED 4-11-89

WIND LOAD DEFLECTIONS

Configuration Attitude/Wind Direction	Primary Pointing Error	2ndary misalignment (Decenter)	(Rotation)
Optical zenith/front wind	.35 microrad .073 arcsec	.00013 in. .0033 mm	.18 microrad .037 arcsec
Infrared zenith/front wind	.33 microrad .069 arcsec	.000154 in. .0039 mm	.076 microrad .016 arcsec
Optical zenith/side wind	.134 microrad .028 arcsec	.000175 in. .0044 mm	.249 microrad .051 arcsec
Infrared zenith/side wind	.13 microrad .027 arcsec	.00019 in. .005 mm	.143 microrad .029 arcsec
Optical horizon/front wind	.40 microrad .082 arcsec	.000142 in. .0036 mm (defocus)	.011 microrad .002 arcsec
Infrared horizon/front wind	.38 microrad .079 arcsec	.000001 in. .000025 mm (defocus)	.012 microrad .0025 arcsec
Optical horizon/side wind	.612 microrad .126 arcsec	.000072 in. .0018 mm	.211 microrad .043 arcsec
Infrared horizon/side wind	.525 microrad .11 arcsec	.000073 in. .0018 mm	.063 microrad .013 arcsec

NATURAL FREQUENCIES AND MODESHAPES

REVISED 4-11-89

Model	Mode	Frequency Hertz	Modeshape Description
AADTELM1	1	(2.7)*	Secondary Rotation, Optical Axis
"	2	7.2	Lateral Translation
"	3	8.6	Locked Rotor Altitude Axis
"	4	11.0	Locked Rotor Azimuth Axis
"	5	12.7	Fore-Aft Translation + Secondary Piston
"	6	14.3	Secondary Piston + Main Plane Lcl
"	7	14.6	Main Plane Lcl + Secondary Piston
"	8	15.4	2nd Main Plane Lcl + Secondary
"	9	17.3	2nd Lateral Translation
"	10	19.5	Diagonal Distortion of O.S.S.
AADTELM2	2	(4.5)^	Locked Rotor Altitude
"	4	(9.6)^	Fore-Aft Translation
OP2NDRY	1	5.2**	Wide Field Secondary Rotation About Optical Axis
"	2	11.7	Infrared Secondary Rotation About Optical Axis
"	3	12.7	Front Vanes "Guitar String"
"	4	12.7	(Orthogonal of Mode 3)
"	5	12.7	(Orthogonal of Mode 3)

*This mode not valid. See Modal Analysis discussion in body of report.

^One altitude drive effective. See Modal Analysis discussion in body of report.

**Maximum possible without antirotation wires. See Modal Analysis discussion in body of report.

(OP2NDRY cont'd)

"	6	12.9	Back Vane Nodes + "Guitar String"
"	7	12.9	(Orthogonal of Mode 6)
"	8	12.9	(Orthogonal of Mode 6)
"	9	13.1	2nd Front Vanes "Guitar String"
"	10	13.9	Secondary Piston
"	11	20.5	2nd Back Vanes
"	12	21.0	(Orthogonal of Mode 11)
"	13	21.0	(Orthogonal of Mode 11)
IR2NDRY	1	5.9	Front Vane Nodes
"	2	6.0	(Orthogonal of Mode 1)
"	3	6.0	(Orthogonal of Mode 1)
"	4	6.0	(Orthogonal of Mode 1)
"	5	10.4	Secondary Rotation, Optical Axis
"	6	11.6	Back Vane Nodes
"	7	11.6	(Orthogonal of Mode 6)
"	8	11.6	(Orthogonal of Mode 6)
"	9	14.0	Front Vanes "Guitar String"
"	10	14.2	(Orthogonal of Mode 9)
"	11	14.2	(Orthogonal of Mode 9)
"	12	14.2	(Orthogonal of Mode 9)
"	13	16.4	Secondary Piston

FINITE ELEMENT ANALYSIS

LIST OF FIGURES

FIGURE 1 - Model AADTELM1 dimetric view of entire model at 17 degrees off zenith.

FIGURE 2 - Side view of model AADTELOH (optical configuration, horizon pointing.

FIGURE 3 - Front view of model AADTELOH.

FIGURE 4 - Front quartering view of primary mirror cell, with hidden lines removed. Perimeter structure in this intermediate level model was artificially thick to simplify model. Detail design modelling should include some optimization of this property to potentially reduce the size of the structure.

FIGURE 5 - Back quartering view of primary mirror cell.

FIGURE 6 - Mirror cell radial webs to assure that front and back plates of cell are effective. Optimization of these should be done in the detail design modelling to maximize cell stiffness/weight ratio.

FIGURE 7 - Circumferential stiffening plates to limit local deflection of front and back plates of cell. This might be accomplished more efficiently in the real telescope by the use of local stiffeners on the inside surfaces of the front and back plates of the cell.

FIGURE 8 - Primary mirror target at the optical (node 322) and infrared (node 658) mirror vertices. These rigid, weightless beams provide a point of reference for determining relative motion of the primary and secondary mirrors, but are mounted to the cell in such a way that they do not stiffen it.

FIGURE 9 - Instrument (node 321), instrument mounting base (node 320), and focal plane (node 657) give references for relative motions of these elements. Mounted on rigid, weightless beams with nodal loads applied at their appropriate c.g.'s, these simplified members do not include deflection effects of the instrument mounting base or instrument.

FIGURE 10 - Altitude disks were modelled with beam elements representing the effective structural properties of the real fabricated box members. Nodes 3 and 40 are support points for the primary mirror cell.

FIGURE 11 - Truss main plane weldments have additional nodal loads applied to represent the substantial machined pads that will be necessary at all bolted joints.

FIGURE 12 - Lateral braces which connect the two altitude disks and one main plane weldment have been optimized considerably and are very significant in limiting the lateral translation vibration mode to an acceptable level.

FIGURE 13 - The secondary main truss, including square frame, are pure axially-loaded members and thus can be small in diameter for low wind area. These members have considerably more exposure to wind than the lower primary support structure.

FIGURE 14 - The "universal vane system" can support either or both secondary assemblies, eliminate the need for an "exchangeable top end", with proper pretension have acceptable modal performance, and yet offer a very small sail area to the wind.

FIGURE 15 - The secondary assemblies were modelled with rigid, weightless structures with nodal loads/masses applied to represent the real mirrors, mirror cells, chopping assemblies, etc.

FIGURE 16 - The support system shown defines both the azimuth and altitude axes as well as modelling the "locked rotor" stiffnesses of the drives. Hydrostatic pad spring rates are included within the structural properties of these members.

FIGURE 17 - The azimuth disk carries only in-plane loads and stresses, and thus could be modelled as a 1" thick (2" in areas of local high stress) plate. This represents a real structure which would have 1/2" thick top and bottom plates which are separated by a small distance; 18" or 24", for example. Nodal masses were distributed to represent the dead weight of internal bulkheads and stiffeners, as well as heavy fittings at the hydrostatic pad locations.

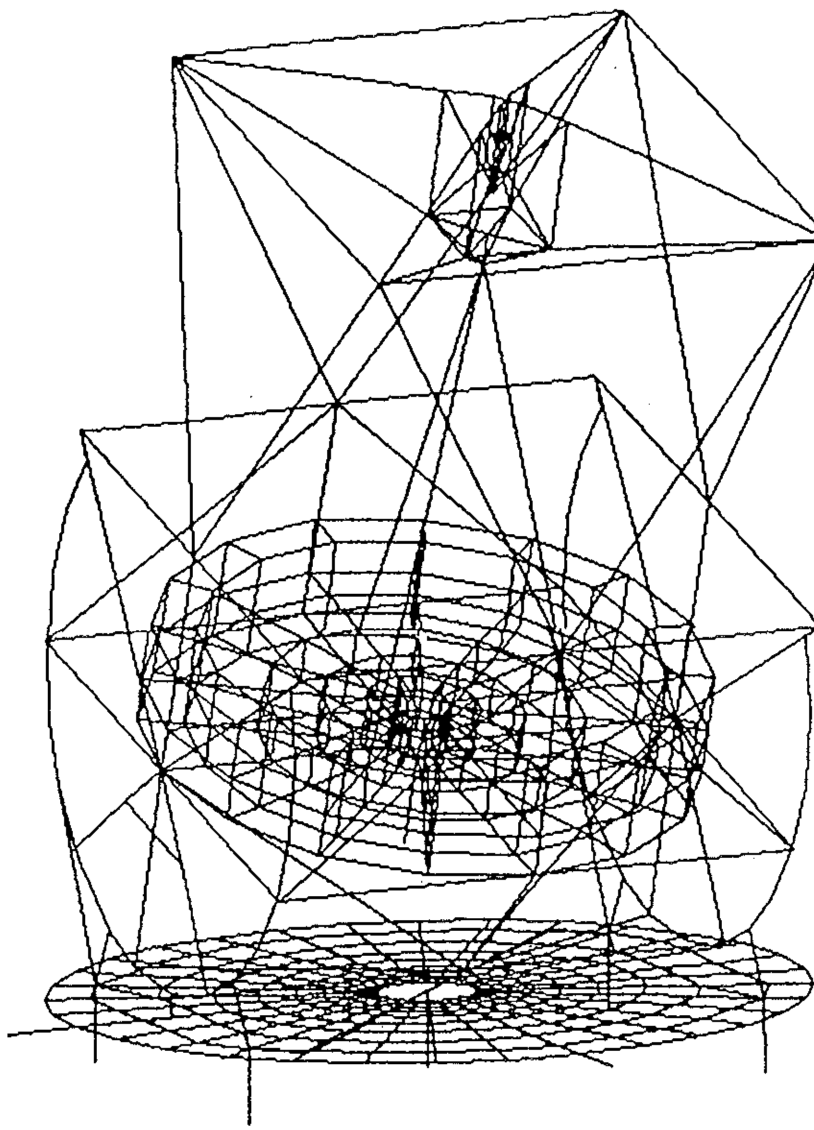

FIGURE 1

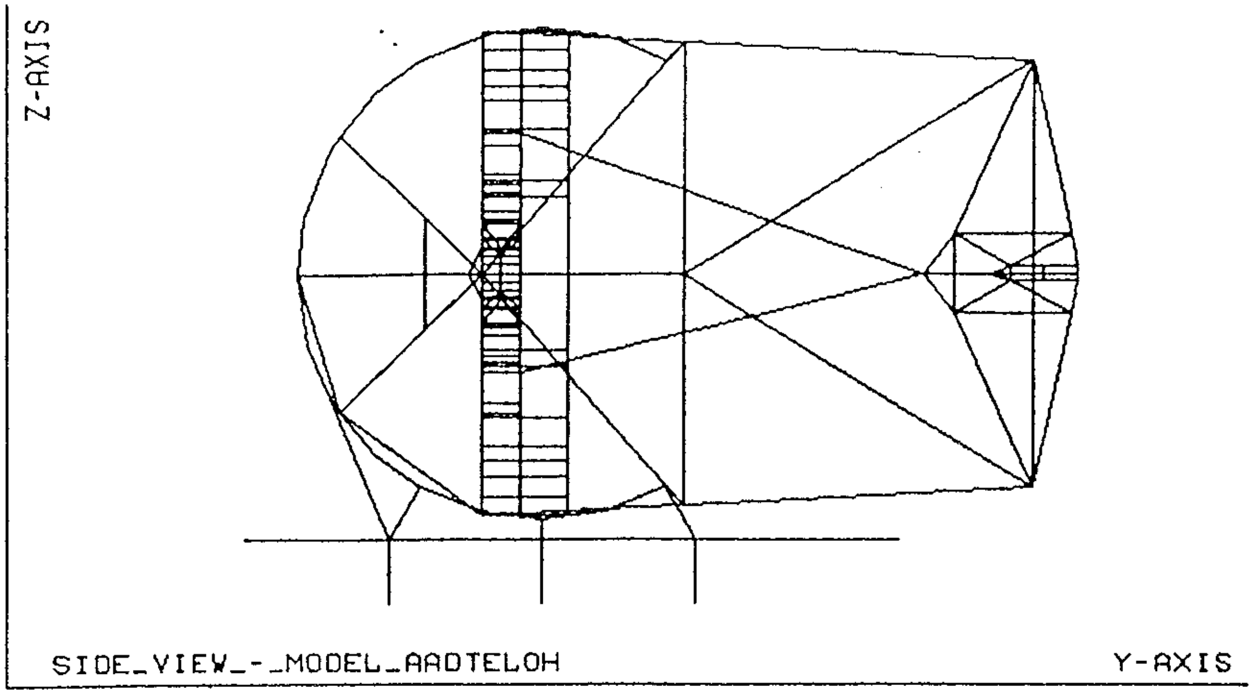

FIGURE 2

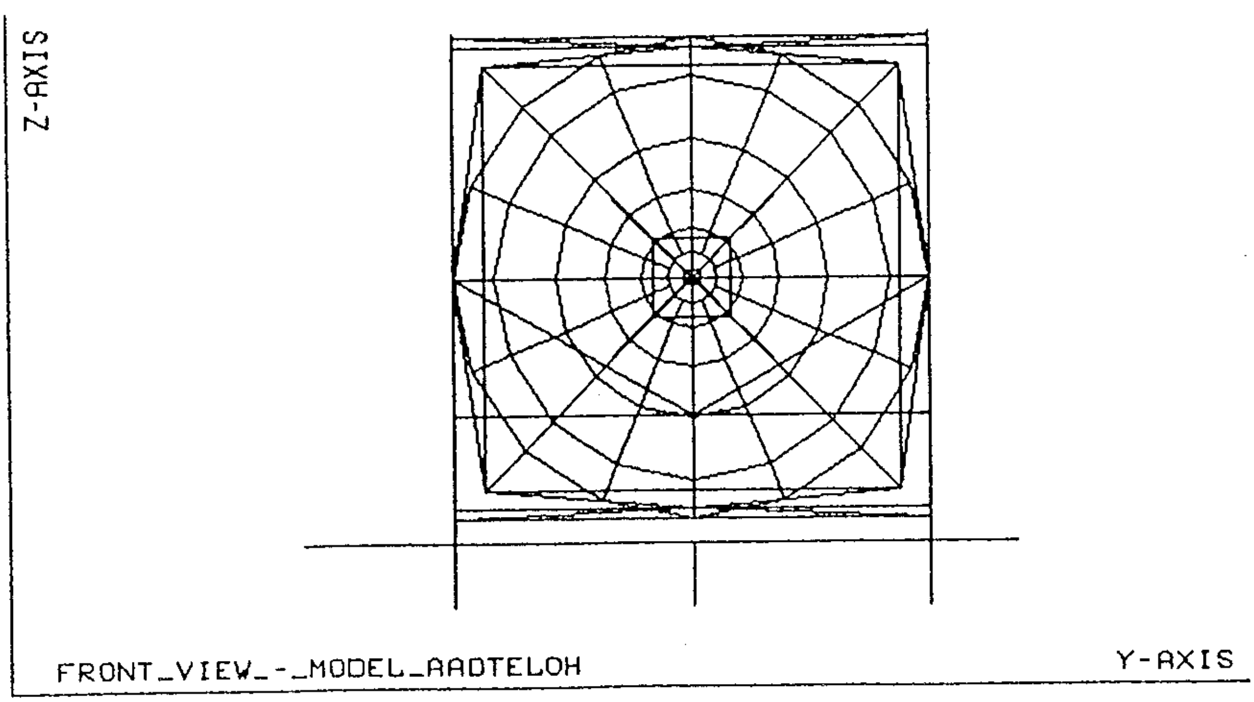

FIGURE 3

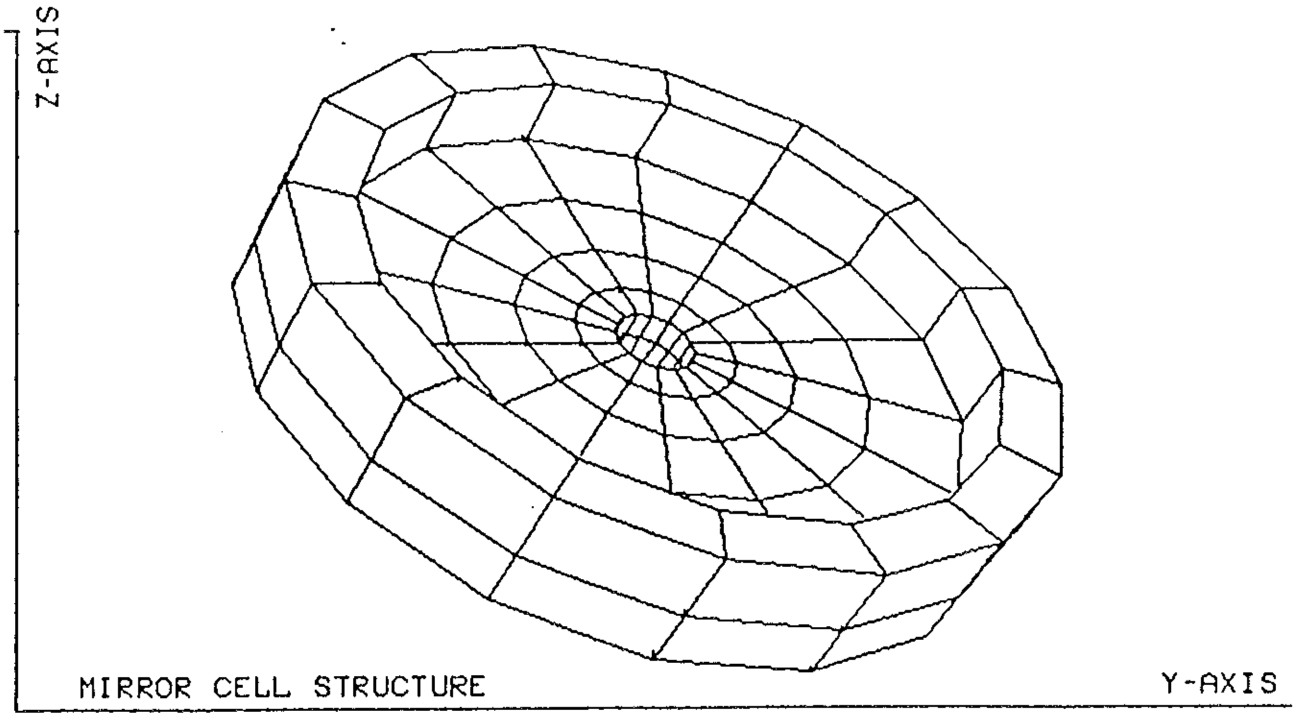

FIGURE 4

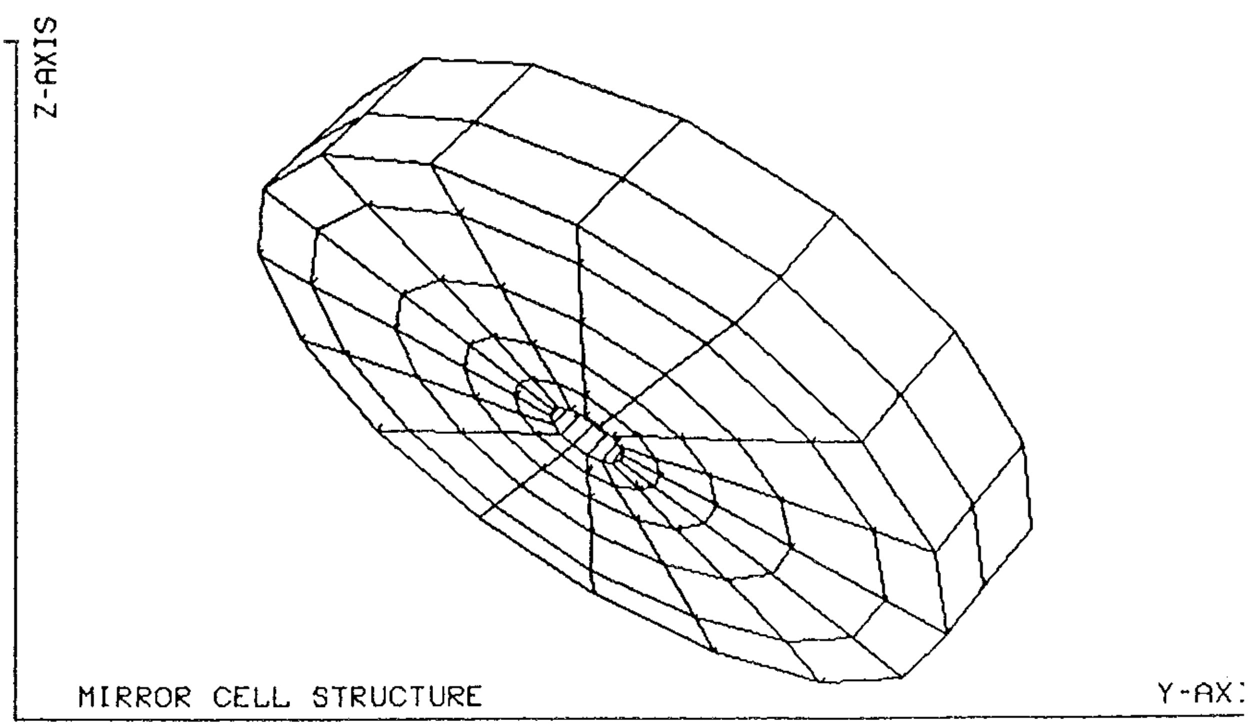

FIGURE 5

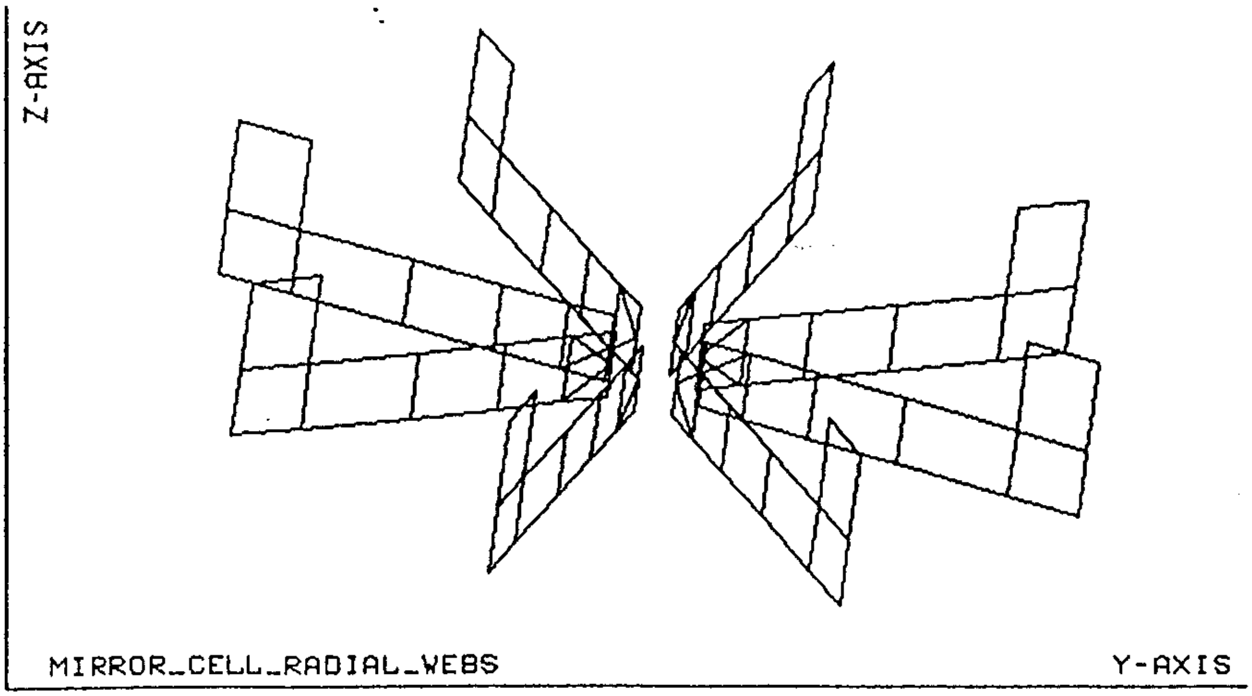

FIGURE 6

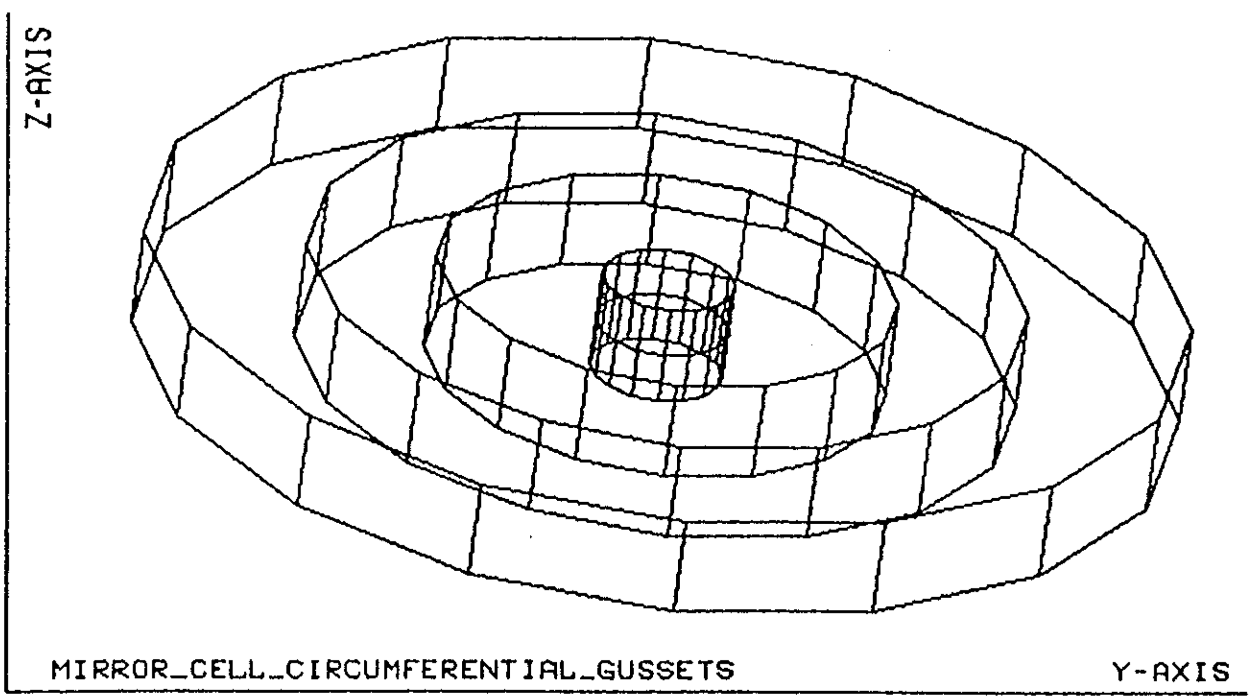

FIGURE 7

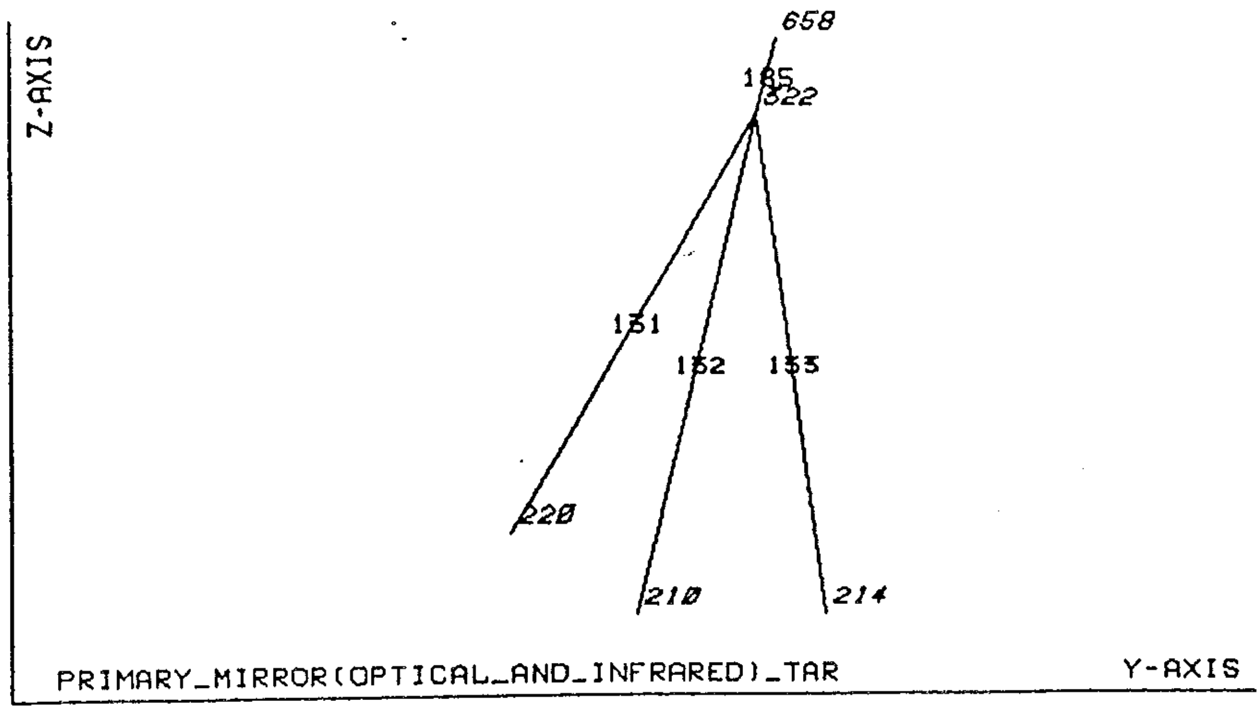

FIGURE 8

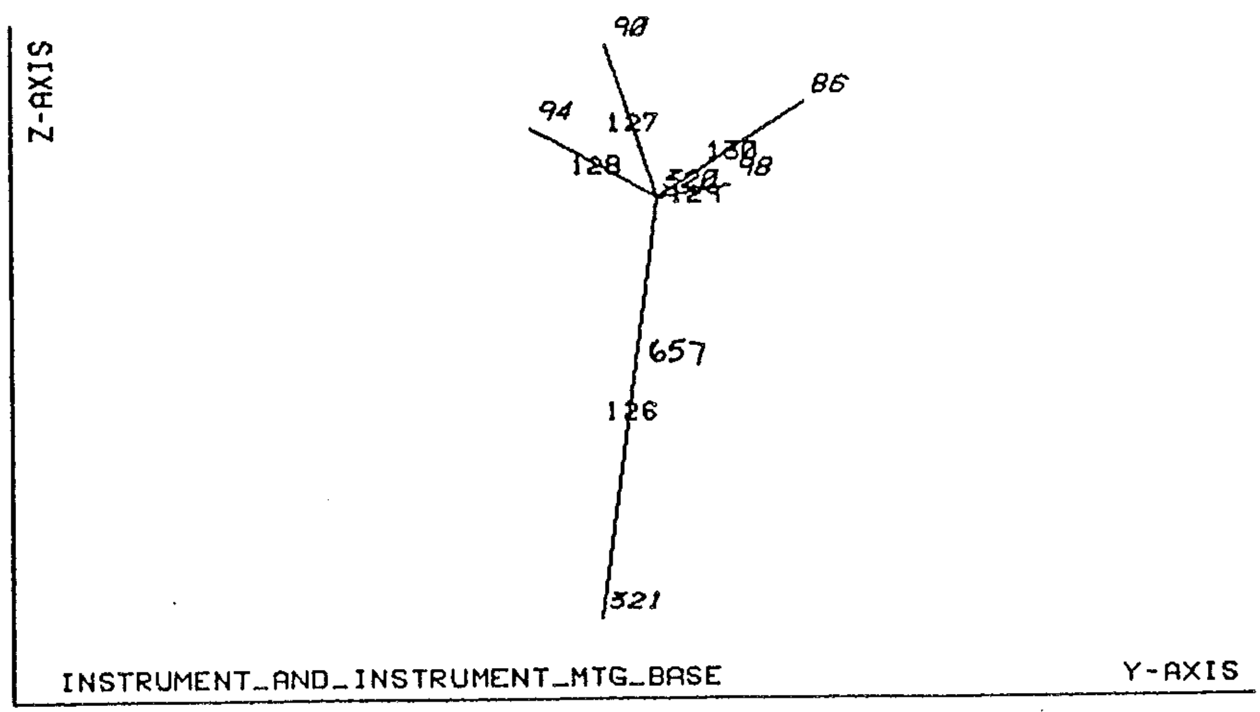

FIGURE 9

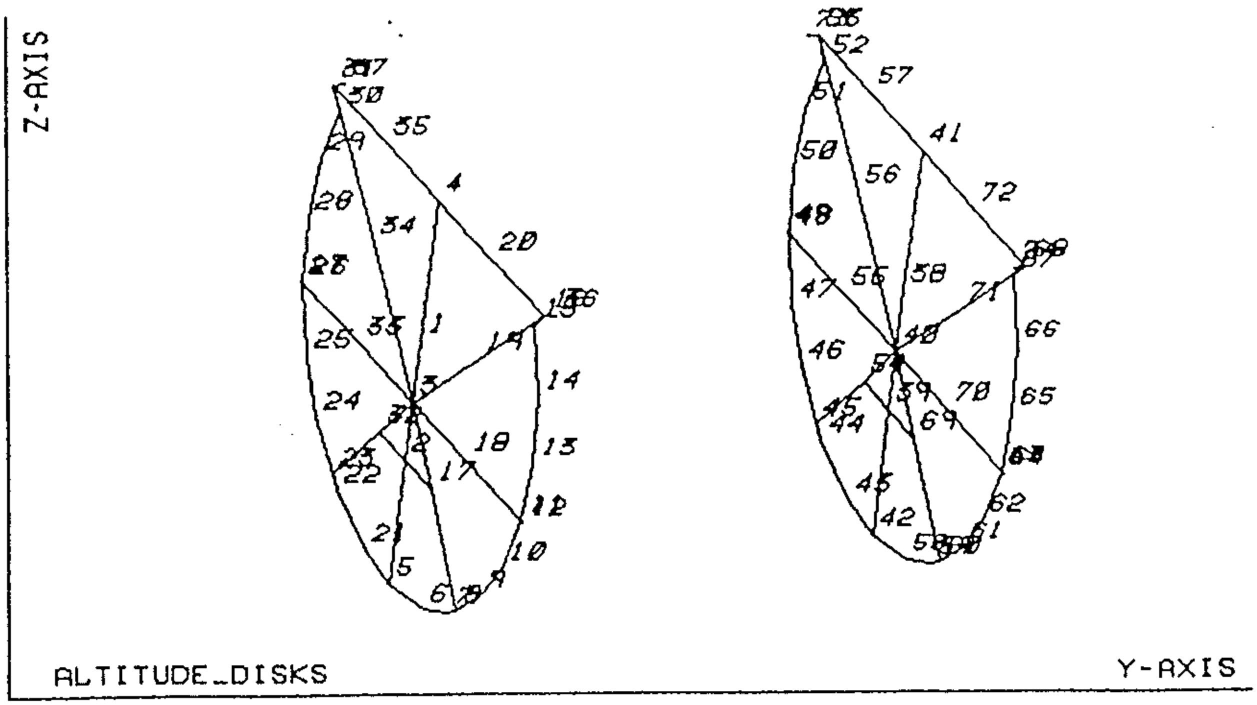

FIGURE 10

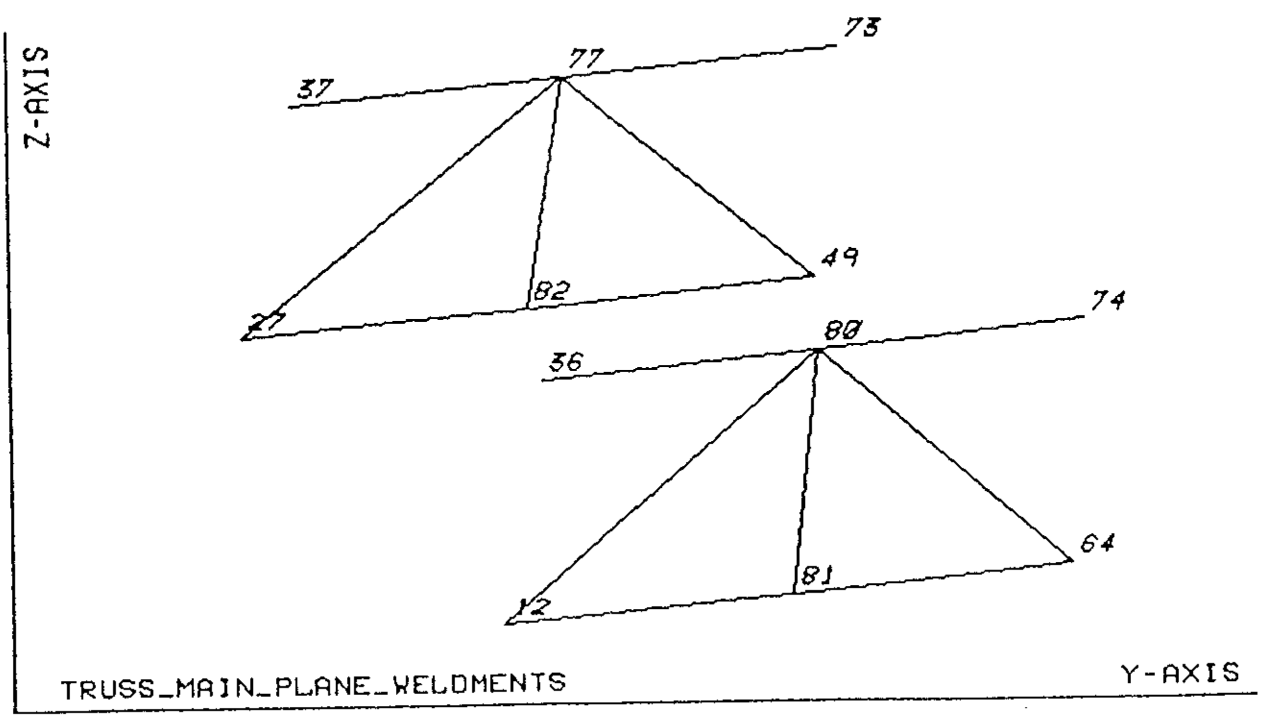

FIGURE 11

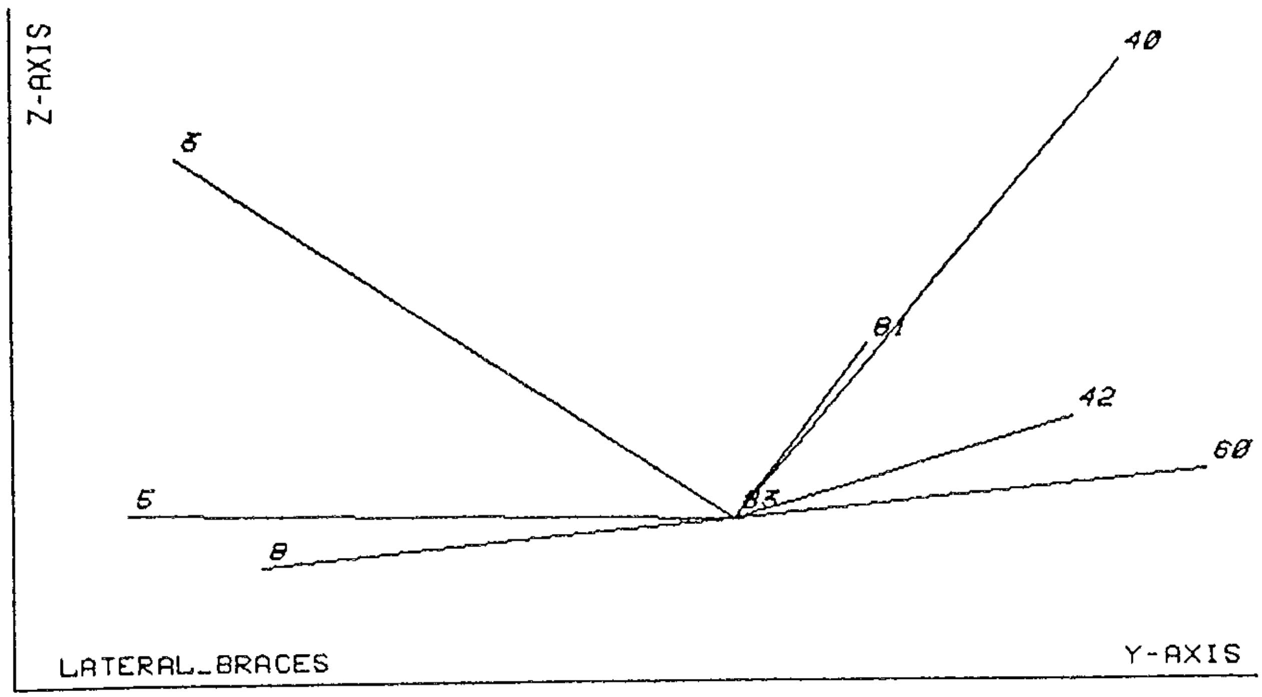

FIGURE 12

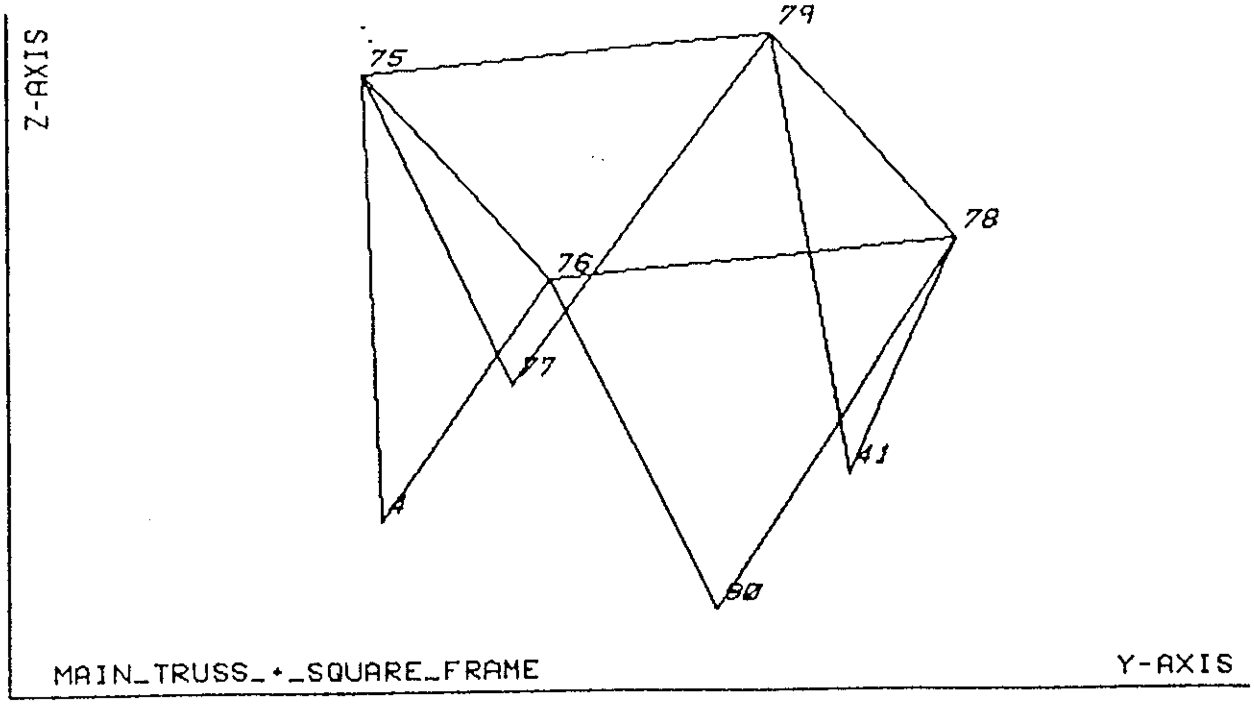

FIGURE 13

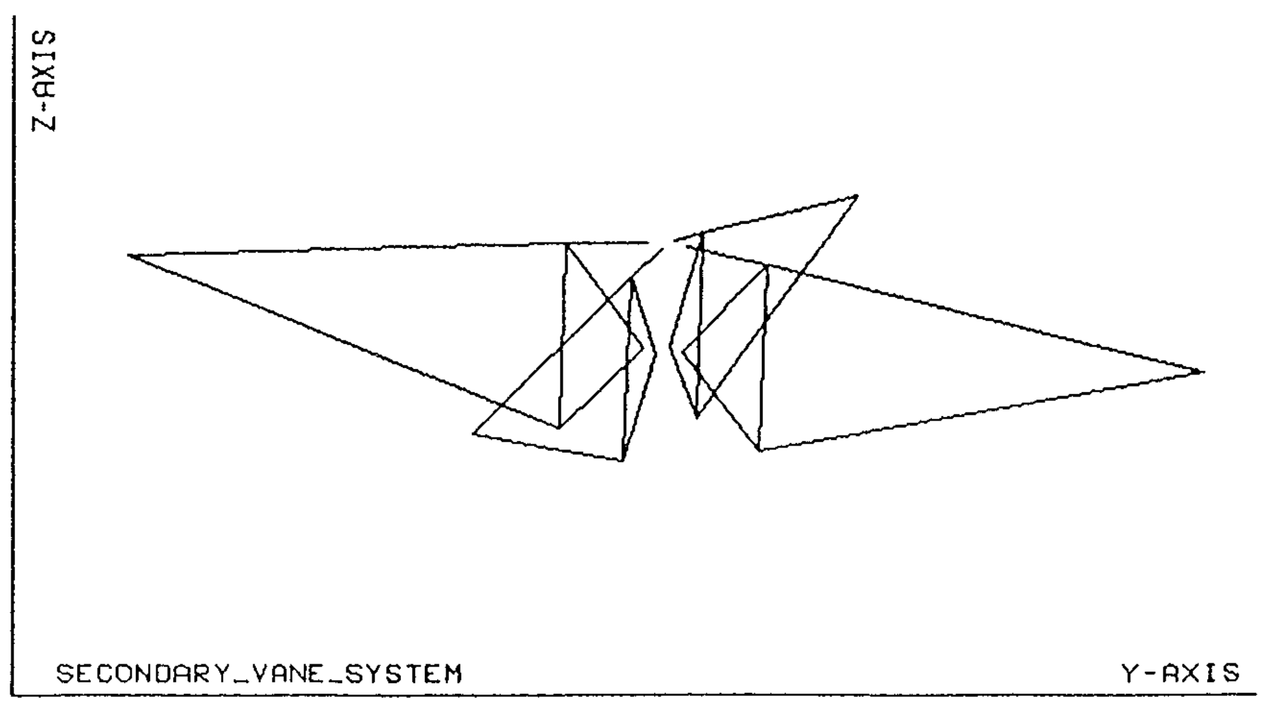

FIGURE 14

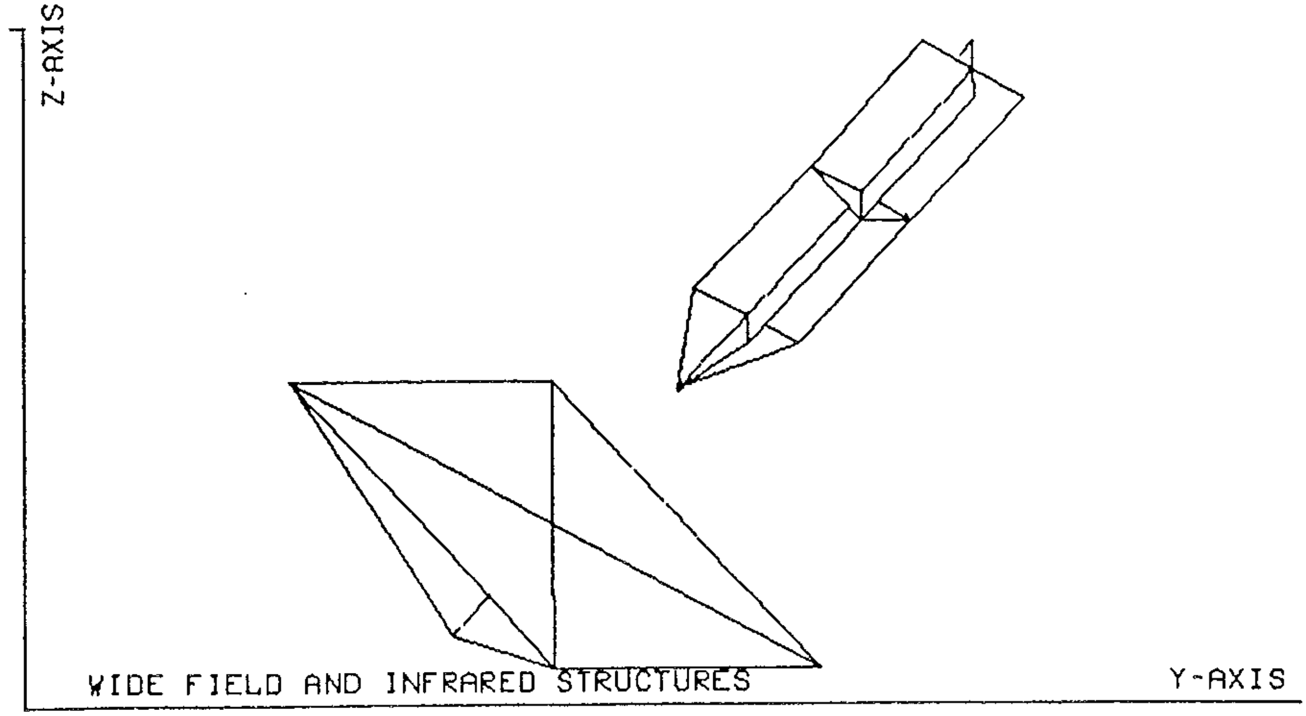

FIGURE 15

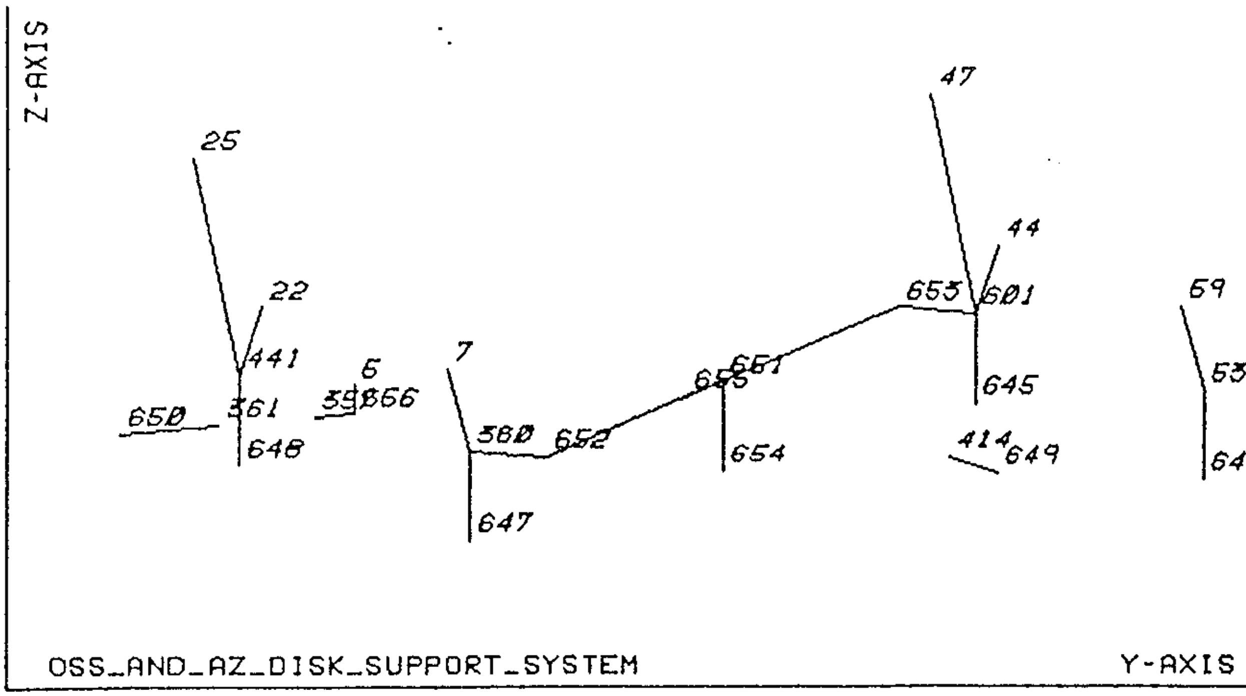

FIGURE 16

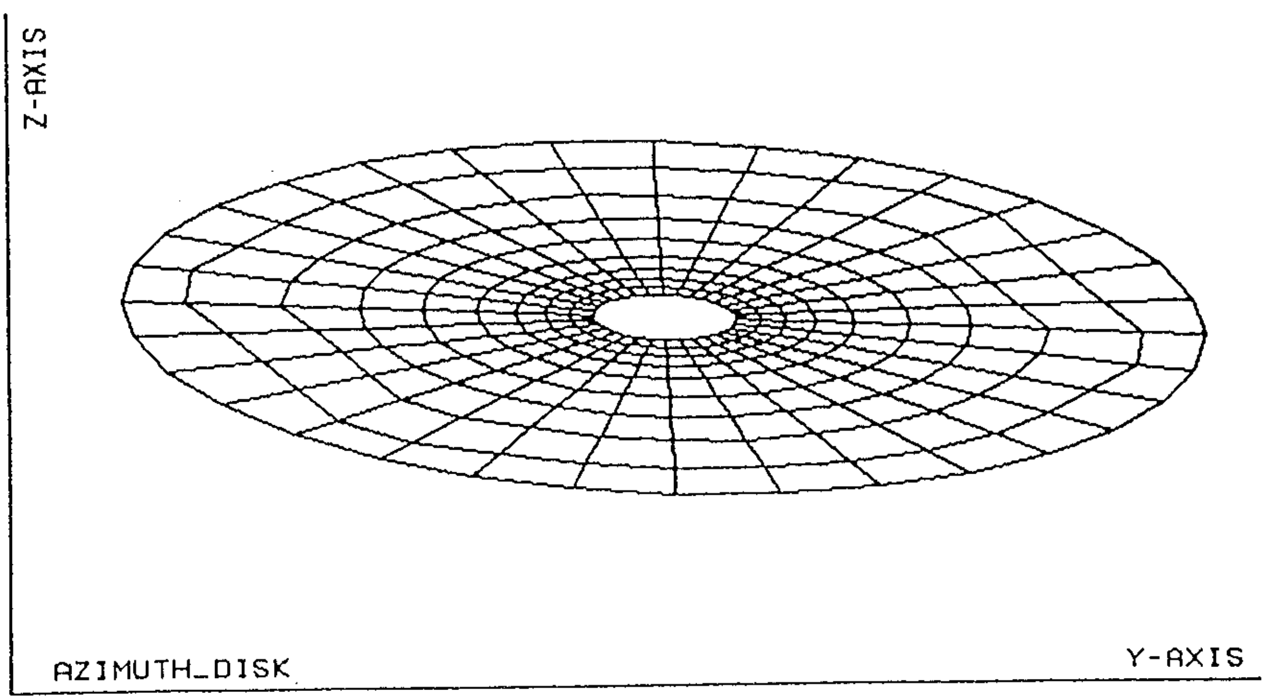

FIGURE 17

AADTEL ___ DATA REDUCTION 1/6

REVISED 4-11-89

SMG
4-11-9

I. ROTATING THRU GRAVITY FIELD (Z TO H)

A.) NET PISTON

(ZTXL) LET Z = DUE TO ZENITH GRAVITY GOING AWAY
(YTXL) " H = " " HORIZON " APPLIED

1.) OPTICAL (NODE 684 VS PMT 322)
Z: .075112 - .035259 = .0399 IN. SEPARATION
H: .001795 - .001662 = .00013 "

NET PISTON OPTICAL = .040 IN. SEPARATION

2.) I.R. (NODE 682 VS 322 PMT)
Z: .06118 - .034877 = .0263 IN. SEPARATION
H: .0021024 - .0019543 = .00015 " "

NET PISTON IR = .027 IN. SEPARATION

3.) FOCAL PLANE (NODE 657 VS PMT 322)
Z: .040735 - .035259 = .00558 IN. APPROACH
H: .001795 - .0016619 = .000133 IN. "

NET PISTON FOCAL PLANE VS. P.M. VERTEX = .0056 IN. APPROACH

B.) NET SAG:

(YTXL) - "Z"
(ZTXL) - "H"

1.) OPTICAL (NODE 684 VS 322 PMT)
Z: .014033 - .010533 = .0035 2ND ABOVE PMT
H: .076661 - .062039 = .01462 " BELOW "

NET SAG OPTICAL = .011 IN. 2NDARY BELOW PMT

SMG
4-11-89

AADTEL ___ DATA REDUCTION 2/6

REVISED 4-11-89

I. B.) NET SAG (CONT'D):

2.) I.R. (NODE 682 VS 322 PMT)
YTXL Z: .016032 - .010366 = .00567 2ND ABOVE PMT
ZTXL H: .067111 - .059 = .00811 " BELOW "

NET SAG IR = .0024 IN. 2NDRY BELOW PMT

C.) NET TILT:

(X-ROTN) - "Z" & "H"

1.) OPTICAL: (NODE 684 VS 322 PMT)
Z: 2.6177E-3 - 2.0466E-3 = -.0005711 DEG 2ND REL PRI
H: (6.5266 - 4.2516) E-3 -.002275 " " " "

NET TILT OPTICAL = -.00285 DEG 2NDRY REL PRI

2.) IR: (NODE 682 VS 322 PMT)
(X-ROTN) Z: (2.5517 - 2.0164) E-3 = -.000535 DEG 2ND REL PRI
" " H: (6.7465 - 6.0779) E-3 = +.000669 " " " "

NET TILT IR = +.000134 DEG 2NDRY REL TO PMT

3.) FOCAL PLANE (NODE 657 VS 322 PMT)

Z: -(2.6693 - 2.0466) E-3 = -.000623 DEG FP REL PMT
H: -(6.5266 - 4.2516) E-3 = -.002275 " " " "

NET TILT FOCAL PLANE = -.0029 DEG F.P. REL P.M.

AADTEL — DATA REDUCTION 3/6

REVISED 4-11-89

SMG
4-11-9

II. ZENITH FRONT WIND

A. PRIMARY POINTING ERROR
(NODE 322 XROTN) = 2.0242E-5 DEG
.353 μRAD
.073 SEC⁻¹
} PRIMARY POINTING ERROR

B. OPTICAL DECENTER (NODE 684 VS 322 PMT YTXL)
(2.8179 - 1.519)E-4 = .00013 IN. OPTICAL DECENTER

C. IR DECENTER (NODE 682 VS 322 PMT YTXL)
(2.9695 - 1.4293)E-4 = .000154 IN. IR DECENTER

D. OPTICAL NET ROTN (NODE 684 VS 322 PMT XROTN)
-(3.0565 - 2.0242)E-5 = -.0000103 DEG
-.18 μRAD
-.037 ARCSEC
} OPTICAL NET ROTN 2NDRY REL P.M.

E. IR NET ROTN (NODE 682 VS 322 PMT XROTN)
-(2.3409 - 1.9075)E-5 = -.0000043 DEG
-.076 μRAD
-.016 ARCSEC
} IR NET ROTN 2NDRY REL P.M.

AADTEL ___ DATA REDUCTION 4/6

REVISED 4-11-89

SMG

III. ZENITH SIDE WIND

A. PRIMARY POINTING ERROR (NODE 322 YROTN)

= 7.662 E-6 DEG
.134 μRAD
.028 ARCSEC
} PRIMARY POINTING ERROR

B. OPTICAL DECENTER (NODE 684 VS 322 PMT XTXL)

(4.6782 - 2.9281) E-4 = .000175 IN. OPTICAL DECENTER

C. IR DECENTER (NODE 682 VS 322 PMT XTXL)

(4.775 - 2.8717) E-4 = .00019 IN. IR DECENTER

D. OPTICAL NET ROTN (NODE 684 VS 322 PMT YROTN)

(2.192 - .76621) E-5 = 1.426 E-5 DEG
.249 μRAD
.051 ARCSEC
} OPTICAL NET ROTN

E. IR NET ROTN (NODE 682 VS 322 PMT) YROTN

1.5647 E-5 - 7.4683 E-6 = 8.18 E-6 DEG
.143 μRAD
.029 ARCSEC
} I.R. NET ROTN

AADTEL ___ DATA REDUCTION 5/6

REVISED 4-11-89

SMG
4-11-9

IV. HORIZON FRONT WIND:

A.) PRIMARY POINTING ERROR (NODE 322 X ROTN)

= 2.2907 E-5 DEG
0.4 μRAD
.082 ARCSEC
} PRIMARY POINTING ERROR

B.) OPTICAL DECENTER (NODE 684 VS 322 PMT ZTXL)

1.2619E-4 - 7.7261E-5 = 4.89 E-5 IN. OPTICAL DECENTER

C.) OPTICAL DEFOCUS (NODE 684 VS 322 PMT YTXL)

(3.8797 - 2.4548) E-4 = .000142 IN. OPTICAL DEFOCUS

D.) OPTICAL NET ROTN (NODE 684 VS 322 PMT X ROTN)

(2.2907 - 2.2302) E-5 = 6.05 E-7 DEG
.011 μRAD
.002 ARCSEC
} OPTICAL NET ROTN

E.) IR DECENTER (NODE 682 VS 322 ZTXL)

1.2087E-4 - 9.3927 E-5 = 2.69 E-5 IN. IR DECENTER

F.) IR DEFOCUS (NODE 682 VS 322 PMT YTXL)

(2.3838 - 2.3734) E-4 = 1 E-6 IN. IR DEFOCUS

G.) IR NET ROTN (NODE 682 VS 322 PMT X ROTN)

(2.1942 - 2.1249) E-5 = 6.9 E-7 DEG
.012 μRAD
.0025 ARCSEC
} IR NET ROTN

AADTEL ____ DATA REDUCTION

6/6

REVISED 4-11-89

SMG
4-11-9

V. HORIZON SIDE WIND:

A) PRIMARY POINTING ERROR (NODE 322 ZROTN)

= 3.5074 E-5 DEG
.612 μRAD
.126 ARCSEC
} PRIMARY POINTING ERROR

B) OPTICAL DECENTER (NODE 684/322 X TXL)

(5.8815 - 5.1645) E-4 = 7.17 E-5 IN. OPTICAL DECENTER

C) IR DECENTER (NODE 682/322 XTXL)

(5.4298 - 4.7033) E-4 = 7.265 E-5 IN. IR DECENTER

D) OPTICAL NET ROTN (NODE 684/322 Z ROTN)

(4.7149 - 3.5074) E-5 = 1.208 E-5 DEG
.211 μRAD
.043 ARCSEC
} OPTICAL NET ROTN

E) IR NET ROTN (NODE 682/322 ZROTN)

(3.0064 - 2.6443) E-5 = 3.62 E-6 DEG
.063 μRAD
.013 ARCSEC
} IR NET ROTN

REVISION 4-11-89

**** DISPLACEMENT POST-PROCESSING OF AADTELOZ.DO

LOAD CASE 1 SCALE FACTOR -1.000E+00

ZENITH GRAVITY GOING AWAY

NODE	GLOBAL X TRANSLATION	GLOBAL Y TRANSLATION	GLOBAL Z TRANSLATION	GLOBAL X ROTATION (DEGREE)	GLOBAL Y ROTATION (DEGREE)	GLOBAL Z ROTATION (DEGREE)
322	-7.3366E-03	1.0533E-02	3.5259E-02	-2.0466E-03	8.7800E-07	2.4059E-04
657	-7.3427E-03	-4.2704E-03	4.0735E-02	-2.6693E-03	8.6661E-07	2.4059E-04
684	-7.3368E-03	1.4033E-02	7.5112E-02	-2.6177E-03	8.6150E-07	2.4059E-04

**** DISPLACEMENT POST-PROCESSING OF AADTELOZ.DO

LOAD CASE 2 SCALE FACTOR 1.000E+00

ZENITH FRONT WIND

NODE	GLOBAL X TRANSLATION	GLOBAL Y TRANSLATION	GLOBAL Z TRANSLATION	GLOBAL X ROTATION (DEGREE)	GLOBAL Y ROTATION (DEGREE)	GLOBAL Z ROTATION (DEGREE)
322	-6.1146E-06	1.5190E-04	3.9303E-06	-2.0242E-05	-3.0393E-10	9.8457E-08
657	-6.1125E-06	1.2550E-05	3.9238E-06	-2.0290E-05	-3.2401E-10	9.8456E-08
684	-6.1150E-06	2.8179E-04	4.4008E-06	-3.0565E-05	-3.3005E-10	9.8463E-08

**** DISPLACEMENT POST-PROCESSING OF AADTELOZ.DO

LOAD CASE 3 SCALE FACTOR 1.000E+00

ZENITH SIDE WIND

NODE	GLOBAL X TRANSLATION	GLOBAL Y TRANSLATION	GLOBAL Z TRANSLATION	GLOBAL X ROTATION (DEGREE)	GLOBAL Y ROTATION (DEGREE)	GLOBAL Z ROTATION (DEGREE)
322	2.9281E-04	-3.4452E-05	-1.4886E-05	7.3448E-06	7.6621E-06	-1.5544E-06
657	2.3906E-04	1.7580E-05	-1.3726E-05	7.8744E-06	7.6234E-06	-1.4986E-06
684	4.6782E-04	-1.6977E-05	-9.6031E-06	6.5104E-06	2.1920E-05	-1.8249E-06

NOTES:

NODE 322 - PRIMARY MIRROR TARGET
NODE 657 - FOCAL PLANE
NODE 684 - OPTICAL SECONDARY VERTEX

REVISION 4-11-89

**** DISPLACEMENT POST-PROCESSING OF AADTELOH.DO

LOAD CASE 1 SCALE FACTOR 1.000E+00

HORIZON GRAVITY DEVELOPING

NODE	GLOBAL X TRANSLATION	GLOBAL Y TRANSLATION	GLOBAL Z TRANSLATION	GLOBAL X ROTATION (DEGREE)	GLOBAL Y ROTATION (DEGREE)	GLOBAL Z ROTATION (DEGREE)
322	2.0594E-03	1.7950E-03	-6.2039E-02	6.5266E-03	-9.2543E-07	-2.4067E-04
657	3.7166E-03	1.6497E-03	-2.1984E-02	-2.0165E-04	-9.2661E-07	-2.4066E-04
684	2.0583E-03	1.6619E-03	-7.6661E-02	4.2516E-03	-8.9586E-07	-2.3943E-04

**** DISPLACEMENT POST-PROCESSING OF AADTELOH.DO

LOAD CASE 2 SCALE FACTOR 1.000E+00

HORIZON FRONT WIND

NODE	GLOBAL X TRANSLATION	GLOBAL Y TRANSLATION	GLOBAL Z TRANSLATION	GLOBAL X ROTATION (DEGREE)	GLOBAL Y ROTATION (DEGREE)	GLOBAL Z ROTATION (DEGREE)
322	3.4356E-06	2.4548E-04	1.2619E-04	-2.2907E-05	-5.1744E-10	-8.1308E-07
657	9.0346E-06	2.6159E-04	-3.0449E-05	-2.1797E-05	-5.1968E-10	-8.1309E-07
684	3.4314E-06	3.8797E-04	7.7261E-05	-2.2302E-05	-5.0067E-10	-8.0894E-07

**** DISPLACEMENT POST-PROCESSING OF AADTELOH.DO

LOAD CASE 3 SCALE FACTOR 1.000E+00

HORIZON SIDE WIND

NODE	GLOBAL X TRANSLATION	GLOBAL Y TRANSLATION	GLOBAL Z TRANSLATION	GLOBAL X ROTATION (DEGREE)	GLOBAL Y ROTATION (DEGREE)	GLOBAL Z ROTATION (DEGREE)
322	5.1645E-04	5.5318E-06	-2.5453E-05	3.7773E-06	1.7442E-05	3.5074E-05
657	2.8561E-04	4.9409E-06	9.4868E-07	4.2499E-06	1.7577E-05	2.8565E-05
684	5.8815E-04	5.9137E-06	-1.5992E-05	4.7061E-06	2.3482E-05	4.7149E-05

NOTES:
NODE 322 - PRIMARY MIRROR TARGET
NODE 675 - FOCAL PLANE
NODE 684 - OPTICAL SECONDARY VERTEX

REVISION 4-11-89

**** DISPLACEMENT POST-PROCESSING OF AADTELIZ.DO

LOAD CASE 1 SCALE FACTOR -1.000E+00

ZENITH GRAVITY GOING AWAY

NODE	GLOBAL X TRANSLATION	GLOBAL Y TRANSLATION	GLOBAL Z TRANSLATION	GLOBAL X ROTATION (DEGREE)	GLOBAL Y ROTATION (DEGREE)	GLOBAL Z ROTATION (DEGREE)
322	-7.1915E-03	1.0366E-02	3.4877E-02	-2.0164E-03	8.7988E-07	2.3681E-04
657	-7.1975E-03	-4.2119E-03	4.0374E-02	-2.6224E-03	8.6852E-07	2.3681E-04
682	-7.1908E-03	1.6032E-02	6.1180E-02	-2.5517E-03	8.5749E-07	2.3681E-04

**** DISPLACEMENT POST-PROCESSING OF AADTELIZ.DO

LOAD CASE 2 SCALE FACTOR 1.000E+00

ZENITH FRONT WIND

NODE	GLOBAL X TRANSLATION	GLOBAL Y TRANSLATION	GLOBAL Z TRANSLATION	GLOBAL X ROTATION (DEGREE)	GLOBAL Y ROTATION (DEGREE)	GLOBAL Z ROTATION (DEGREE)
322	-5.7989E-06	1.4293E-04	3.6981E-06	-1.9075E-05	-2.8492E-10	9.4033E-08
657	-5.7969E-06	1.1614E-05	3.6925E-06	-1.9120E-05	-3.0422E-10	9.4031E-08
682	-5.7995E-06	2.9695E-04	4.1443E-06	-2.3409E-05	-3.0761E-10	9.4038E-08

**** DISPLACEMENT POST-PROCESSING OF AADTELIZ.DO

LOAD CASE 3 SCALE FACTOR 1.000E+00

ZENITH SIDE WIND

NODE	GLOBAL X TRANSLATION	GLOBAL Y TRANSLATION	GLOBAL Z TRANSLATION	GLOBAL X ROTATION (DEGREE)	GLOBAL Y ROTATION (DEGREE)	GLOBAL Z ROTATION (DEGREE)
322	2.8717E-04	-3.3903E-05	-1.4649E-05	7.2278E-06	7.4683E-06	-1.5418E-06
657	2.3478E-04	1.7300E-05	-1.3508E-05	7.7489E-06	7.4539E-06	-1.4892E-06
682	4.7750E-04	-2.2669E-05	-9.3570E-06	6.3698E-06	1.5647E-05	-1.8096E-06

NOTES: NODE 322 - PRIMARY MIRROR TARGET
NODE 657 - FOCAL PLANE
NODE 682 - INFRARED SECONDARY VERTEX

REVISION 4-11-89

**** DISPLACEMENT POST-PROCESSING OF AADTELIH.DO

LOAD CASE 1 SCALE FACTOR 1.000E+00

HORIZON GRAVITY APPLIED

NODE	GLOBAL X TRANSLATION	GLOBAL Y TRANSLATION	GLOBAL Z TRANSLATION	GLOBAL X ROTATION (DEGREE)	GLOBAL Y ROTATION (DEGREE)	GLOBAL Z ROTATION (DEGREE)
322	1.8320E-03	2.1024E-03	-5.8997E-02	6.0779E-03	-9.2626E-07	-2.3689E-04
657	3.4632E-03	1.9539E-03	-2.2024E-02	-6.4679E-04	-9.2737E-07	-2.3688E-04
682	1.6116E-03	1.9543E-03	-6.7111E-02	6.7465E-03	-8.9764E-07	-2.3403E-04

**** DISPLACEMENT POST-PROCESSING OF AADTELIH.DO

LOAD CASE 2 SCALE FACTOR 1.000E+00

HORIZON FRONT WIND

NODE	GLOBAL X TRANSLATION	GLOBAL Y TRANSLATION	GLOBAL Z TRANSLATION	GLOBAL X ROTATION (DEGREE)	GLOBAL Y ROTATION (DEGREE)	GLOBAL Z ROTATION (DEGREE)
322	3.2299E-06	2.3734E-04	1.2087E-04	-2.1942E-05	-4.9549E-10	-7.7951E-07
657	8.5977E-06	2.5352E-04	-2.9186E-05	-2.0891E-05	-4.9762E-10	-7.7952E-07
682	2.5040E-06	2.3838E-04	9.3927E-05	-2.1249E-05	-4.7965E-10	-7.7015E-07

**** DISPLACEMENT POST-PROCESSING OF AADTELIH.DO

LOAD CASE 3 SCALE FACTOR 1.000E+00

HORIZON SIDE WIND

NODE	GLOBAL X TRANSLATION	GLOBAL Y TRANSLATION	GLOBAL Z TRANSLATION	GLOBAL X ROTATION (DEGREE)	GLOBAL Y ROTATION (DEGREE)	GLOBAL Z ROTATION (DEGREE)
322	4.7033E-04	5.3878E-06	-2.4315E-05	3.6031E-06	1.6111E-05	3.0064E-05
657	2.7343E-04	4.8314E-06	8.6551E-07	4.0482E-06	1.6245E-05	2.4000E-05
682	5.4298E-04	5.7069E-06	-1.9576E-05	4.4414E-06	2.1511E-05	2.6443E-05

NOTES: NODE 322 - PRIMARY MIRROR TARGET
NODE 657 - FOCAL PLANE
NODE 682 - INFRARED SECONDARY VERTEX

A	REVISED SECONDARY SPRT TO UNIVERSAL VANE SYS

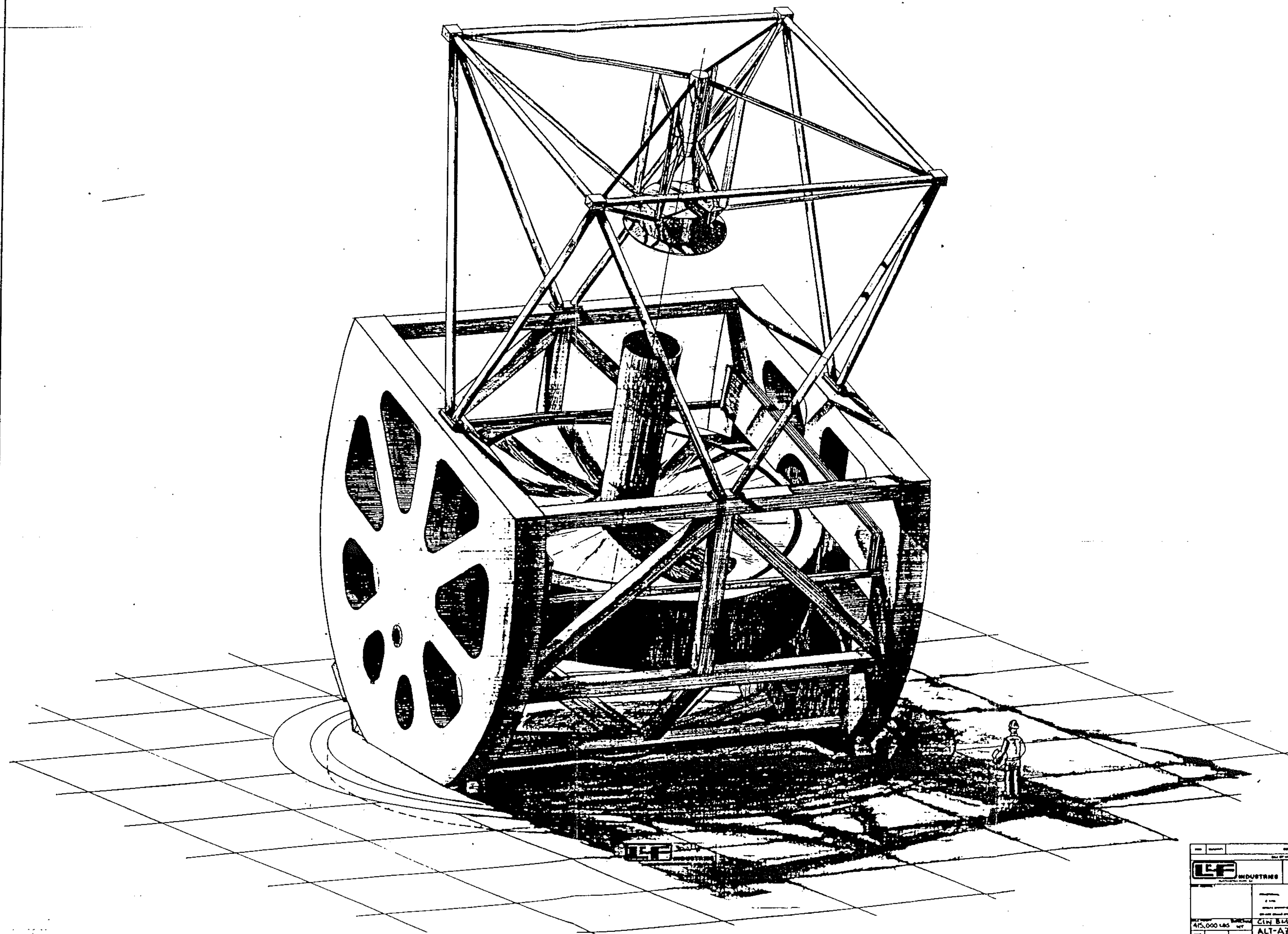

L&F INDUSTRIES

415,000 LBS WT

SMG 2-4-88

CIW BM - MAGELLAN PROJECT

ALT-AZ DISK TELESCOPE
OBLIQUE VIEW

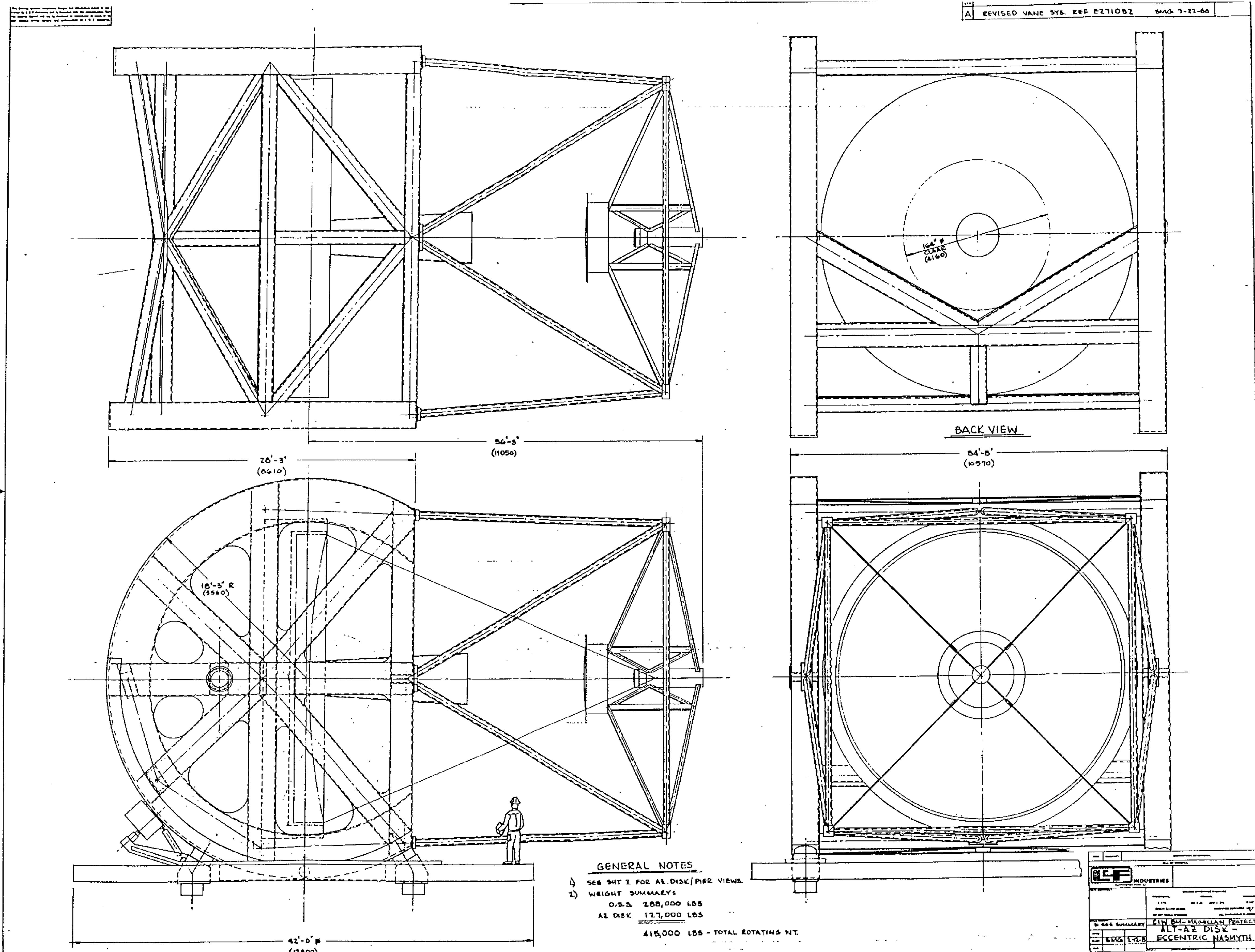
A REVISED VANE SYS. REF E271082 BMG 7-22-88
BACK VIEW
164" ⌀ CLEAR (4160)
56'-3" (11050)
28'-3" (8610)
34'-8" (10570)
18'-3" R (5560)
42'-0" ⌀ (12800)
GENERAL NOTES
1) SEE SHT 2 FOR AZ. DISK/PIER VIEWS.
2) WEIGHT SUMMARY:
O.S.S. 288,000 LBS
AZ DISK 127,000 LBS
415,000 LBS - TOTAL ROTATING WT.
L&F INDUSTRIES
6.5M MMT-MAGELLAN PROJECT
ALT-AZ DISK -
ECCENTRIC NASMYTH

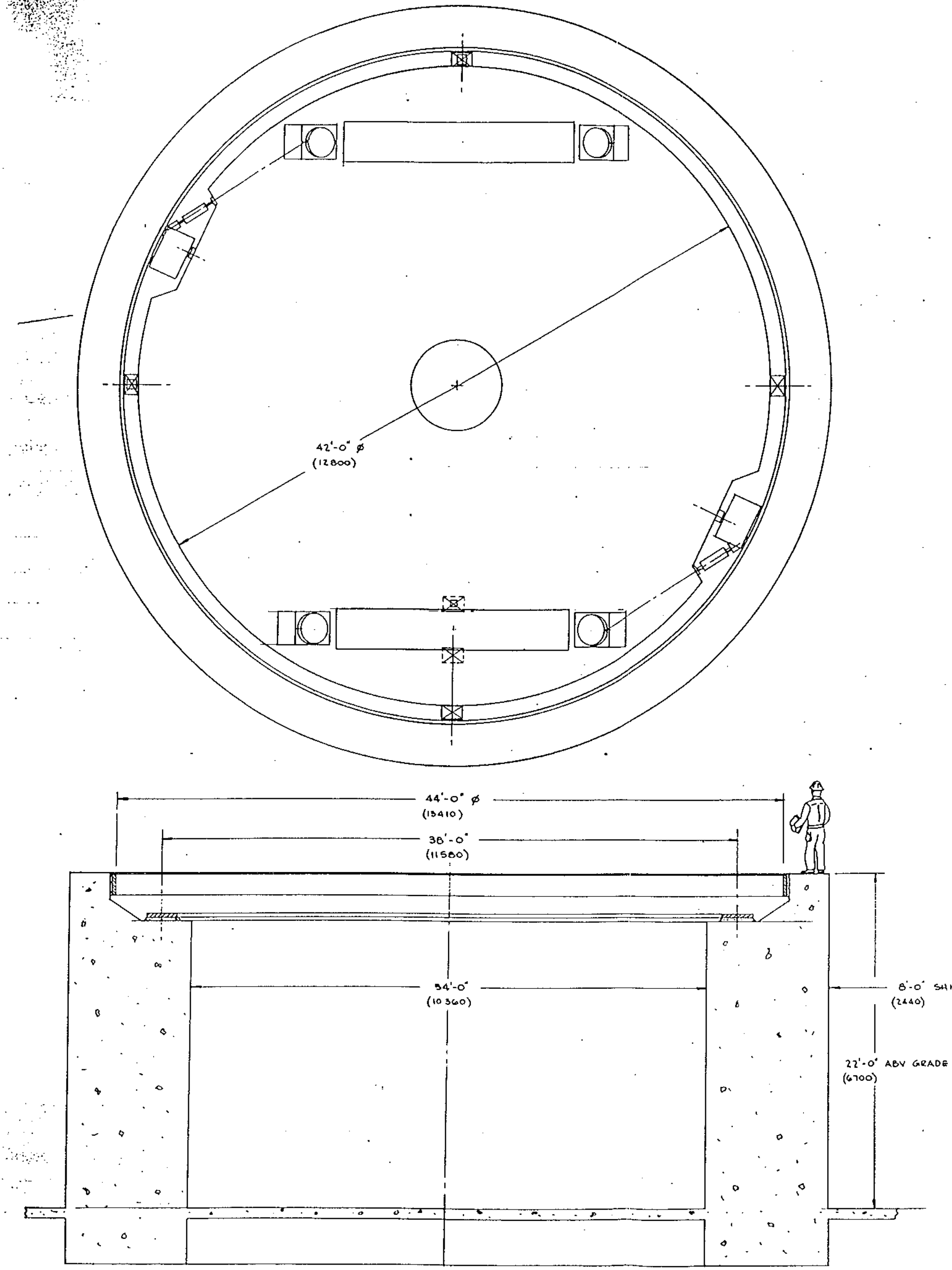

⊠ INDICATES PRELOADED HYDROSTATIC PAD

⊠ INDICATES RIGIDLY MOUNTED HYDROSTATIC PAD (STIFFNESS LOAD PATH)

L&F INDUSTRIES

CIW BM-MAGELLAN PROJECT

ALT-AZ DISK
ECCENTRIC NASMYTH

SMG 2-11-0
SMG 2-12-0
3/16"=1'0" (1:32)
E271029 SHT 2 of 2

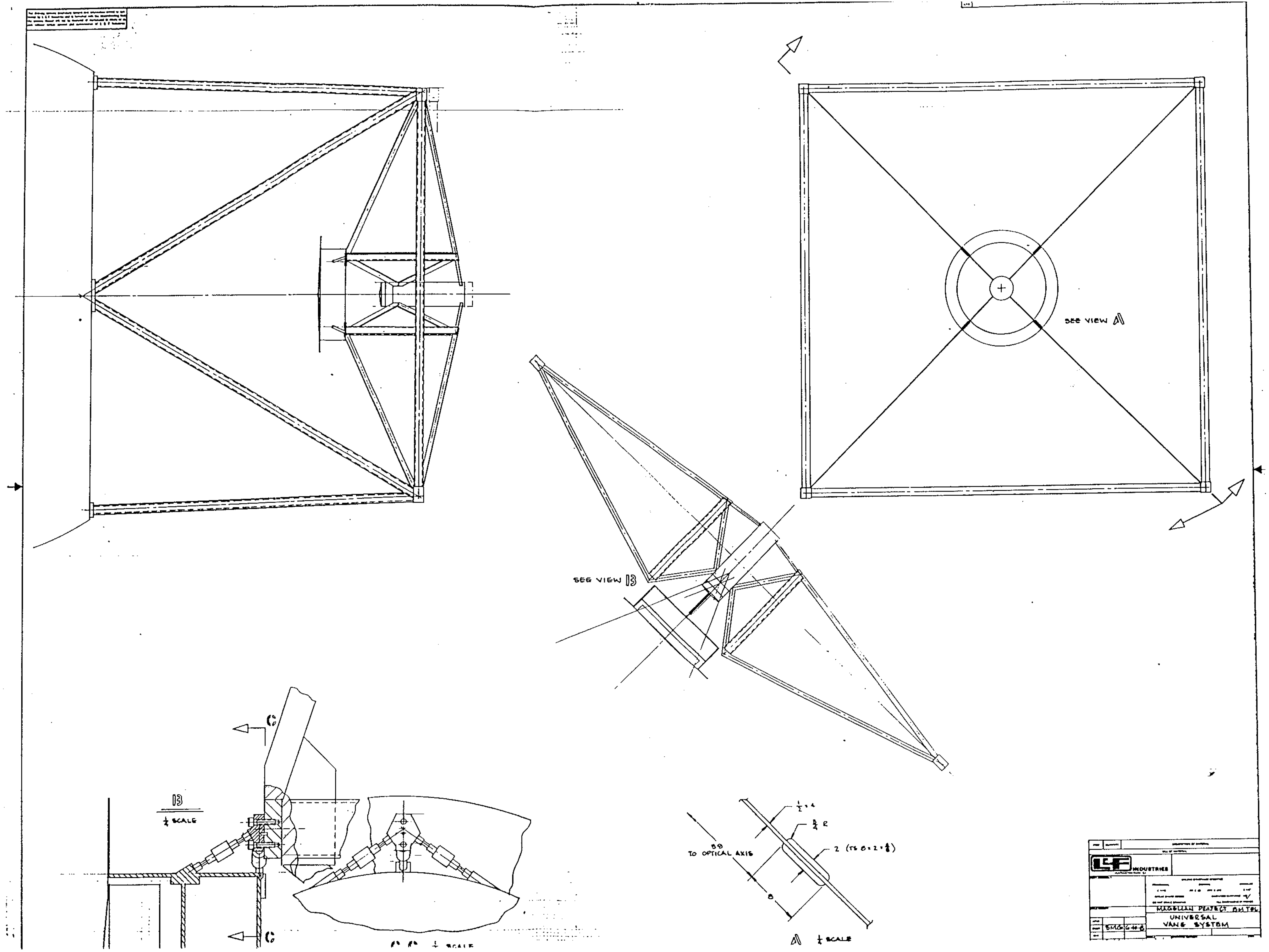

SEE VIEW A
SEE VIEW B
B
1/4 SCALE
C
C
C-C 1/4 SCALE
TO OPTICAL AXIS
A 1/4 SCALE
INDUSTRIES
MAGELLAN PROJECT
UNIVERSAL
VANE SYSTEM

APPENDIX

SUMMARY OF OTHER DESIGN CONFIGURATIONS

LARGE CONVENTIONAL FORK:

The first investigation made after the October 1987 "Phase II Interim Report" was one to see how much the two lowest (translational) vibration modes could be improved by increasing the stiffness of the conventional fork. As can be seen on the chart labelled "Fork Mod. Improvement vs. Large Alt-Az Disk", the two lowest modes could be brought up to about 6.4 hz using this method. However, as shown on the chart, this required the addition of between 100,000 and 245,000 lbs. of material to the fork, adding considerable cost, decreasing thermal response of the structure, etc. Drawings showing the structural designs which were tested are shown following (E271025 shts 1 & 2). However, it should be noted that the braced fork, although shown on the drawing, was not modelled, and thus no conclusive results were gained for a braced fork design.

LARGE (CONCENTRIC NASMYTH) ALT-AZ DISK:

The next concept investigated was one in which the O.S.S. "connects" to the azimuth structure using large diameter journals, or altitude disks. Since this can be done in such a way that bending moments on the azimuth structure are eliminated altogether, the "fork" then becomes a thin flat structure. In this particular design, it is convenient for this azimuth structure to be round (for better interface with the round pier bearing), and thus it is also a disk.

Therefore, since both rotation axes are defined using "disk" structures, the mount is presently being called an "Alt-Az Disk".

The first configuration of this mount which was tested included a conventional Nasmyth location; that is, with the Nasmyth instrument located on the altitude axis. This design requires rather large diameter altitude disks. Three designs were drawn, as shown on drawings E271026, E271027, and E271028. E271028, or "Alt-Az Disk No. 3", in its braced altitude disk configuration, with a braced Primary Support Structure, was the design of choice for the large alt-az disk system.

The results of the four major vibrational modes is plotted also on the following chart labelled "Fork Mod. Improvement vs. Large Alt-Az Disk". As can be seen, the performance for the two lowest (translation) modes is improved, and with a lower weight than even the lightest "conventional fork". Note that one of the areas that required considerable optimizing was that of the lateral bracing between the altitude disks on the back side of the primary mirror cell. Some of the results of these bracing studies are shown in tabular form in the following data.

SMALL (ECCENTRIC NASMYTH) ALT-AZ DISK:

At this point in the recent work it was realized that the simple act of moving the Nasmyth instrument location behind the primary mirror cell would allow the use of considerably smaller altitude disks. This not only reduces weight and cost, but makes the disks more feasibly made in one piece - a very desirable move from the aspect of hysteresis, etc.

These first modal analysis results are then shown on the chart labelled "braced structures". Of course, since this has turned out to be the final configuration, much more detailed results are presented in the body of this report, prior to this appendix. A plot showing the relative size of the large and small alt-az disks (at equal scale) is shown in this section.

PLATE STRUCTURE ALT-AZ DISK:

The next investigation was to see the effect of making the entire Primary Support Structure as a plate, or monocoque, structure. In order for its weight to not become much greater than in the braced system, 3/8" plate thickness was initially used for both the altitude disks and the curved shear panels which joined them together.

Since this initial result was a little disappointing in lateral translation, and since it was recognized that much strain was occuring near the bottom of the O.S.S. near its bottom end (when pointing to zenith), it was decided to increase the plate thicknesses locally in that area. The results of these analyses are presented in the chart labelled "Plate vs. Braced Structure", following.

It was concluded that 1.) the modal performance was a little worse, 2.) the weight was a little higher, and 3.) thermal effects on seeing would be considerably worse, than in the braced alt-az disk structure. Therefore this design was not considered further. Plots showing this design, as well as drawing E271031, are included later in this appendix.

DUAL VANE SYSTEM:

One detail configuration which was considered (and which was included in most of the modelling described above) was that of the dual vane system shown on drawing E271029 "no change revision". In this system, the wide field secondary is supported by a second set of vanes, half of which attach to the Primary Support Structure. When static analyses were finally run using this vane configuration, it was found that 1.) piston and decenter ("sag") motions were much lower than in the previously used vane system, but 2.) net tilt motions were far greater than in the previous system. Results are presented near the end of this appendix section, especially in the chart labelled "Comparison of Secondary Misalignments".

It was found that this large tilt effect could be improved considerably by adjusting relative stiffnesses of the front and back (wide field secondary support) vanes. In fact, it can be reduced to zero for any particular tilt motion. However, since there are many tilt motions (due each to different load conditions), others will not be zero.

Another disadvantage to the dual vane system is an operational one. In order to remove or install the wide field secondary it becomes necessary to either remove or replace, or at least move that vane set into or out of position. Although this can certainly be done, it will be somewhat time consuming and one wonders whether, in the "out-of-the-way" position, the vanes' local bending vibration might be a problem.

UNIVERSAL VANE SYSTEM:

The universal vane system was then created as a solution to the disadvantages of the dual vane system, but still with the attribute that the secondary end need not be exchanged when changing to or from the infrared configuration.

This is the current vane system of choice, and therefore is presented in the body of this report.

CARNEGIE INSTITUTION OF WASHINGTON

MAGELLAN PROJECT

NATURAL FREQUENCIES AND MODESHAPES

SMG 2-11-8

FORK MOD. IMPROVEMENT VS LARGE ALT-AZ DISK

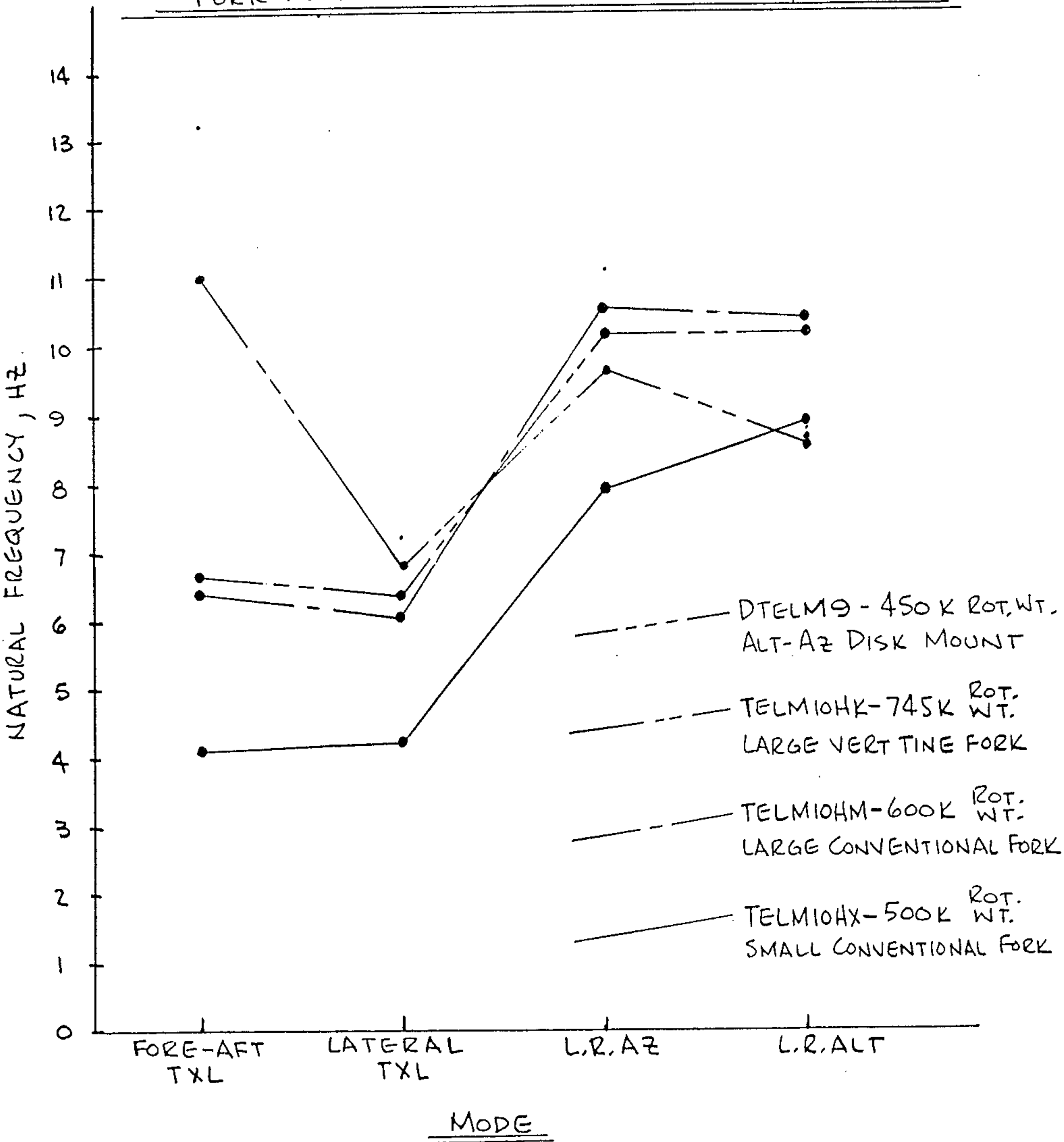

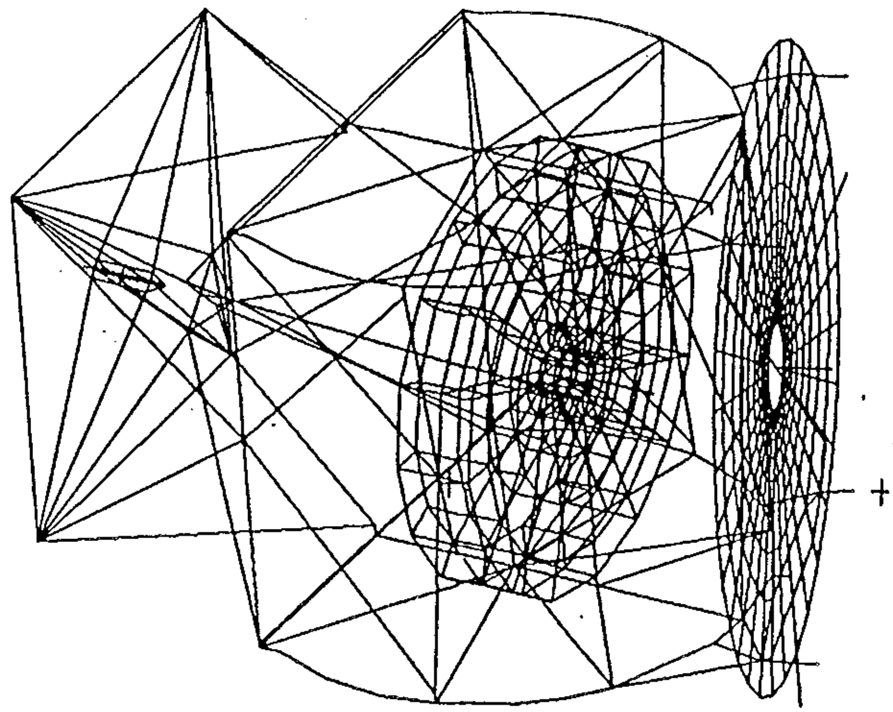

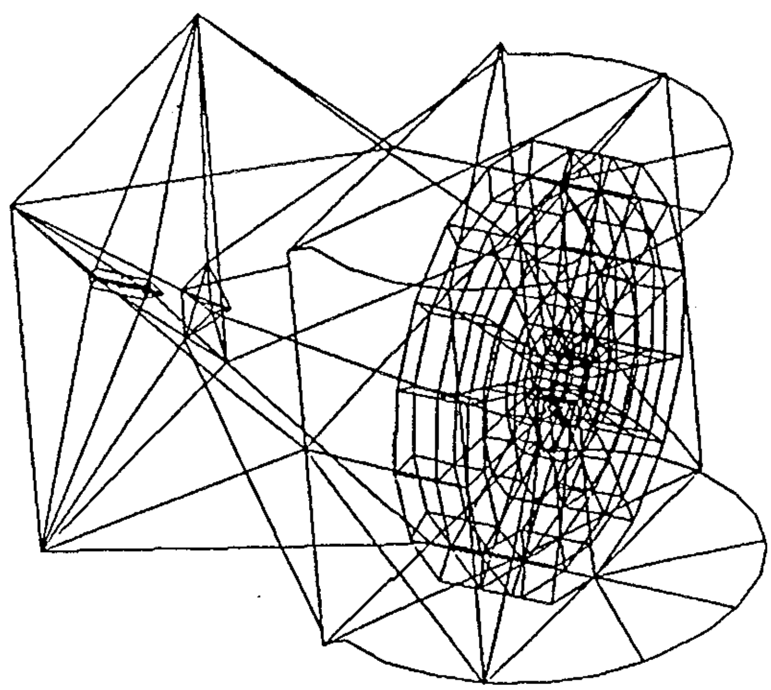

CARNEGIE INSTITUTION OF WASHINGTON

ECCENTRIC NASMYTH ALT-AZ DISK TELESCOPE

LATERAL TRANSLATION VIBRATIONAL MODE - OPTIMIZING RUNS

Note: The following results are from FEA models with a highly simplified mirror cell (including point mass and mass moment of inertia representing the primary mirror, mirror cell, instrument and instrument mounting base) as well as a lateral spring support for the O.S.S. (i.e. no az disk). These results therefore do not accurately represent the true lateral vibrational mode, but are sufficiently accurate for optimizing purposes. Optimizing runs are **shown in bold type.** Other miscellaneous runs are also included for reference.

MODEL	LATERAL MODE	DESCRIPTION
SDOSSGMP	11.4	Upper limit due to both bracing and rim. (SDOSS4MP plus unrealistically stiff rim)
SDOSS4MP	10.5	Upper limit due to bracing only. Uses ideal material properties without regard to instrument clearance (i.e. not an achievable upper limit).
SDOSS3MP	8.7	Back view of bracing: 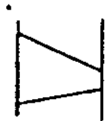
SDOSSIMP	8.25	Back view of bracing: 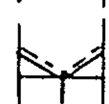 This version used in subsequent complete models.
SDOSSJMP	8.25	SDOSSIMP with heavier main truss plane.
SDOSSHMP	8.2	SDOSSIMP with heavier spokes.
SDOSSEMP	8.1	SDOSSIMP with heavier rim.
SDOSS1MP	7.5	SDOSSMP with heavier rim.
SDOSSMP	7.4	Back view of bracing: 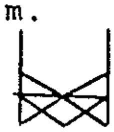
SDOSS8MP	7.2	Back view of bracing: 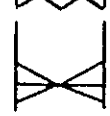
SDOSS9MP	6.4	Back view of bracing: 
SDOSS5MP	5.6	No back bracing, stiff rim.
SDOSSFMP	8.1	SDOSSIMP at zenith.
SDOSSGMP	8.6	SDOSSIMP at 30˚ above horizon.

ALT-AZ DISK TELESCOPE

FINITE ELEMENT ANALYSIS

PRELIMINARY SUMMARY OF RESULTS

An intermediate-level finite element model of an alt-az disk telescope structure has been created for the Carnegie Institution of Washington (Magellan Project) 8 Meter Telescope.

The complete system has been modelled (although with only an "intermediate" level of complexity), including the O.S.S., Azimuth Disk, and drives and support system. It has been assumed that the reinforced concrete pier structure is infinitely stiff as compared to the telescope structure. Modal analyses were performed for various azimuth disk structures (with point masses applied to represent the O.S.S.) to first determine its most efficient structural configuration. Then complete models were created and run to include the effects of the O.S.S. "non-stiffness".

Significant results are listed below, with a narrative summary following:

MODEL	FREQ HZ.	MODESHAPE	DESCRIPTION/CONCLUSION
AZD1	7.2 8.2 11.3	LATERAL TXL FORE-AFT TXL L.R.AZ	Azimuth Disk Modal Analysis, braced structure using TS 18 x 6 x 1/2" rectangular tubing, XY positioning hydrostatic pads at 45° to global axes.
AZD2	9.8 11.6 12.2	LATERAL TXL FORE-AFT TXL L.R.AZ	AZD1 but with doubled structural tubing areas.
AZDA1	18.1 10.5 12.5	LATERAL TXL FORE-AFT TXL L.R.AZ	Still a braced structure but with support system rotated 45° (i.e. XY positioning hydrostatic pads aligned with global axes.
AZDA3	19.3 14.1 12.5	LATERAL TXL FORE-AFT TXL L.R.AZ	AZDA1 but with doubled structural tubing areas.
AZDB1	17.9 13.9	FORE-AFT TXL L.R.AZ	Plate (membrane) type structure. Support system as in AZDA1. Lateral mode didn't appear, but should be at least 19.3 hz.
DTELM	5.8 9.1 9.9 12.5	LATERAL TXL L.R.ALT L.R.AZ FORE-AFT TXL	Disk Telescope Modal Analysis using AZDB1 azimuth disk and support sys. Back view of bracing system:

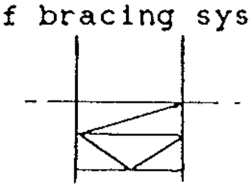

DTELM2	5.7	LATERAL TXL	DTELM1 but with bracing back view: 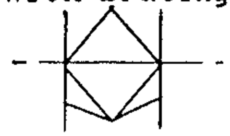
	9.0	L.R.ALT	
	10.0	L.R.AZ	
	12.5	FORE-AFT TXL	
DTELM3	6.0	LATERAL TXL	DTELM2 but with heavier main truss plane.
	8.8	L.R.ALT	
	10.1	L.R.AZ	
DTELM4	6.3	LATERAL TXL	Heavier main truss plane plus back view bracing: 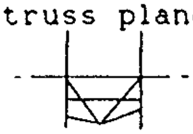
	8.7	L.R.ALT	
	9.9	L.R.AZ	
DTELM6	7.1	LATERAL TXL	Overdefinition (laterally) of entire system; O.S.S. to Az Disk and Az Disk to concrete pier.(DTELM4 structure). Upper limit of frequencies due to lateral support system.
	8.7	L.R.ALT	
	9.9	L.R.AZ	
DTELM7	8.8	LATERAL TXL	Upper limit of frequencies due only to back bracing.
	8.7	L.R.ALT	
	10.0	L.R.AZ	
DTELM8	6.2	LATERAL TXL	Curved shear panel back "bracing".
	8.7	L.R.ALT	
	9.8	L.R.AZ	
DTELM9	6.8	LATERAL TXL	Back bracing: 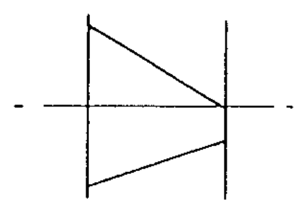
	8.5	L.R.ALT	
	9.5	L.R.AZ	
	11.0	FORE-AFT TXL	

CONCLUSIONS:

The plate-membrane type structure is most efficient for the azimuth disk.

The support system oriented with the XY hydrostatic pads aligned with the global axes and drives at 45° is most efficient.

The back bracing system used in DTELM9 is most efficient of those investigated thus far. However, lateral translation as high as 8 hz may be possible for this system, with an even more efficient bracing system.

The natural frequencies of DTELM9, at least, can be expected. Some further optimizing may further improve this performance.

An approximate weight summary for DTELM9 is as follows:

330,000 lbs	- O.S.S. complete assembly
120,000 lbs	- Az Disk complete Assembly
450,000 lbs	- Total Rotating Weight

A problem which plagues this design is that the O.S.S. is naturally heavy toward the primary end. This means that one cannot add as much bracing steel (to stiffen the Altitude Disks laterally) as one would like. A revised design is being modelled in which the complete optical system is moved forward relative to the altitude axis. In this "Eccentric Nasmyth" system, both the altitude and azimuth disks are measurably smaller. It is anticipated that the total rotating weight will be lowered by between 50,000 and 100,000 lbs. and that the natural frequencies will be measurably improved.

ECCENTRIC NASMYTH ALT-AZ DISK TELESCOPE

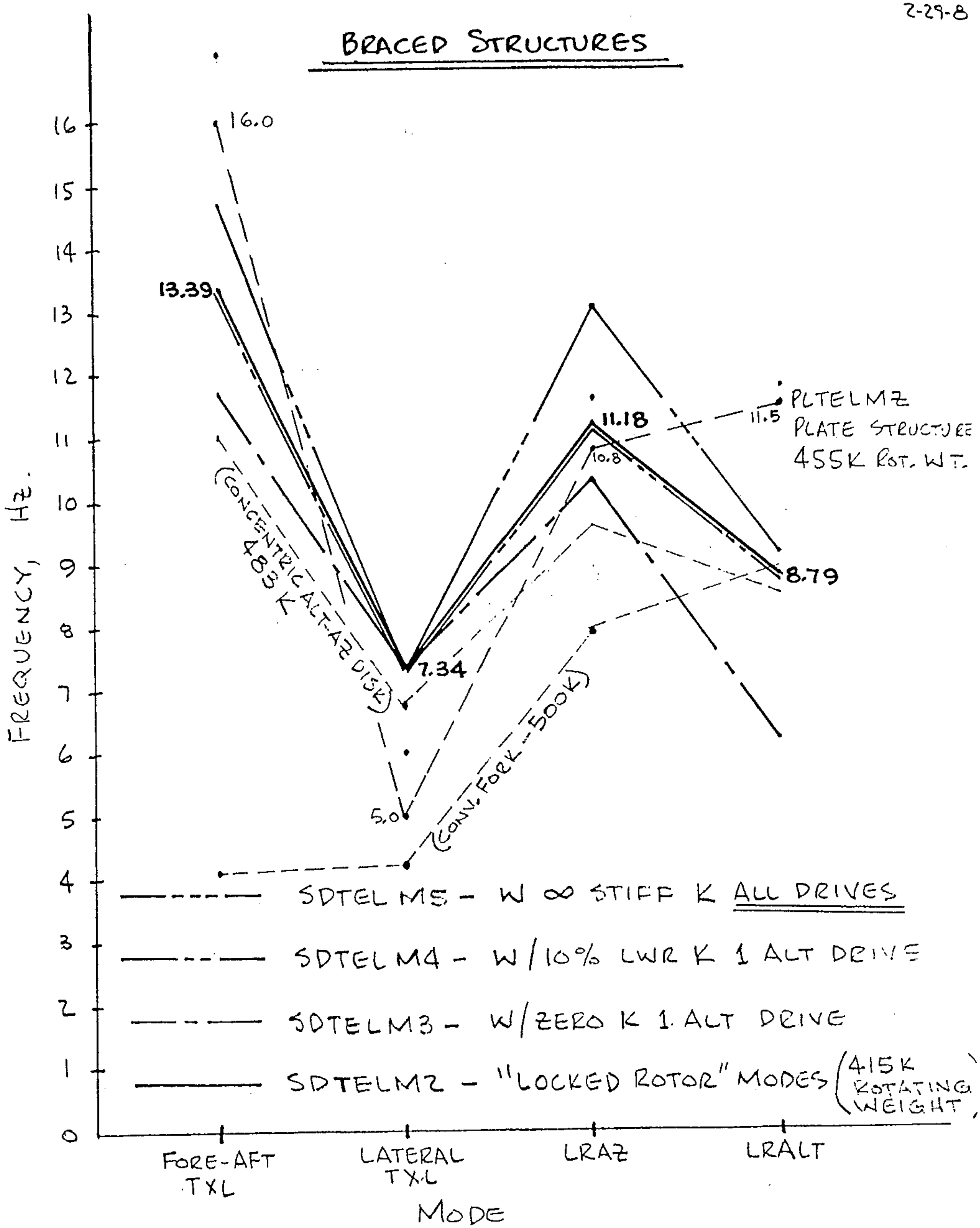

ECCENTRIC NASMYTH ALT-AZ DISK TELESCOPE

PLATE VS. BRACED STRUCTURE

SMG
5-10-8

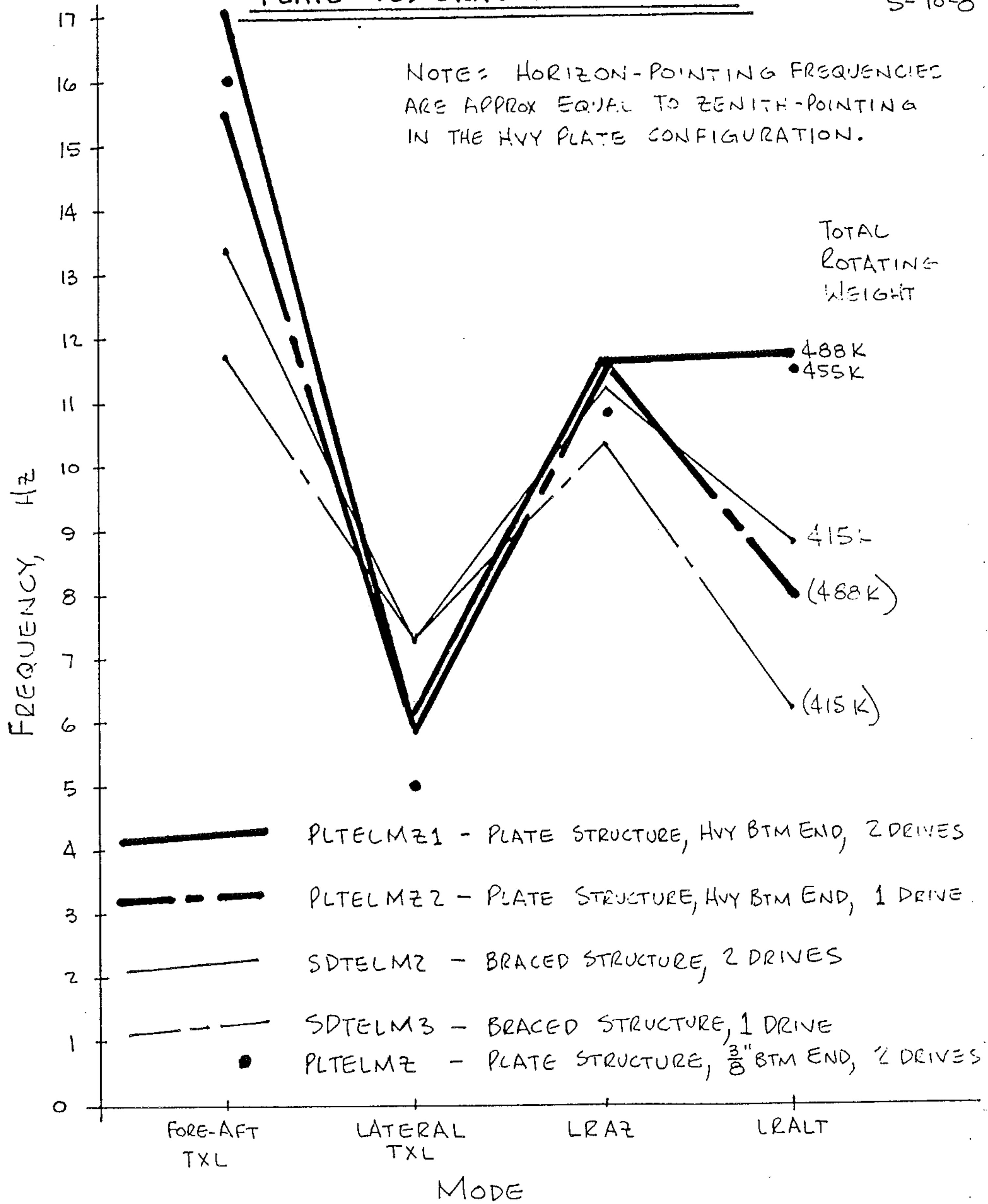

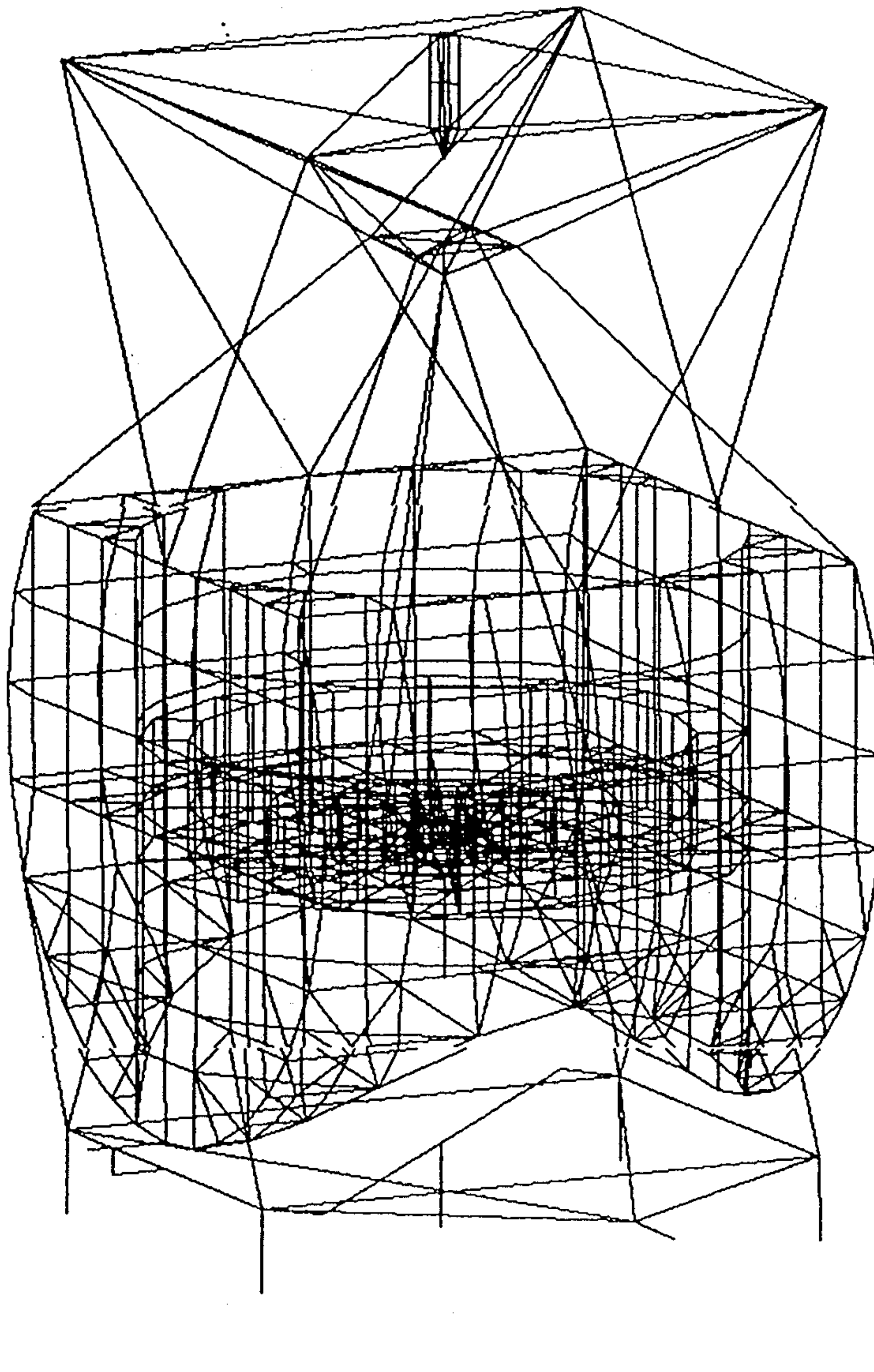

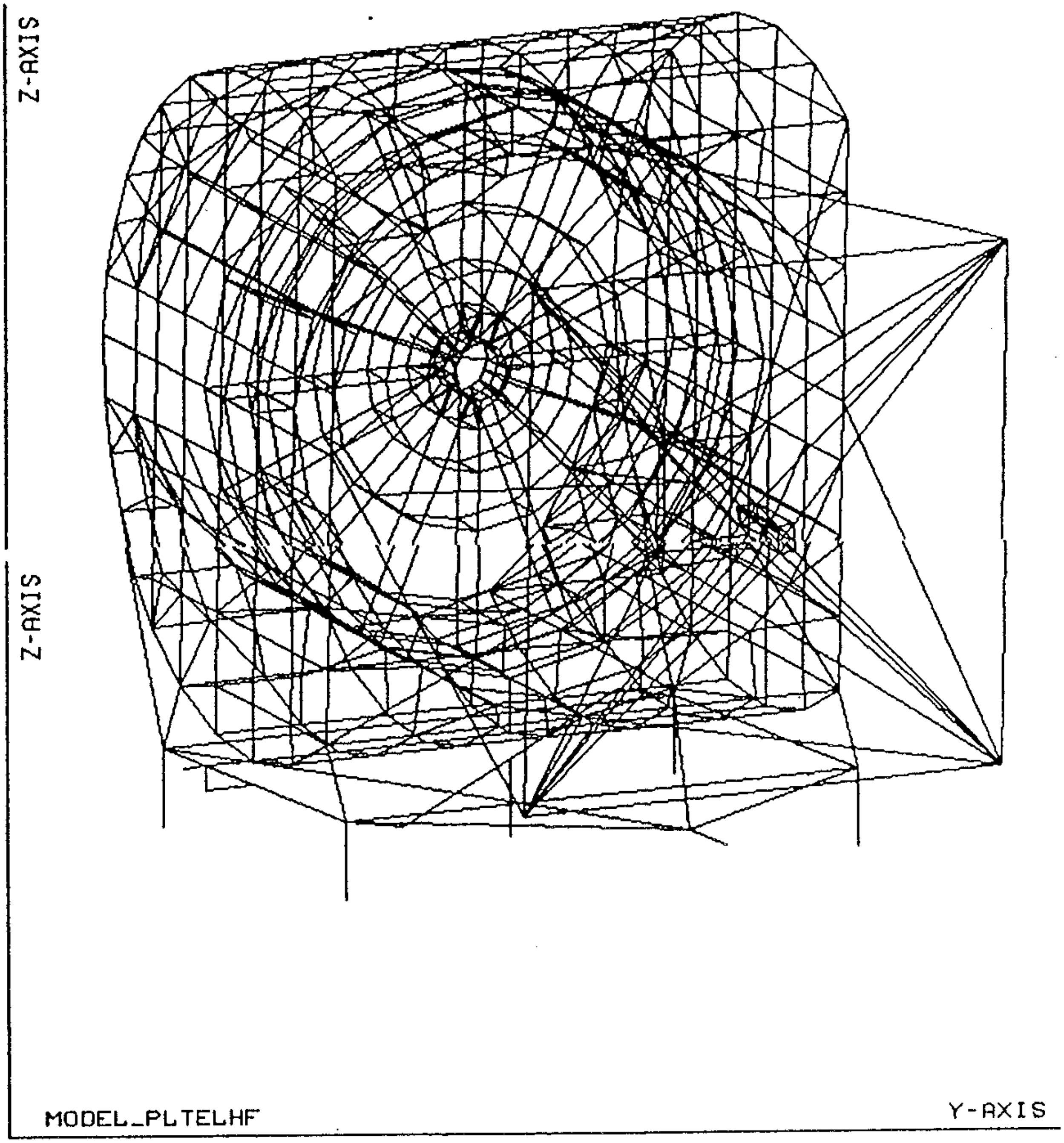
Z-AXIS
Z-AXIS
MODEL_PLTELHF
Y-AXIS

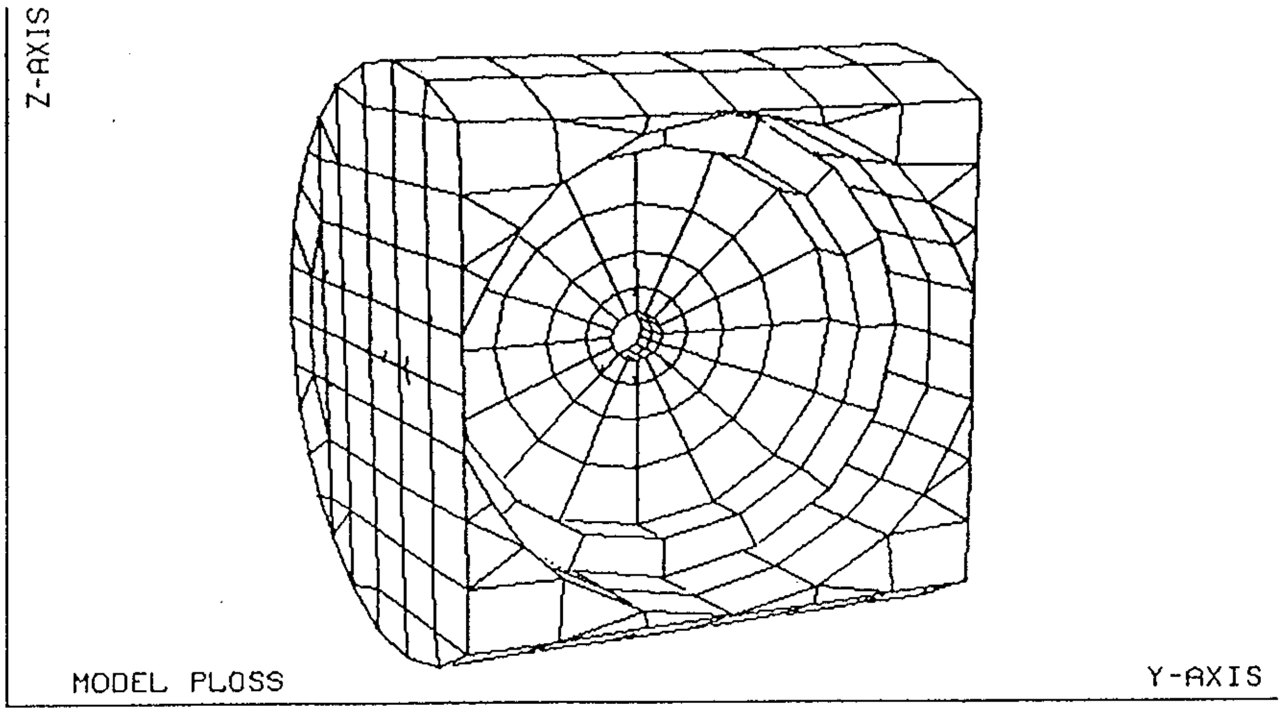
Z-AXIS
MODEL PLOSS
Y-AXIS

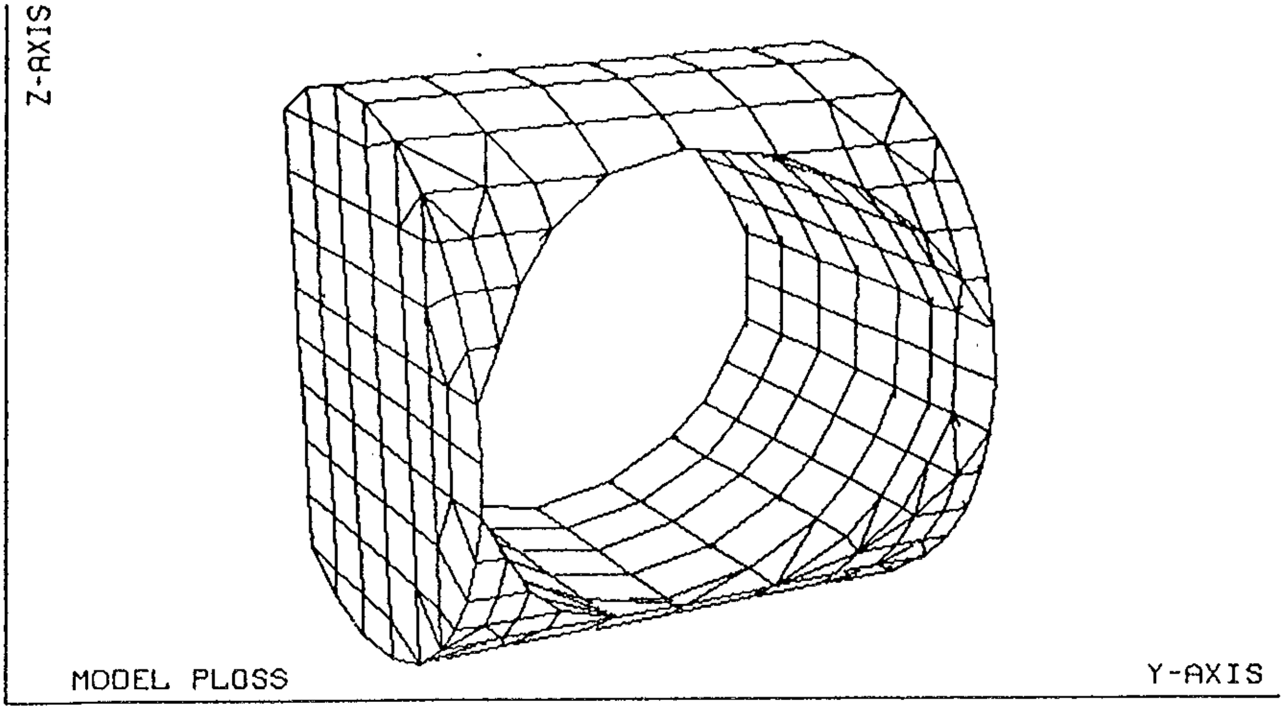
Z-AXIS
MODEL PLOSS
Y-AXIS

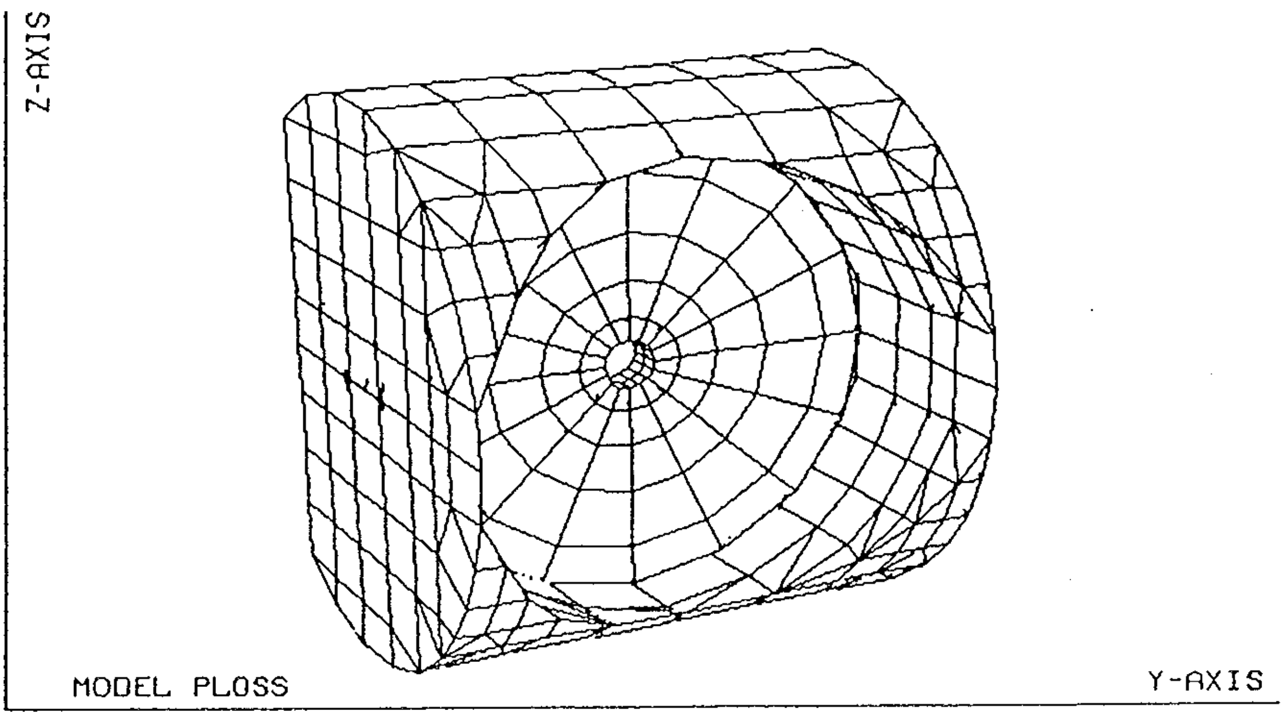
Z-AXIS
MODEL PLOSS
Y-AXIS

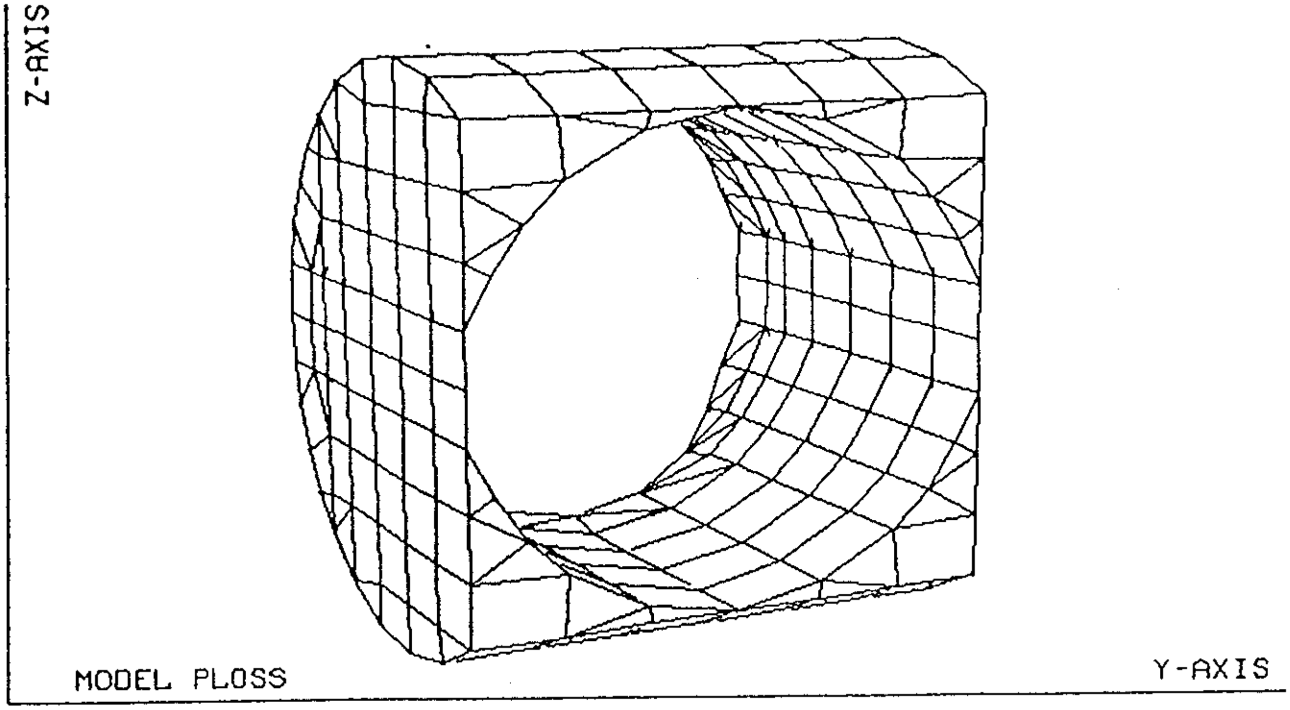
Z-AXIS
MODEL PLOSS
Y-AXIS

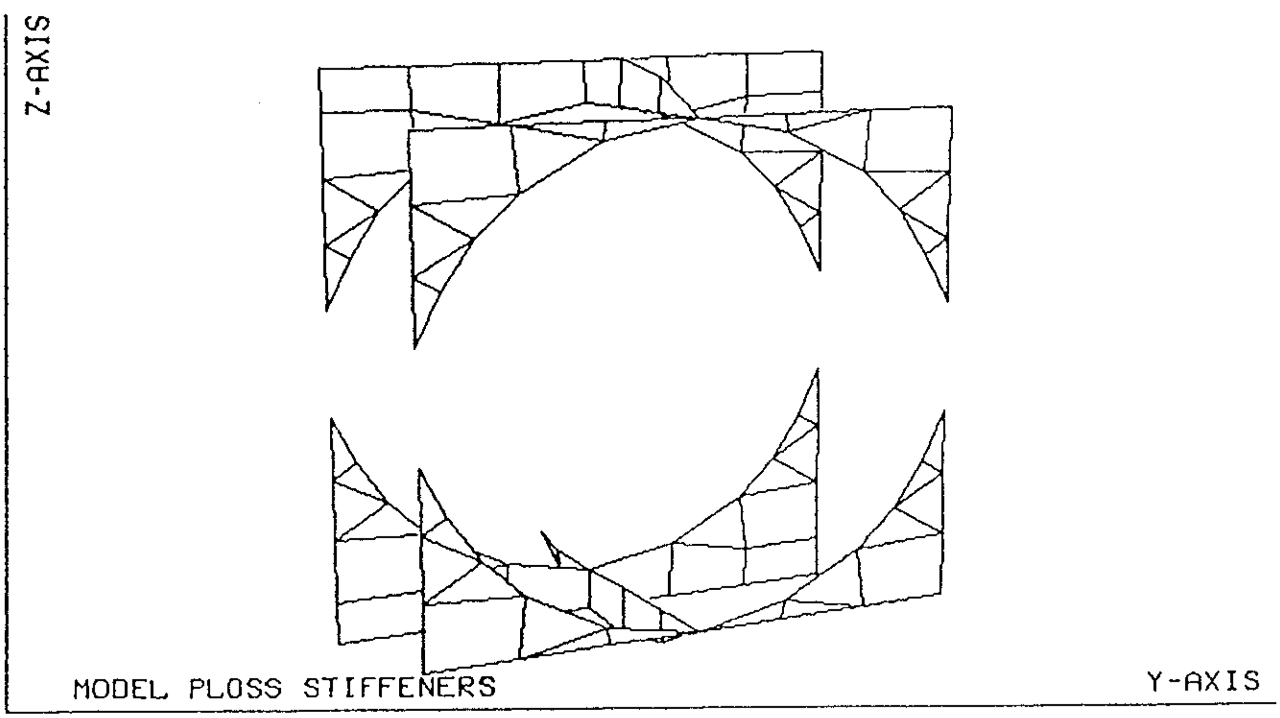
Z-AXIS
MODEL PLOSS STIFFENERS
Y-AXIS

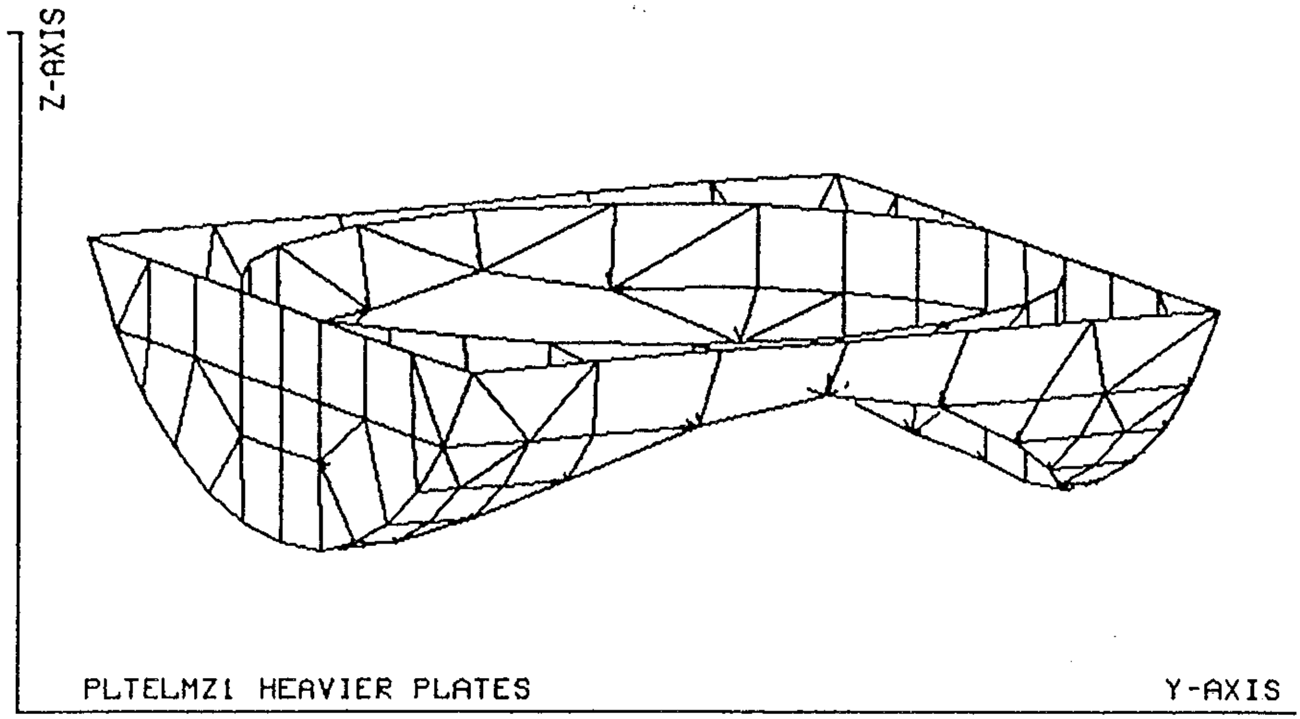
Z-AXIS
PLTELMZ1 HEAVIER PLATES
Y-AXIS

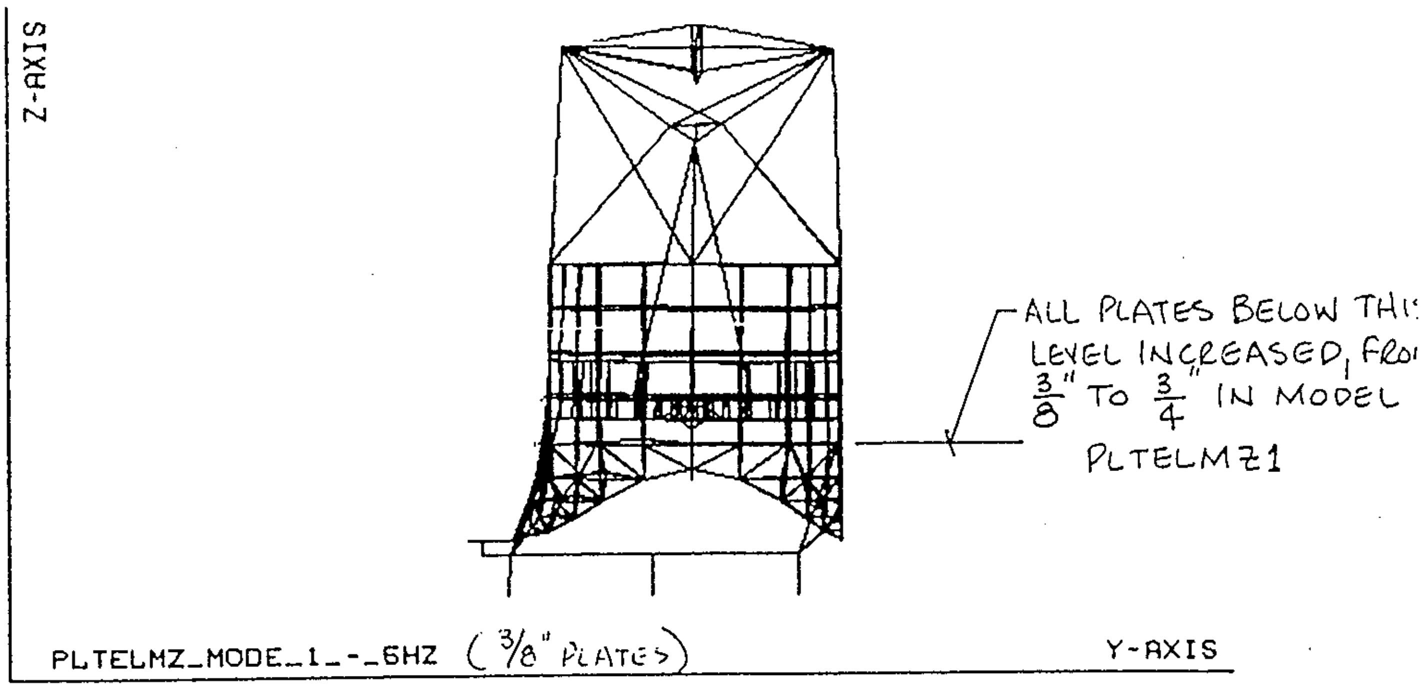
Z-AXIS
ALL PLATES BELOW THIS LEVEL INCREASED, FROM 3/8" TO 3/4" IN MODEL PLTELMZ1
PLTELMZ_MODE_1_-_6HZ (3/8" PLATES)
Y-AXIS

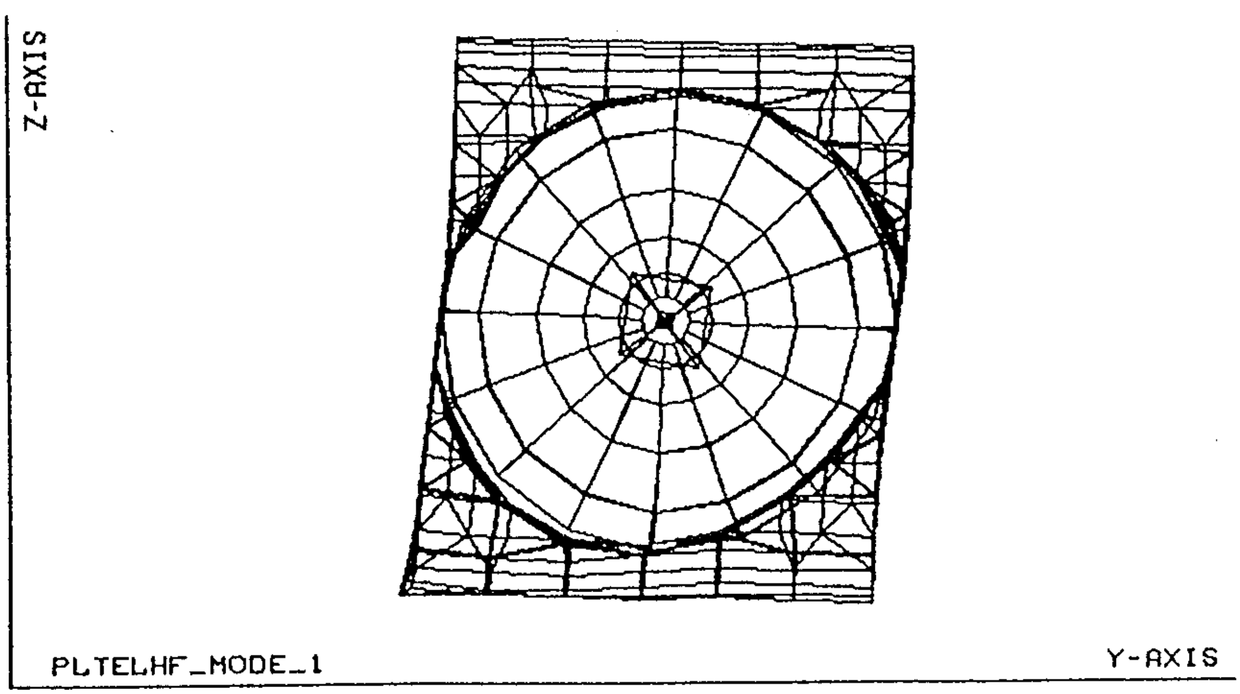
Z-AXIS
PLTELHF_MODE_1
Y-AXIS

DUAL VANE SYSTEM

ECCENTRIC NASMYTH ALT-AZ DISK TELESCOPE

FINITE ELEMENT ANALYSIS

GRAVITY DEFLECTIONS/MISALIGNMENTS

If optics are perfectly aligned at zenith, the following misalignments will develop (between the subject optical element and the primary mirror) as O.S.S. is rotated to horizon.

Results are based on models SDTELZ and SDTELH. See "SDTEL_ Data Reduction" for detail calculations.

Note: "Infrared secondary" results are approximate and are included only for general comparison to "optical secondary" results - Optical secondary and its vanes are in place in all of the following results.

OPTICAL ELEMENT	NET PISTON	NET SAG	NET TILT
OPTICAL SECONDARY	.0023 in.	.0036 in.	.030 deg. 524 microrad 108 arcsec
INFRARED SECONDARY	.0265 in.	.0027 in.	.00032 deg. 5.60 microrad 1.15 arcsec
CASS FOCAL PLANE	.0033 in.	- - -	.003 deg. 52 microrad 11 arcsec

ECCENTRIC NASMYTH ALT-AZ DISK TELESCOPE

FINITE ELEMENT ANALYSIS

WIND LOAD DEFLECTIONS/MISALIGNMENTS

O.S.S. Attitude/ Wind Direction	Primary Pointing Error	Secondary (Decenter)	Misalignment (Rotation)
Zenith Front Wind			
Optical	0.36 microrad 0.074 arcsec	.000112 in.	1.98 microrad .408 arcsec
Infrared	0.36 microrad 0.074 arcsec	.000132 in.	.152 microrad .031 arcsec
Zenith Side Wind			
Optical	0.063 microrad 0.013 arcsec	.00014 in.	1.44 microrad .297 arcsec
Infrared	0.063 microrad 0.013 arcsec	.00016 in.	.126 microrad .026 arcsec
Horizon Front Wind			
Optical	0.404 microrad 0.083 arcsec	.00005 in.	.066 microrad .014 arcsec
(Optical Defocus - .000014 in.)			
Infrared	0.404 microrad 0.083 arcsec	.00005 in.	.010 microrad .002 arcsec
(Infrared Defocus - .000081 in.)			
Horizon Side Wind			
Optical	0.456 microrad 0.094 arcsec	.000047 in.	2.02 microrad 0.42 arcsec
Infrared	0.456 microrad 0.094 arcsec	.000057 in.	0.25 microrad 0.05 arcsec

Note: "Infrared" results are approximate and are included only for general comparison to "Optical" results - Optical secondary and its vanes are in place in all models.

COMPARISON OF SECONDAR MISALIGNMENTS
— — — CONV. FORK VS —— ALT-AZ DISK*

* (W/ MODIFIED VANE SYSTEM)

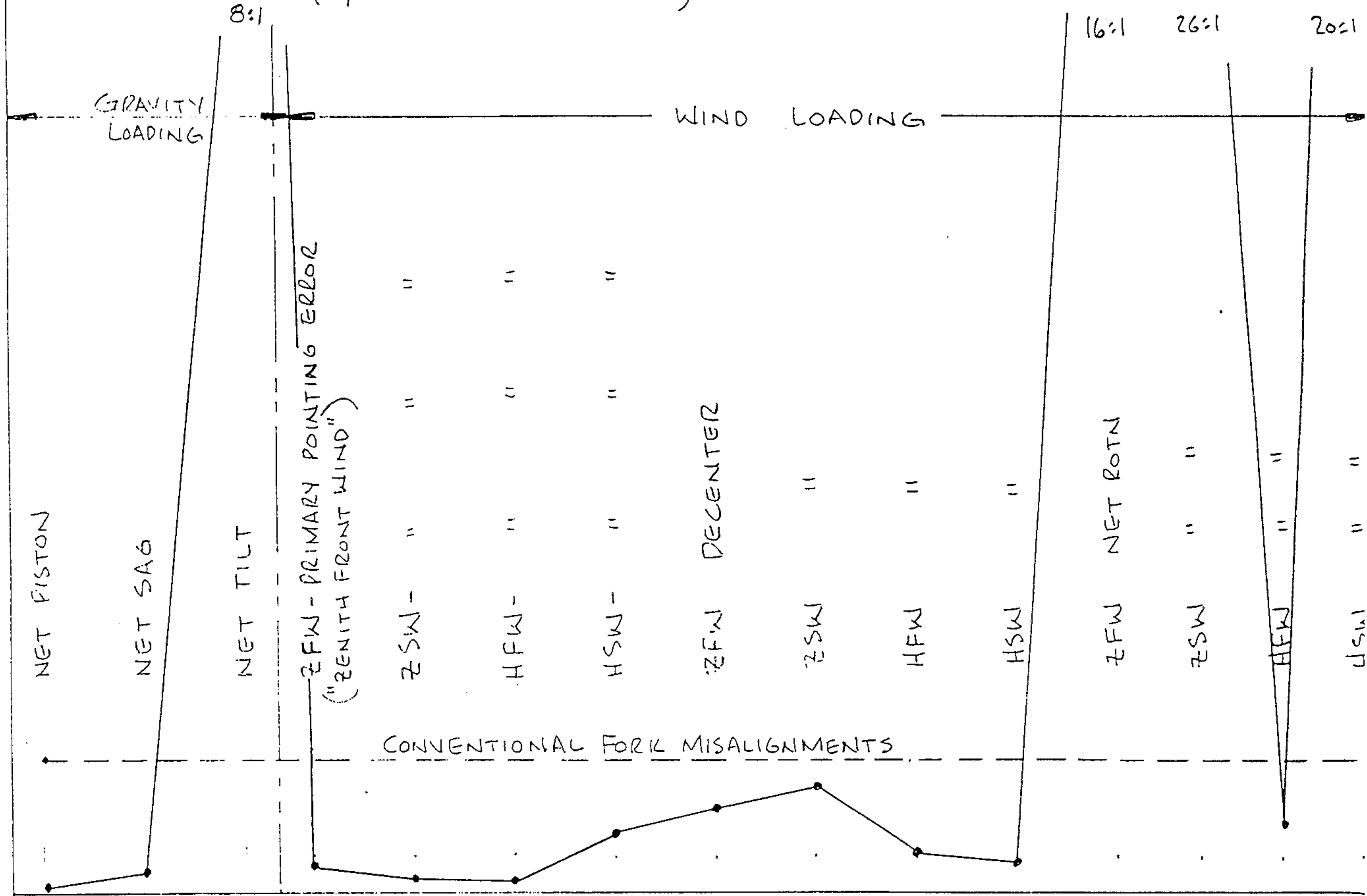

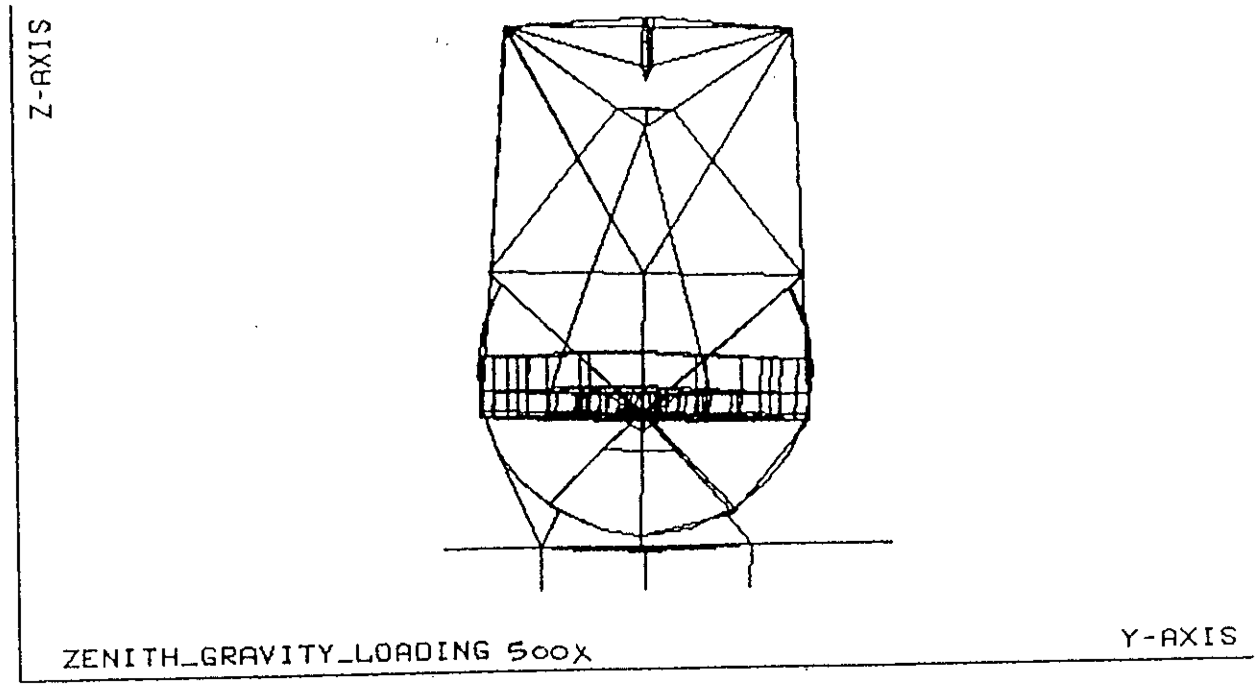
Z-AXIS
Y-AXIS
ZENITH_GRAVITY_LOADING 500X

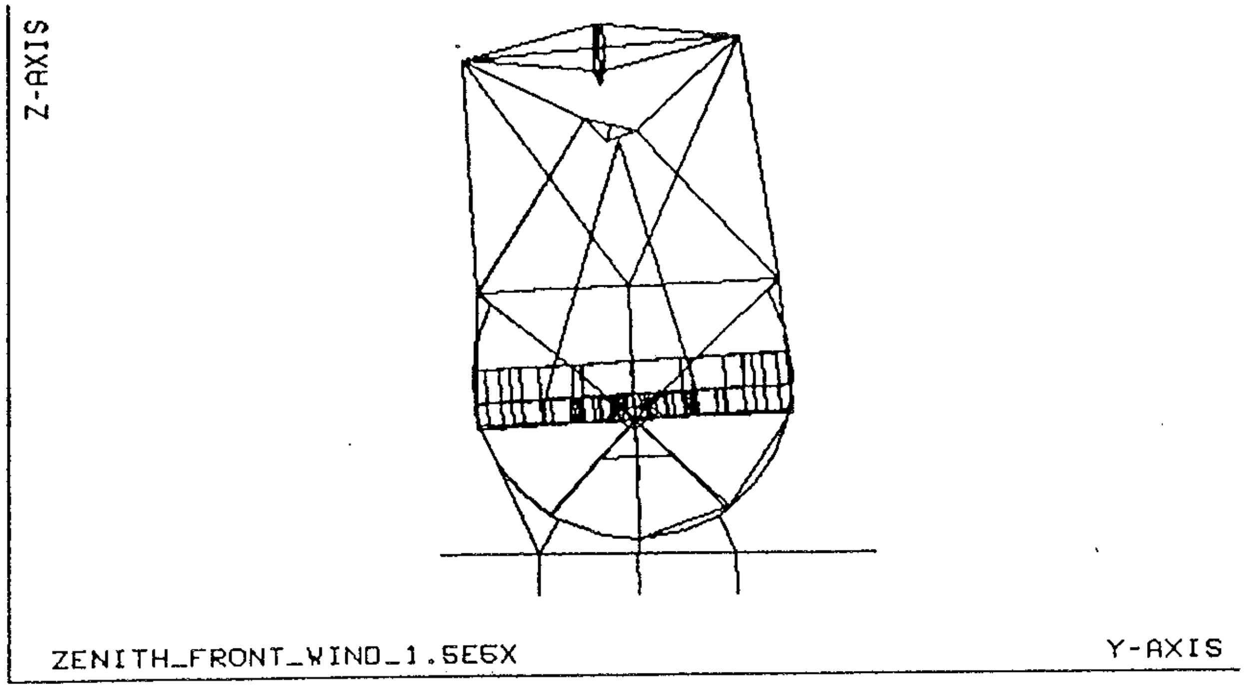
Z-AXIS
ZENITH_FRONT_WIND_1.5E6X
Y-AXIS

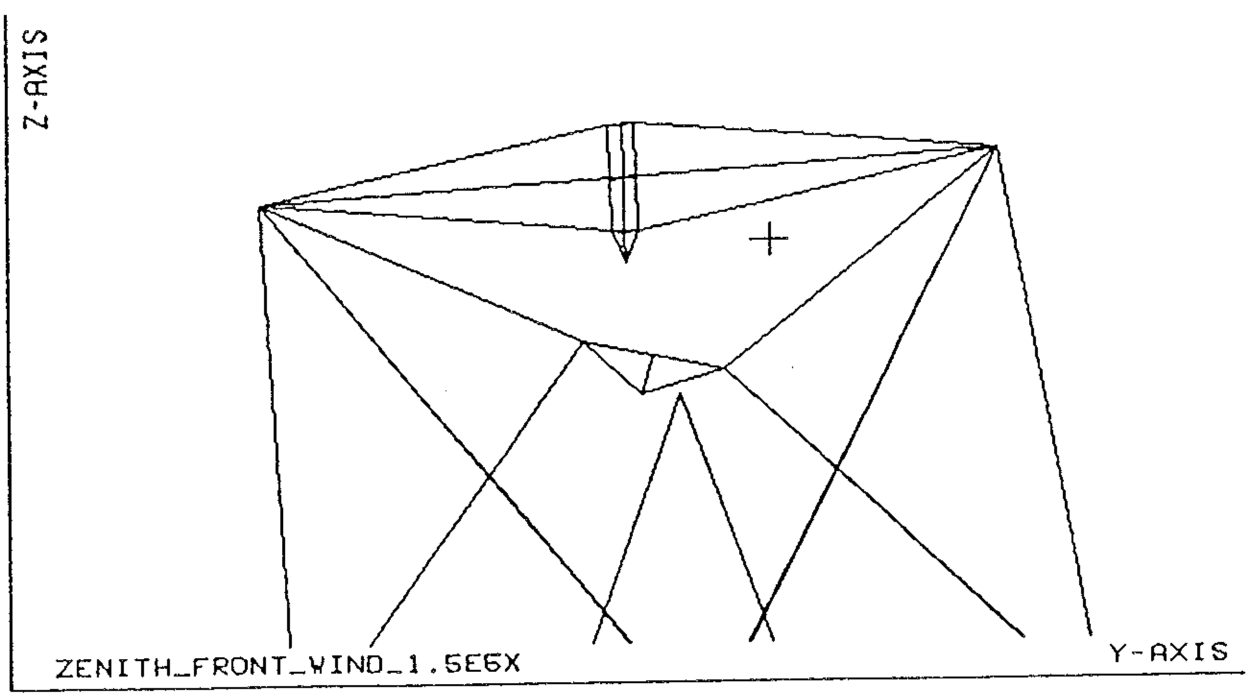
Z-AXIS
ZENITH_FRONT_WIND_1.5E6X
Y-AXIS

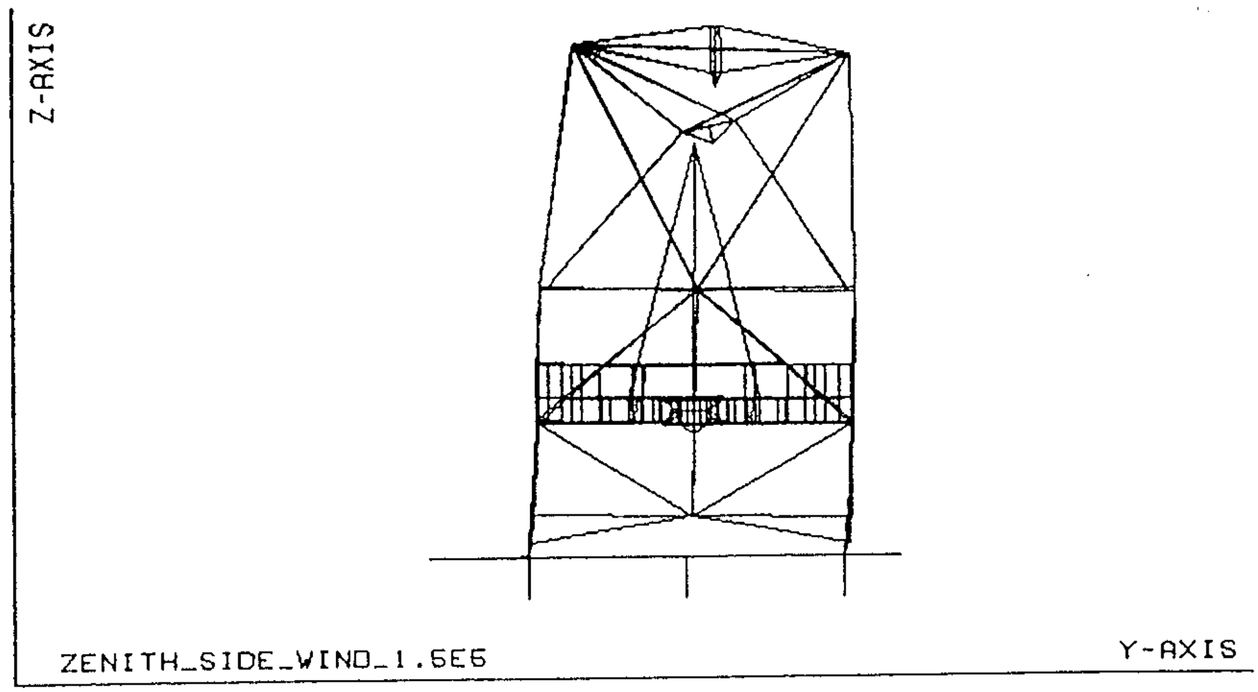
Z-AXIS
ZENITH_SIDE_WIND_1.5E6
Y-AXIS

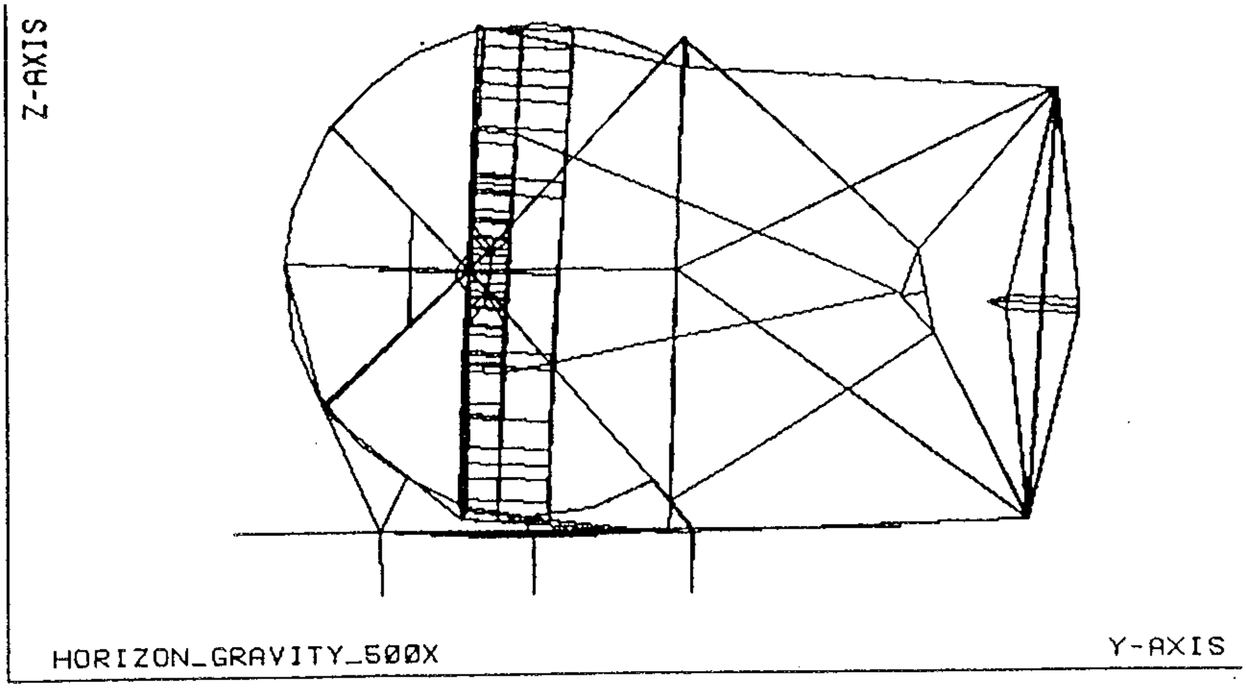
Z-AXIS
HORIZON_GRAVITY_500X
Y-AXIS

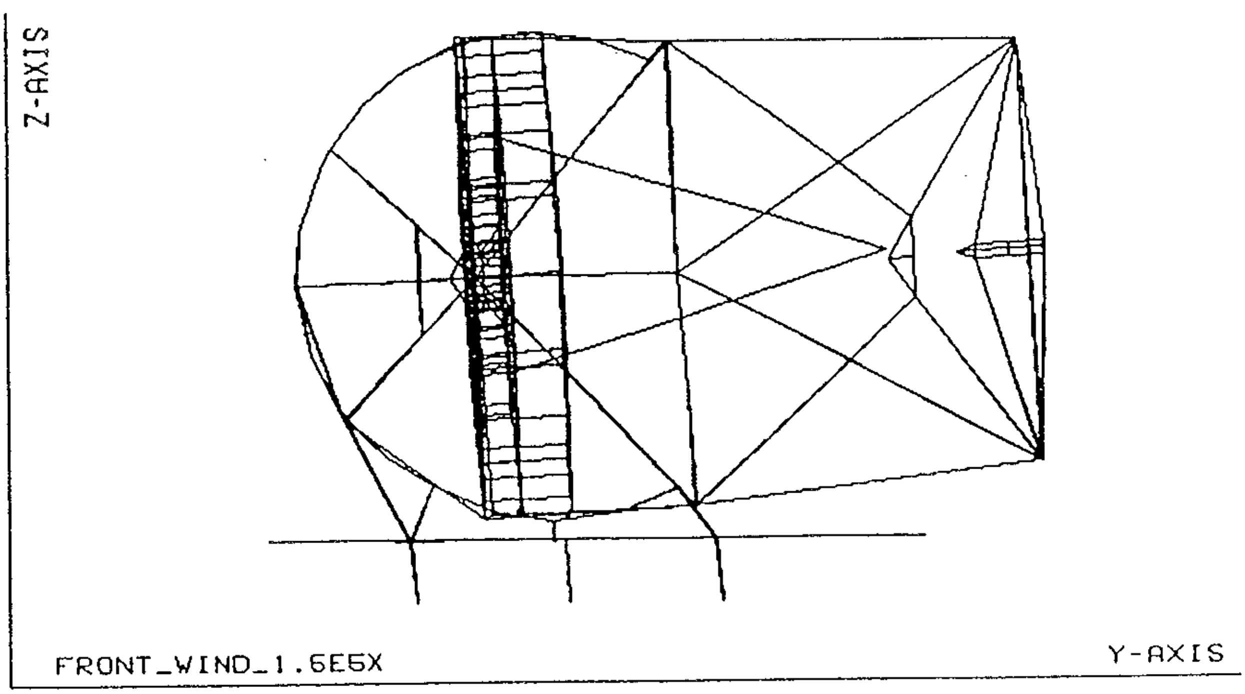
Z-AXIS
FRONT_WIND_1.6E5X
Y-AXIS

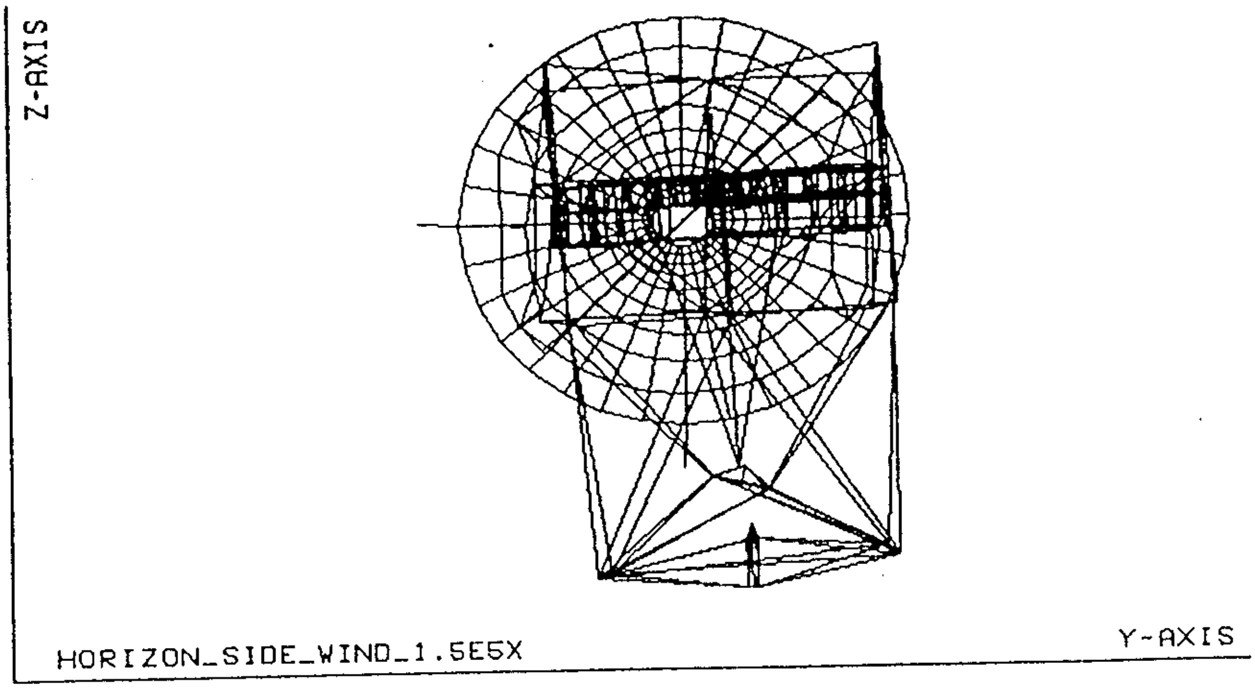
Z-AXIS
Y-AXIS
HORIZON_SIDE_WIND_1.5E5X

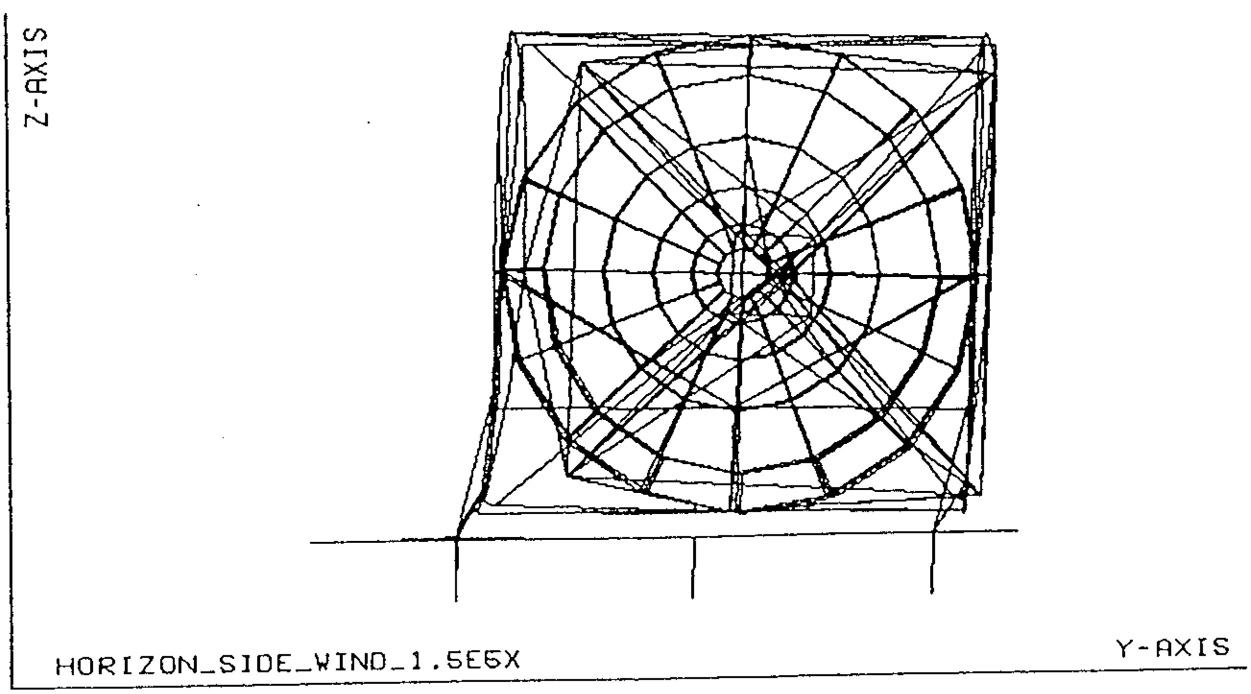
Z-AXIS
Y-AXIS
HORIZON_SIDE_WIND_1.5E5X

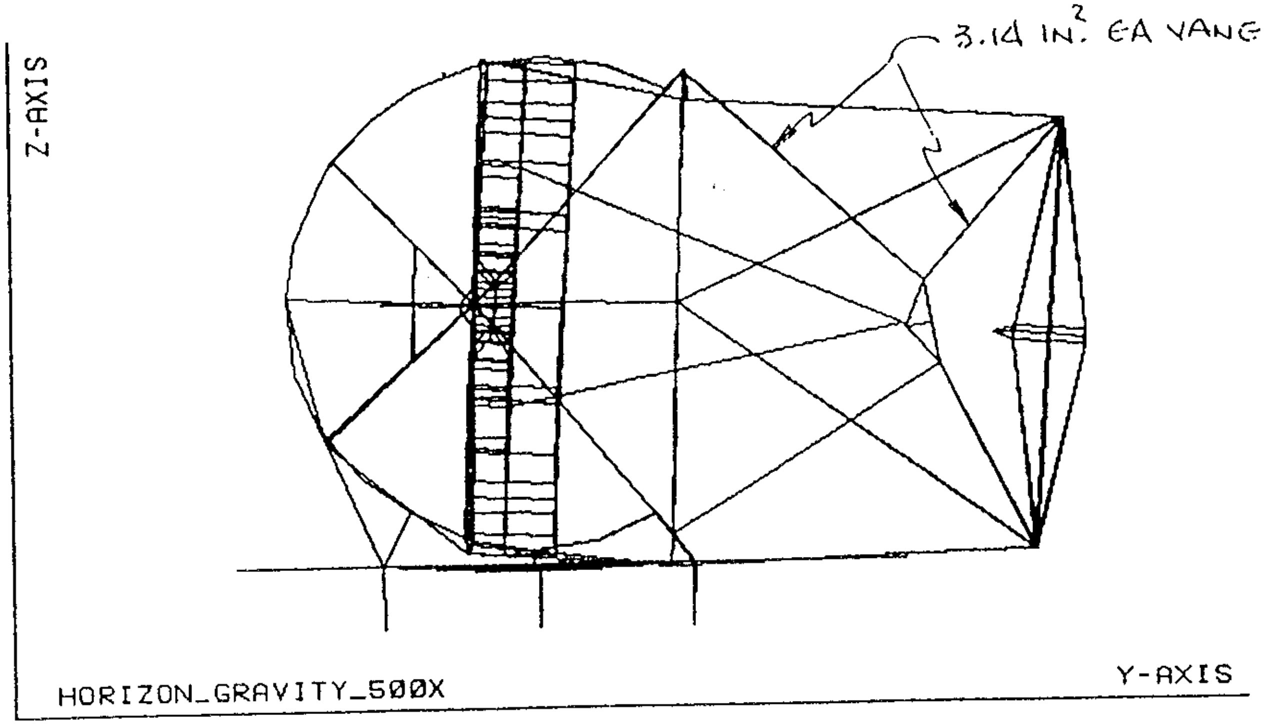
3.14 IN.² EA VANE
Z-AXIS
Y-AXIS
HORIZON_GRAVITY_500X

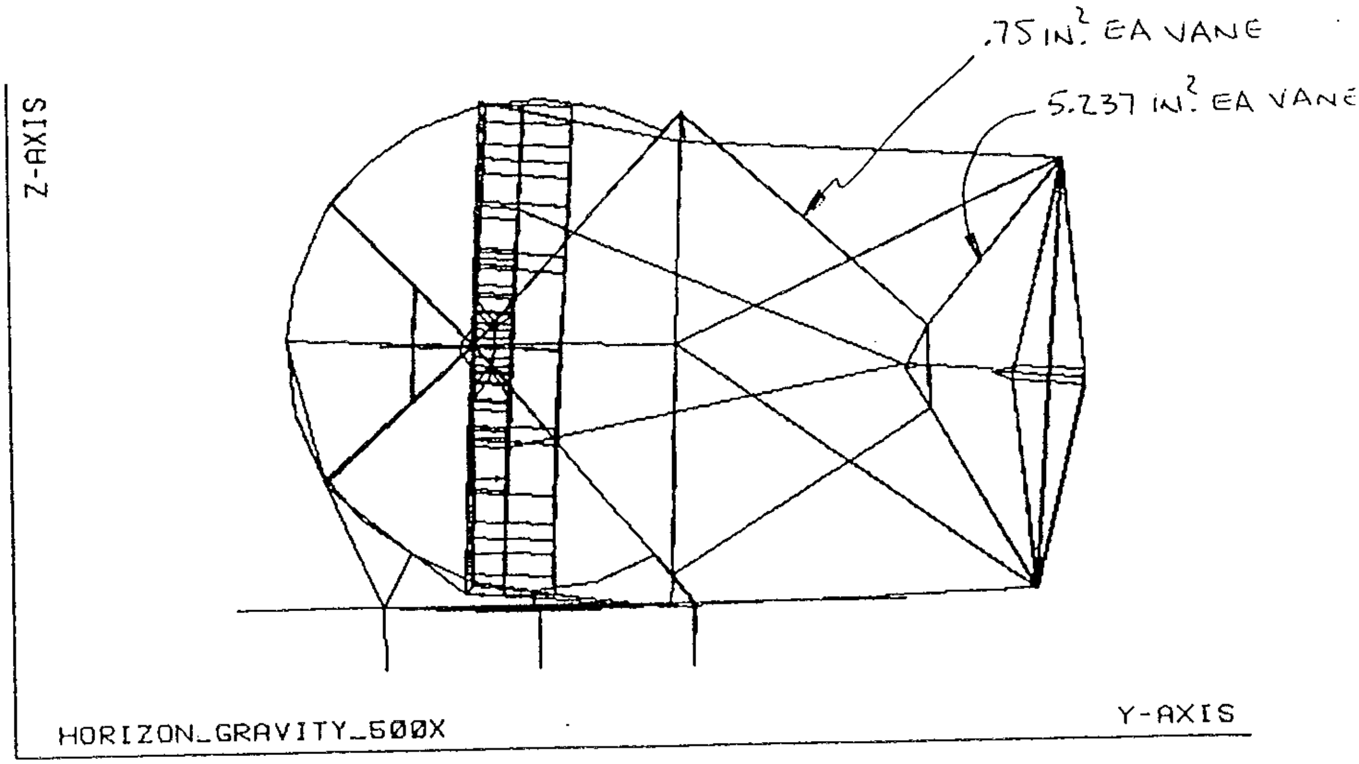
.75 IN.² EA VANE
5.237 IN.² EA VANE
Z-AXIS
Y-AXIS
HORIZON_GRAVITY_500X

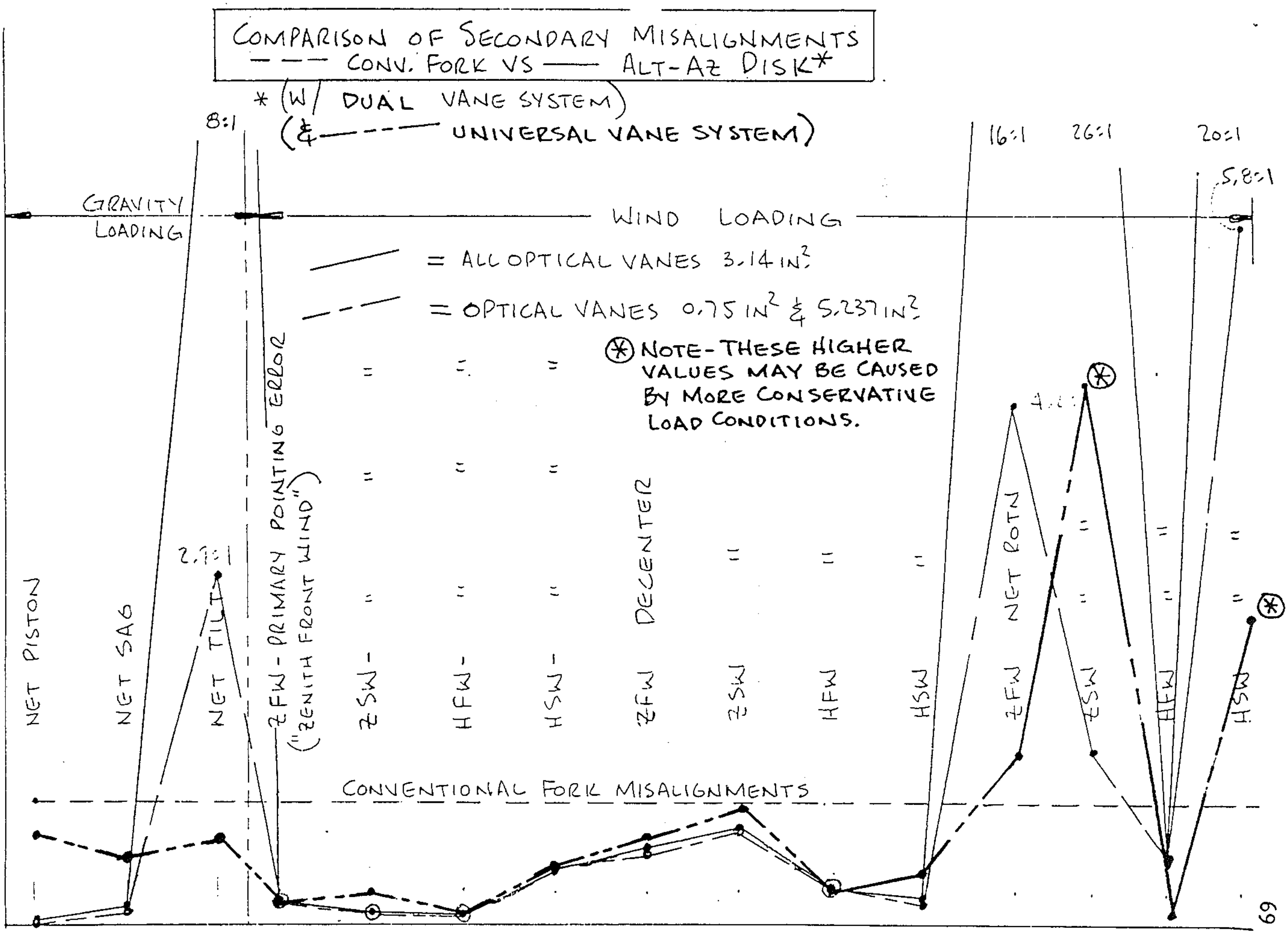
COMPARISON OF SECONDARY MISALIGNMENTS
— — — CONV. FORK VS —— ALT-AZ DISK*
* (W/ DUAL VANE SYSTEM)
(& - - - - UNIVERSAL VANE SYSTEM)
GRAVITY LOADING
WIND LOADING
—— = ALL OPTICAL VANES 3.14 IN²
— — = OPTICAL VANES 0.75 IN² & 5.237 IN²
(*) NOTE - THESE HIGHER VALUES MAY BE CAUSED BY MORE CONSERVATIVE LOAD CONDITIONS.
8:1
2.7:1
16:1
26:1
20:1
5.8:1
NET PISTON
NET SAG
NET TILT
ZFW - PRIMARY POINTING ERROR
("ZENITH FRONT WIND")
ZSW -
HFW -
HSW -
ZFW
DECENTER
ZSW
HFW
HSW
ZFW
NET ROTN
ZSW
HFW
HSW
CONVENTIONAL FORK MISALIGNMENTS

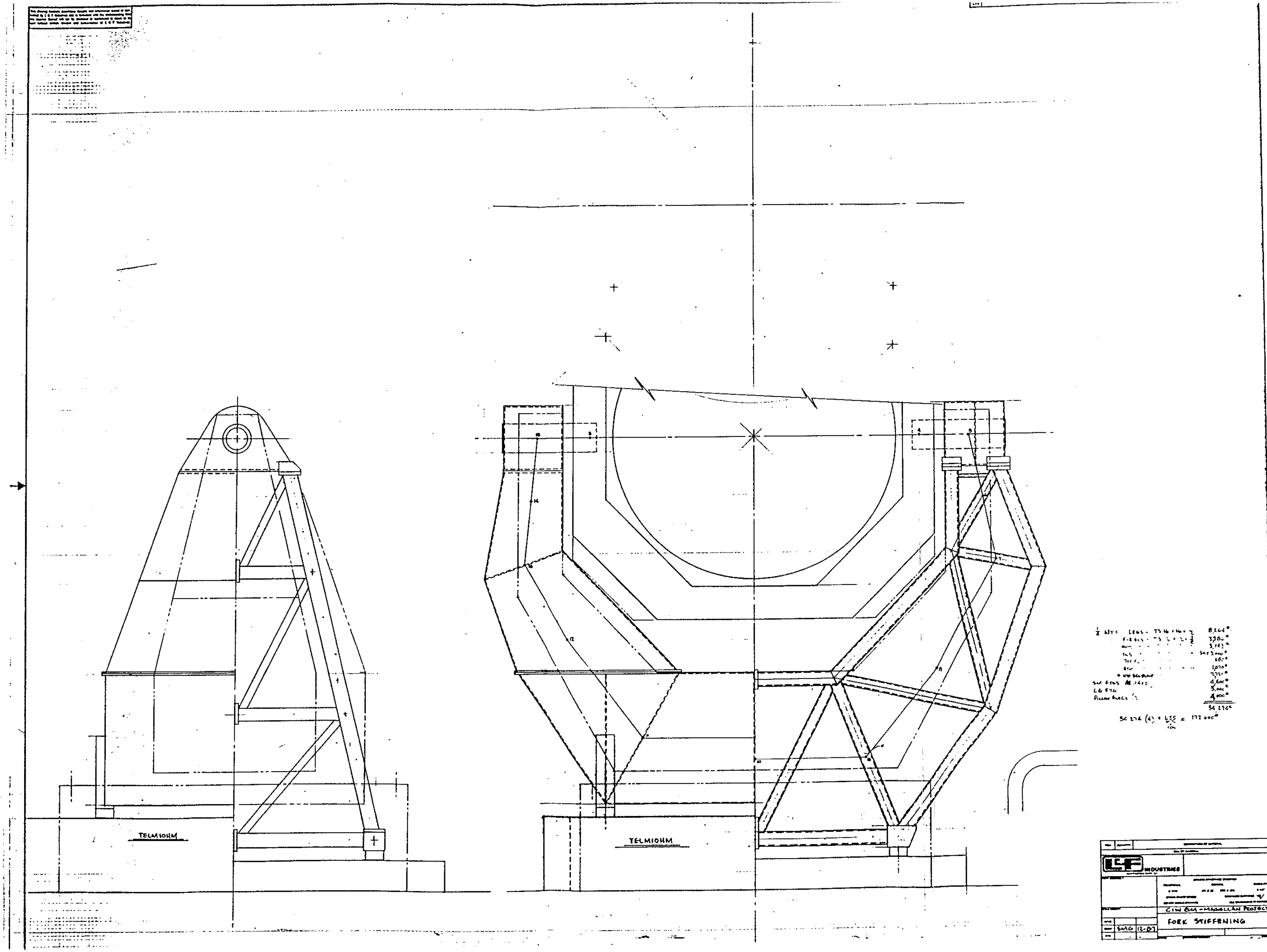
TELMIOHM
TELMIOHM
LEGS
LG FTG
8,264#
1,070#
4,400#
5,000#
4,000#
54,274#
INDUSTRIES
CIW 8M - MAGELLAN PROJECT
FORK STIFFENING
SMG
12-07

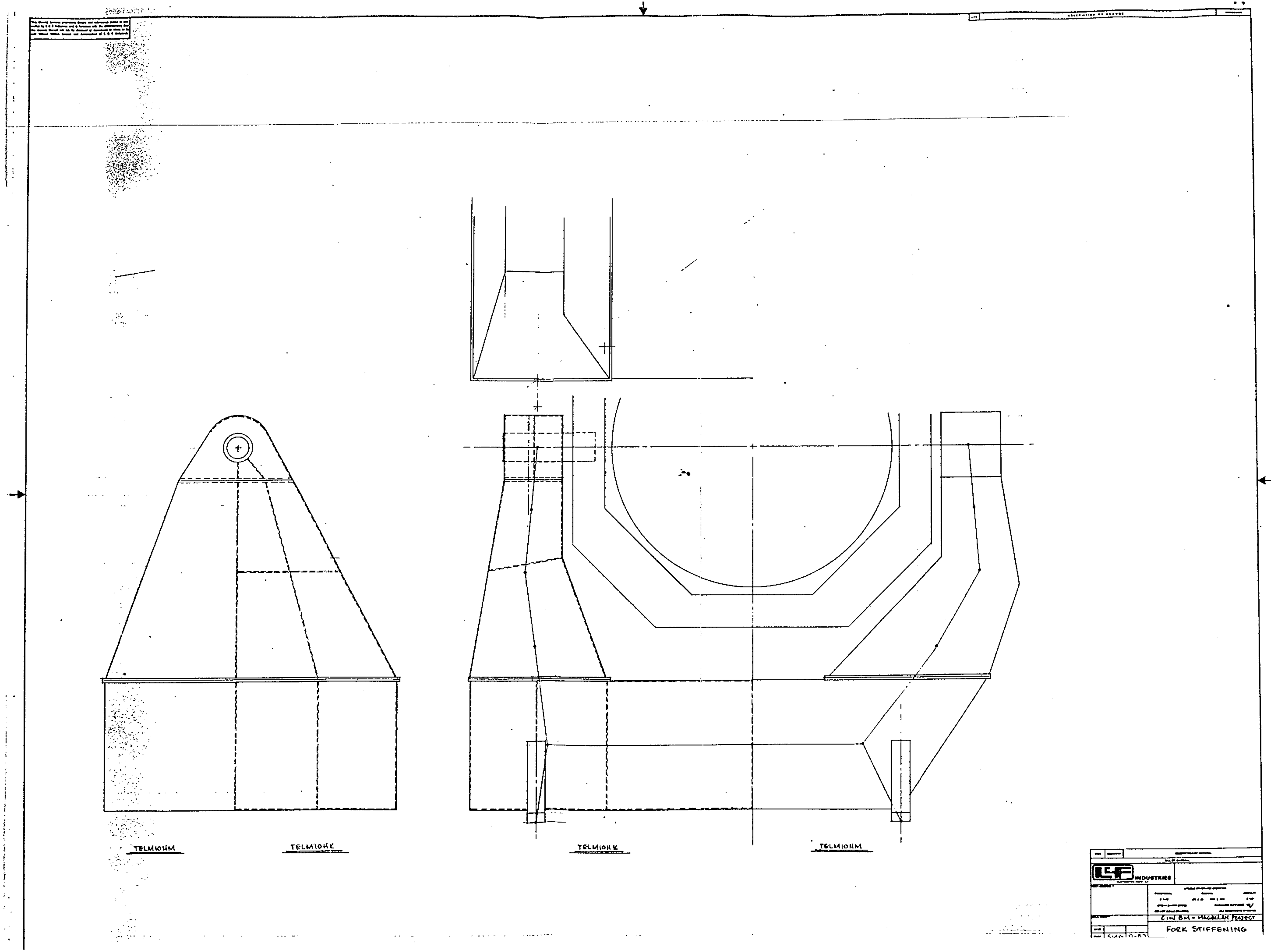

TELM10HM
TELM10HK
TELM10HK
TELM10HM
INDUSTRIES
CIW BM - MAGELLAN PROJECT
FORK STIFFENING
SMG

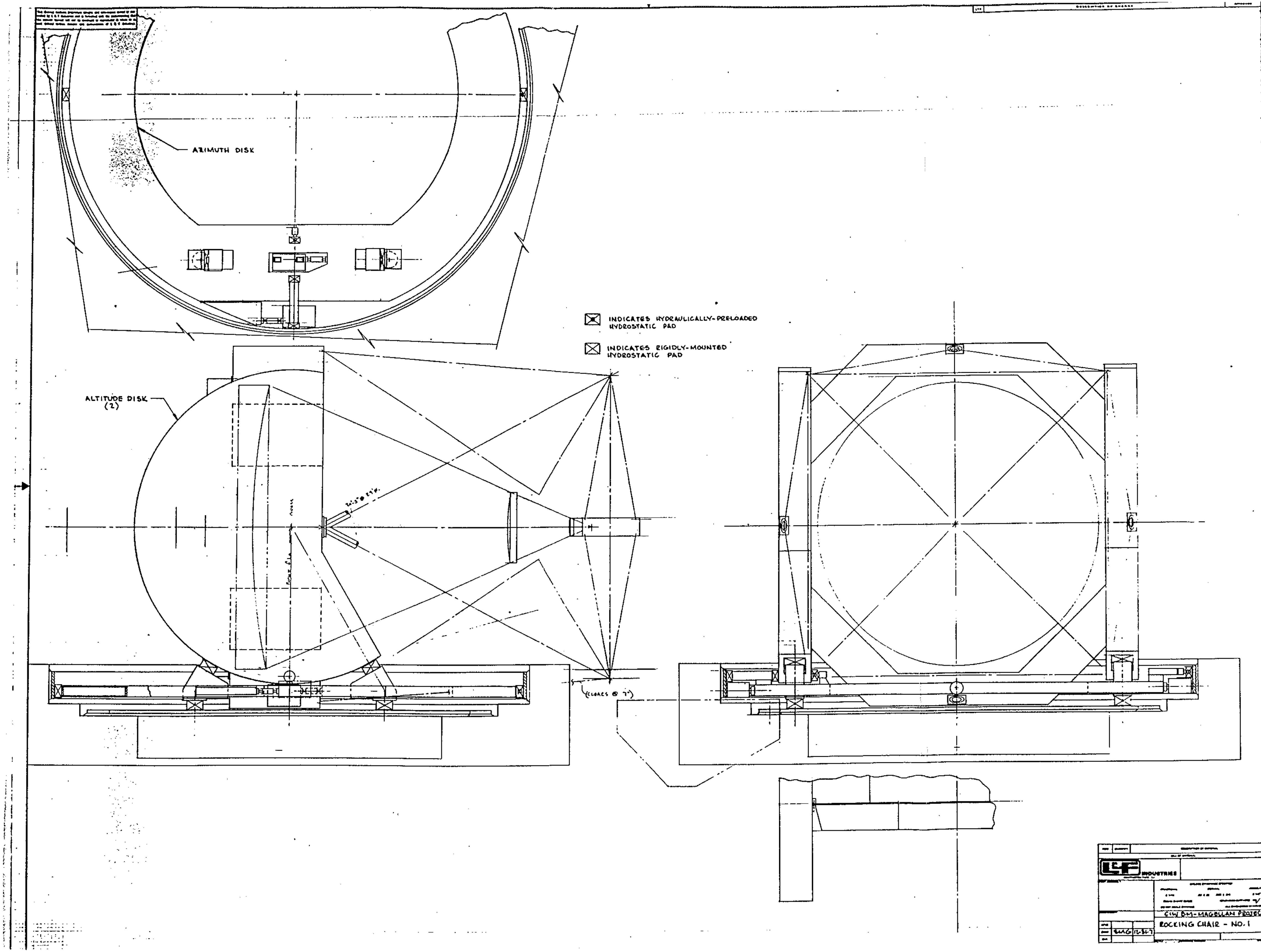
AZIMUTH DISK
ALTITUDE DISK (2)
INDICATES HYDRAULICALLY-PRELOADED HYDROSTATIC PAD
INDICATES RIGIDLY-MOUNTED HYDROSTATIC PAD
INDUSTRIES
CIW DM-MAGELLAN PROJECT
ROCKING CHAIR - NO. 1

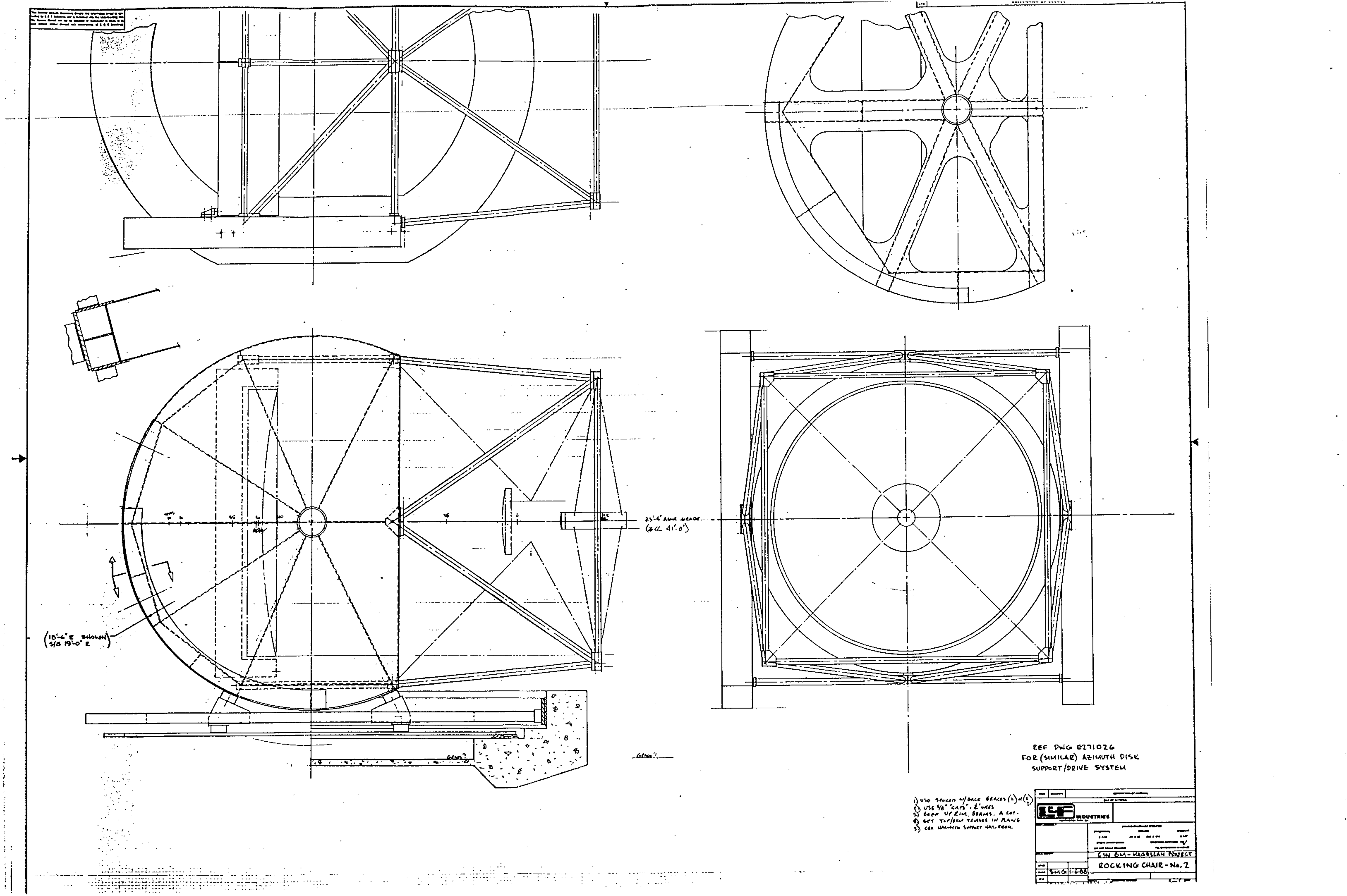
(18'-6" ⌀ SHOWN
S/B 19'-0" ⌀)
REF DWG E271026
FOR (SIMILAR) AZIMUTH DISK
SUPPORT/DRIVE SYSTEM
INDUSTRIES
ROCKING CHAIR - No. 2

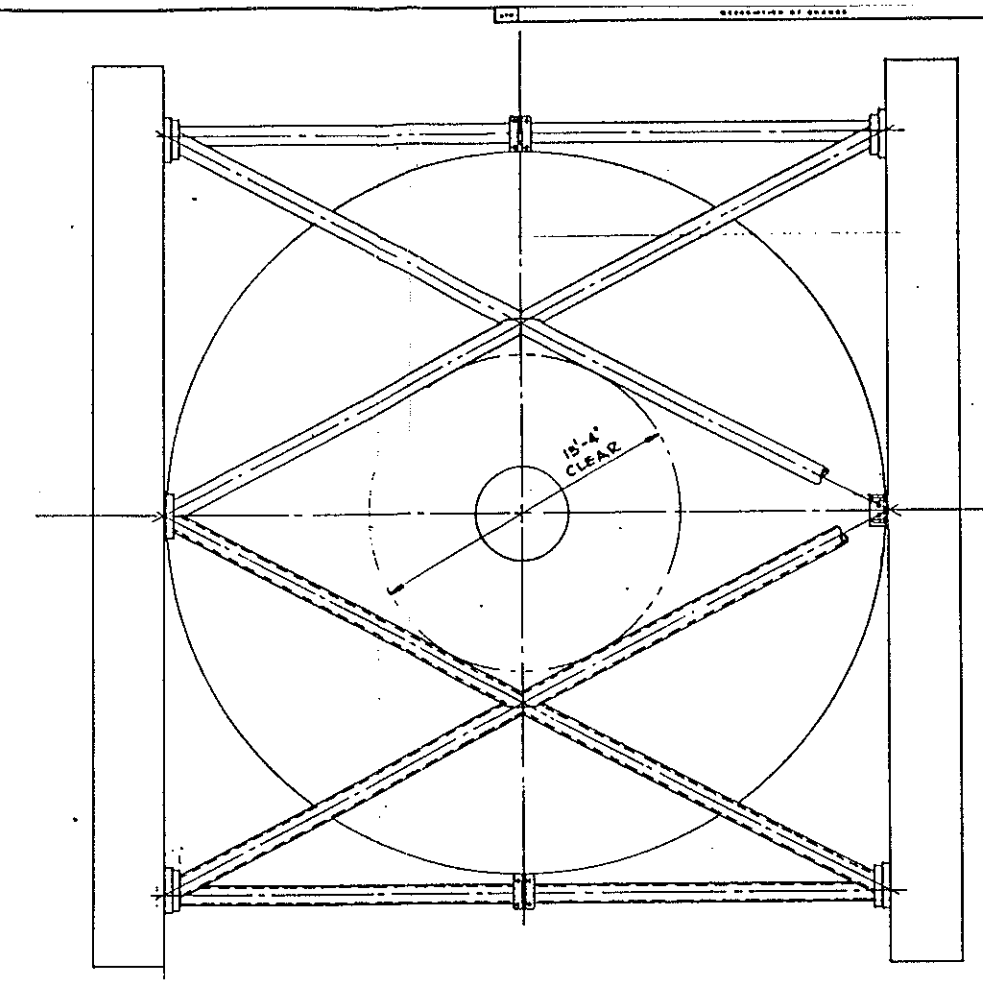

L&F INDUSTRIES

GLW DM – MAGELLAN PROJECT

ROCKING CHAIR – NO. 2

SMG 1-7-B

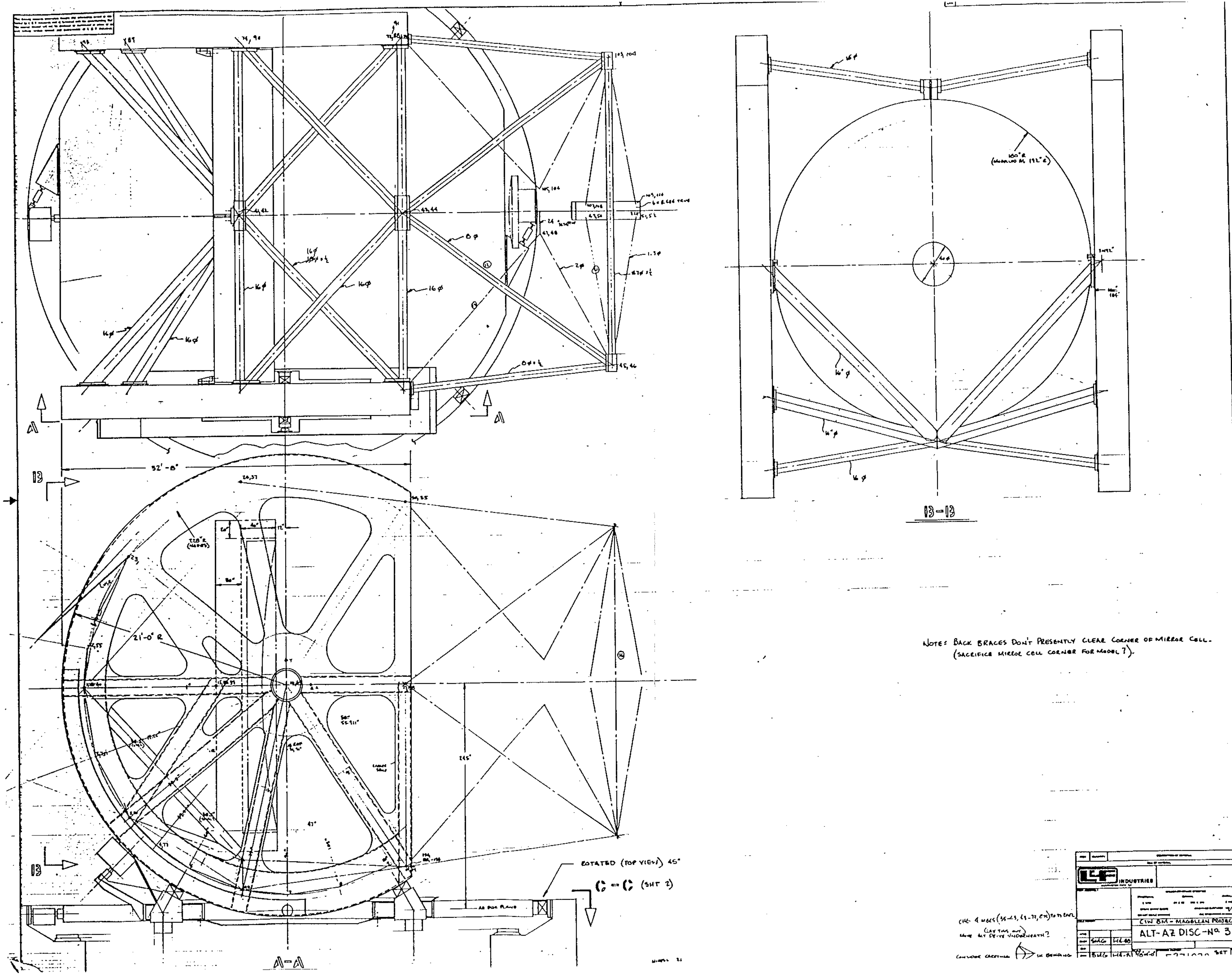
52'-8"
21'-0" R
A-A
B-B
ROTATED (TOP VIEW) 45°
C-C (SHT 2)
NOTE: BACK BRACES DON'T PRESENTLY CLEAR CORNER OF MIRROR CELL.
(SACRIFICE MIRROR CELL CORNER FOR MODEL 7).
L&F INDUSTRIES
CIW 8M - MAGELLAN PROJECT
ALT-AZ DISC-Nº 3

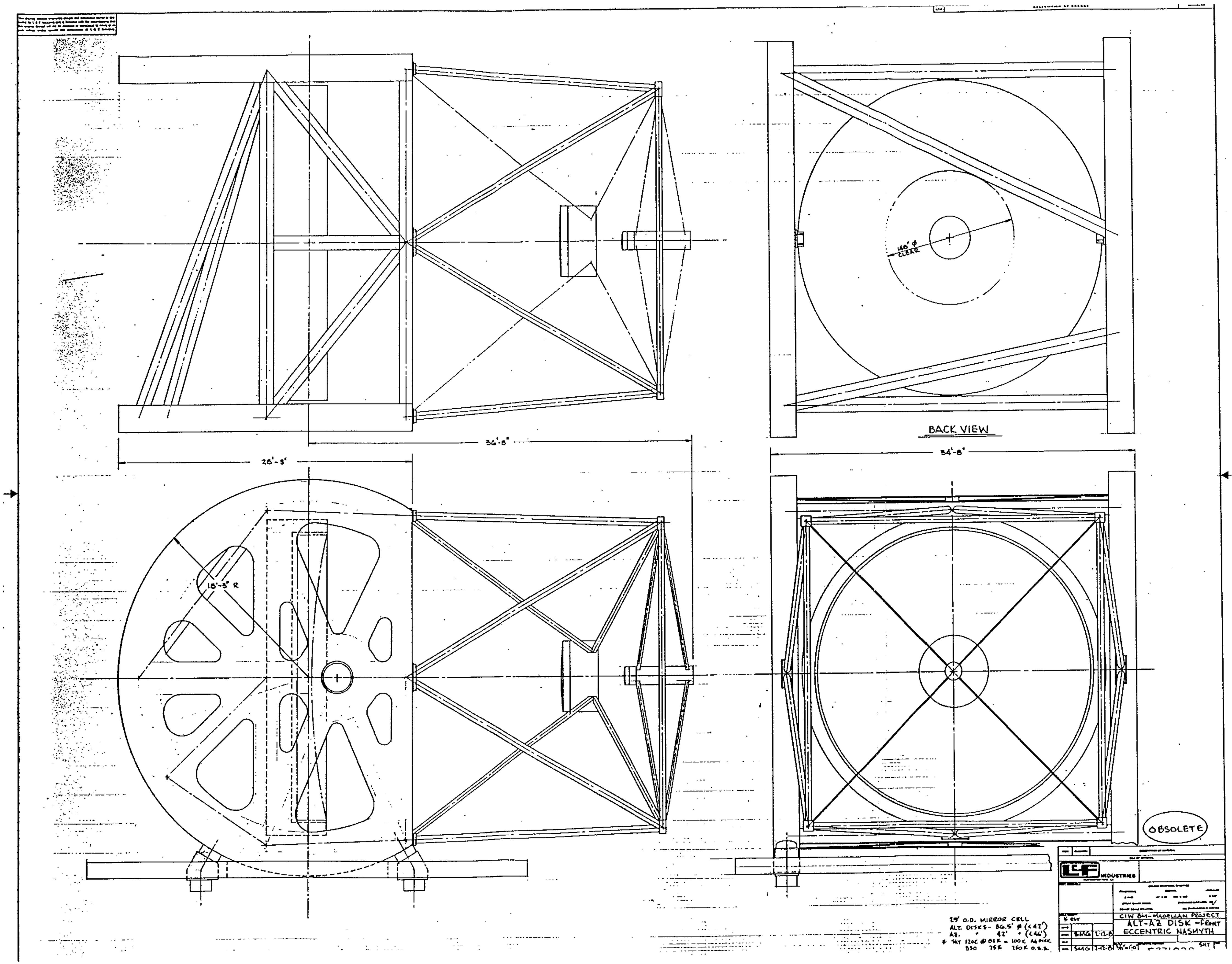
BACK VIEW
148" ϕ CLEAR
36'-8"
28'-3"
34'-8"
18'-3" R
OBSOLETE
INDUSTRIES
29' O.D. MIRROR CELL
ALT. DISKS - 36.5' ϕ (<42')
AZ. " 42' " (<46')
CIW 8M-MAGELLAN PROJECT
ALT-AZ DISK - FRONT
ECCENTRIC NASMYTH
SMG
SHT

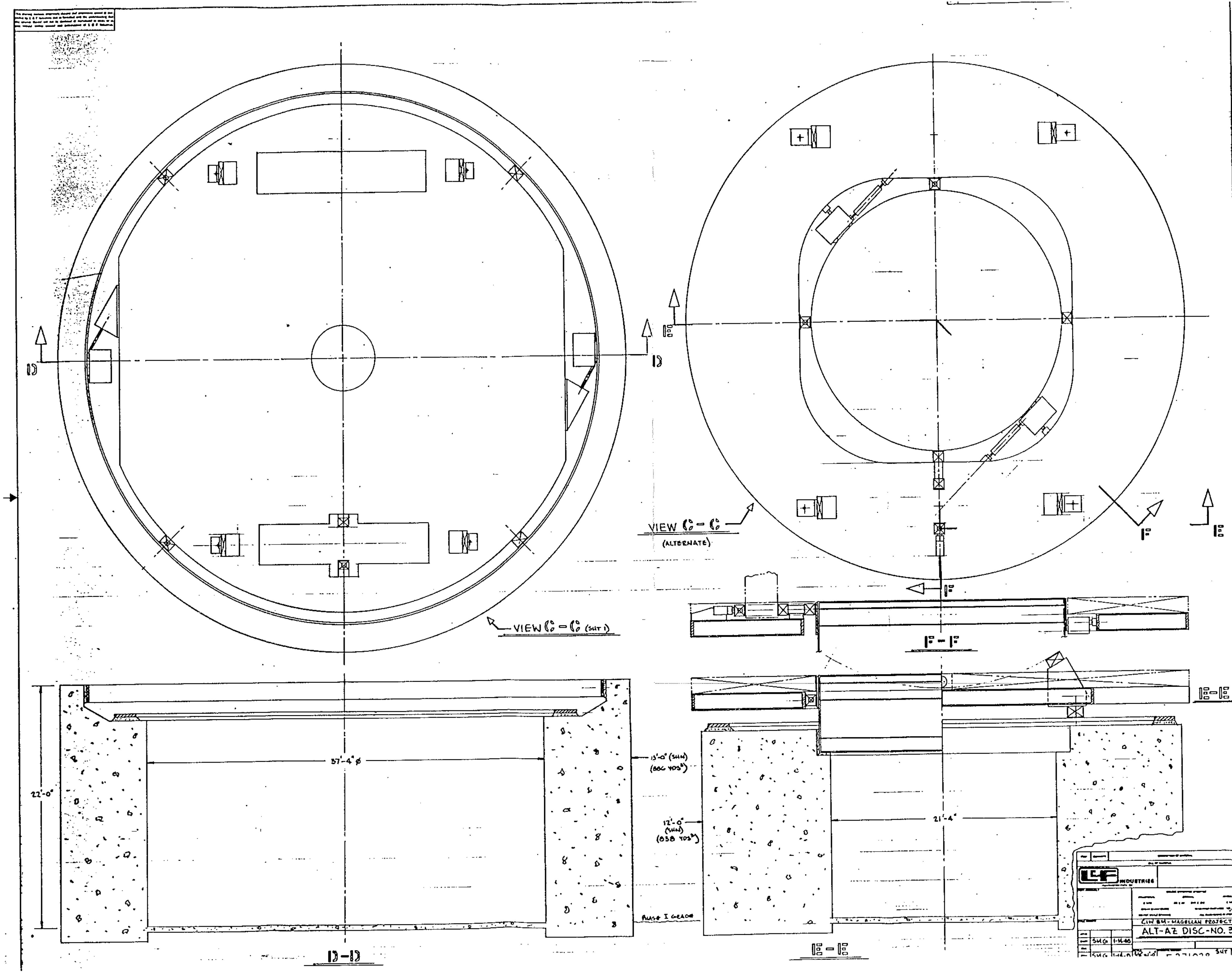

VIEW C-C (SHT 1)
VIEW C-C
(ALTERNATE)
D
E
F
F-F
E-E
D-D
22'-0"
37'-4" ⌀
13'-0" (SHN)
(866 YDS³)
12'-0"
(SHN)
(838 YDS³)
21'-4"
PHASE I GRADE
INDUSTRIES
CIW 8M-MAGELLAN PROJECT
ALT-AZ DISC-NO. 3
SMG
SHT

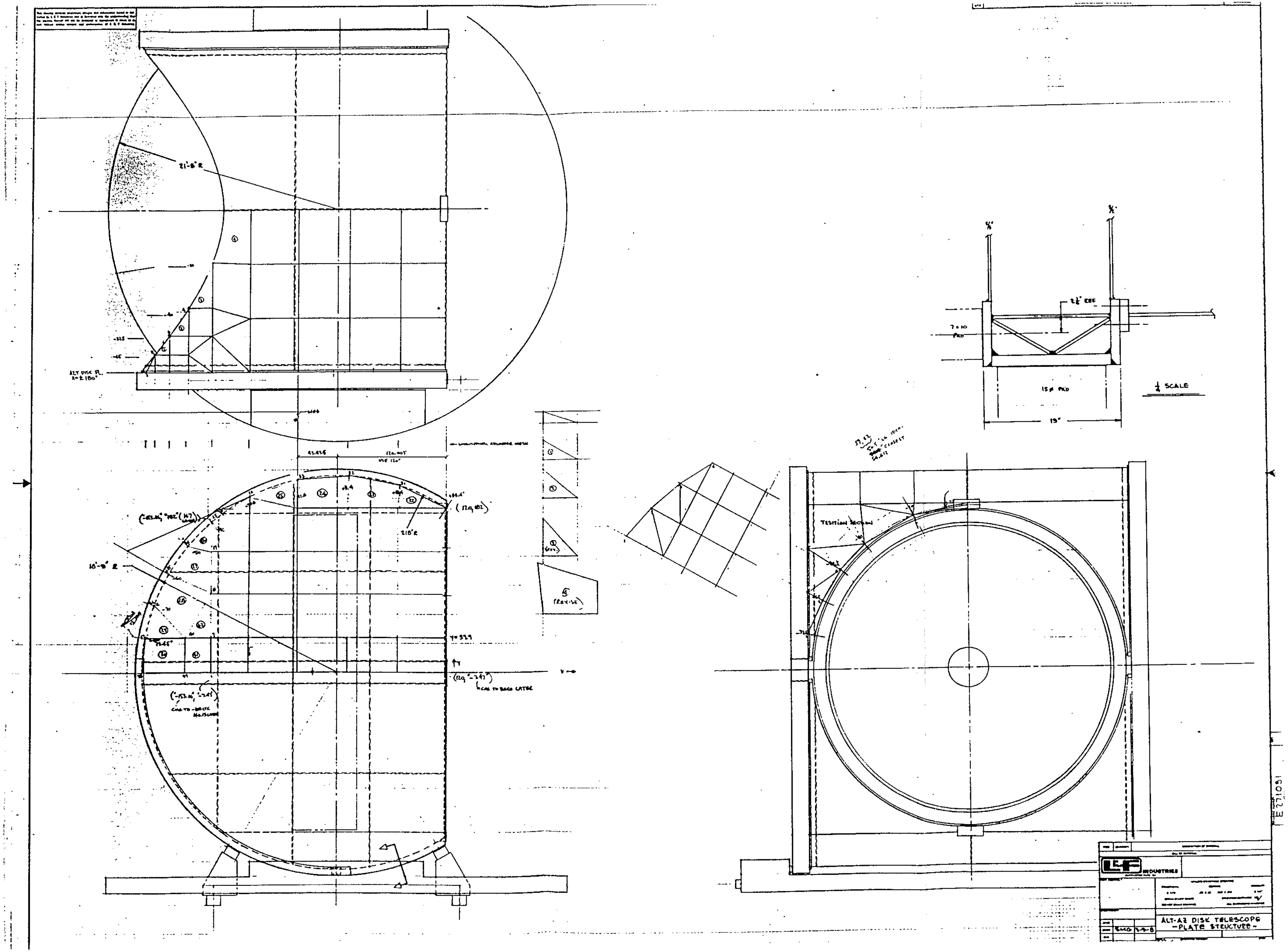
21'-8" R
ALT DISK FL
10'-8" R
210" R
(REVISE)
TESTING SECTION
2 1/2" REF
7 x 10
15# PRD
19"
1/4 SCALE
L&F INDUSTRIES
ALT-AZ DISK TELESCOPE
-PLATE STRUCTURE-
E271051

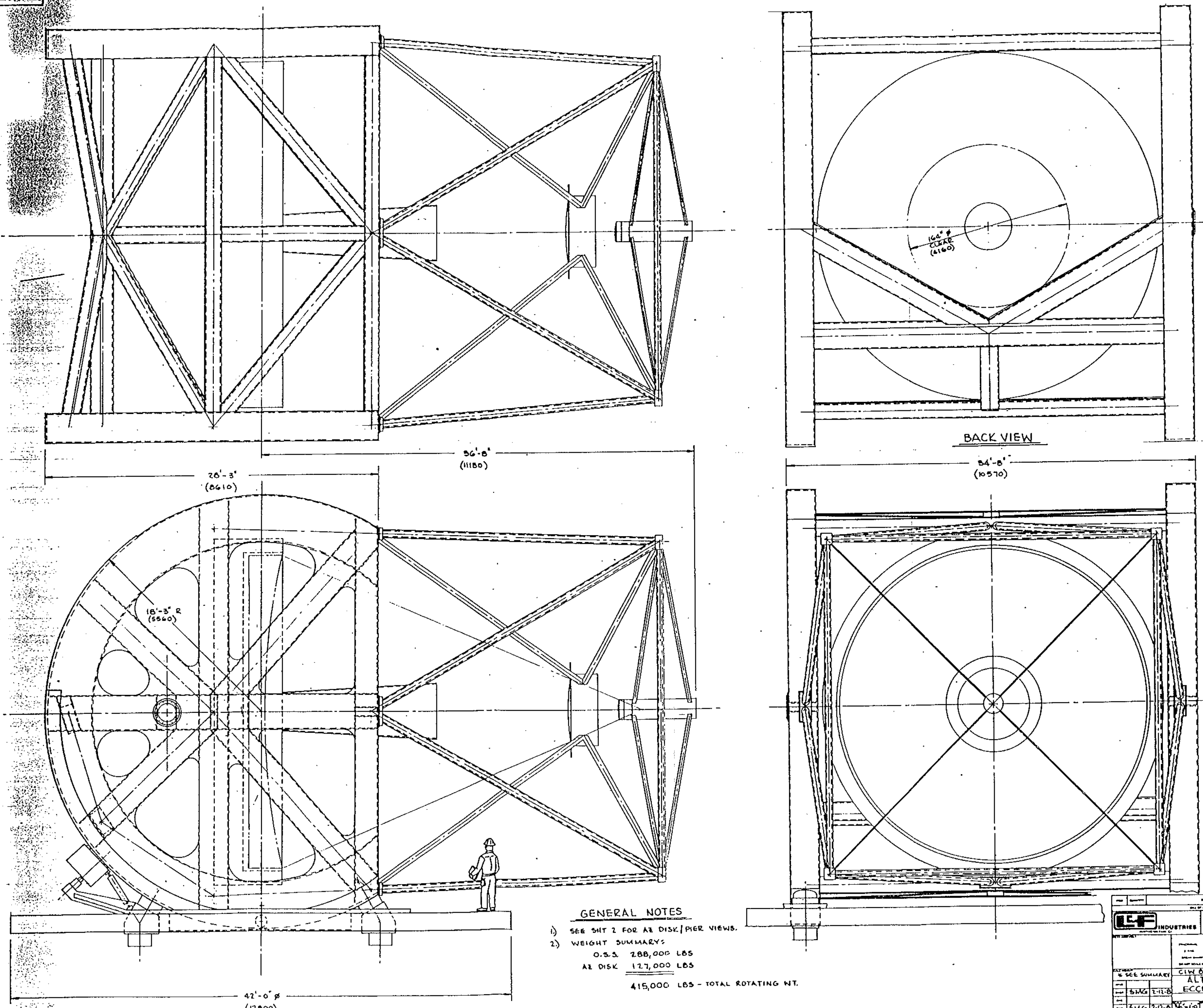

GENERAL NOTES

1) SEE SHT 2 FOR AZ DISK/PIER VIEWS.
2) WEIGHT SUMMARY:
O.S.S. 288,000 LBS
AZ DISK 127,000 LBS
415,000 LBS - TOTAL ROTATING WT.

L&F INDUSTRIES

* SEE SUMMARY

CIW 8M-MAGELLAN PROJECT

ALT-AZ DISK - ECCENTRIC NASMYTH

SMG 2-12-8

SMG 2-12-8

3/8"=1'-0" (1:32)

E271029 SHT 1 of 2